Assessment of Ga$_2$O$_3$ Technology

Dr. Burhan Bayraktaroglu

AFRL/RYDD

burhan.bayraktaroglu@us.af.mil

Ga(1) tetrahedral

Ga(2) octahedral

SEPTEMBER 15, 2016

TABLE OF CONTENT

LIST OF FIGURES

1. INTRODUCTION

In 2002, two well-known professors (Eastman of Cornell University and Mishra of UCSB) have written a provocative article in the IEEE Spectrum announcing the arrival of the "Toughest Transistor Yet". The article was well promoted by the display of the picture of Figure 1 on its front cover [1]. The timely appearance of this article has given the emerging technology of GaN a valuable push in term of encouragement to stay with it while the painful technology development stages can be navigated. The rest of the story is well known to many in this field. With concentrated research activities both at DoD and in commercial laboratories, a new generation of high power transistors were developed and fielded [2-4].
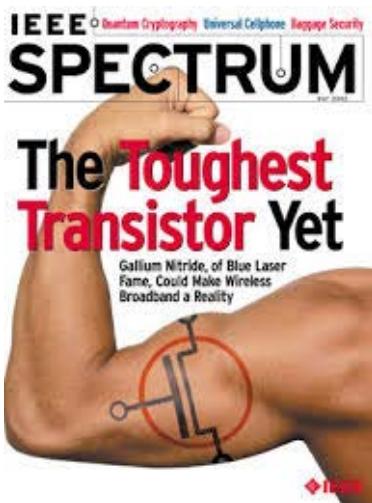
Figure 1: Cover of IEEE Spectrum, Vol. 39, Issue 5

The "toughness" of the GaN transistor refers to its ability to operate at high voltages and at elevated temperatures while generating substantially higher power than the previous generation devices. For military applications, this new "toughness" translates to smaller and cheaper RF electronics that improve radar and communication system ranges while improving bandwidth and power consumption. As pointed out by Kemerley *et.al.* "... *the RF electronics portion of most electromagnetic (EM) systems generally constitutes over 50% of the system cost, and EM systems constitute from 38 to 60% of the overall cost of most major Department of Defense (DoD) combatant platforms. The major application areas include radar, electronic warfare (EW), communications, and smart munitions*"[5].

A similar story can be told about a prior "tough" transistor technology based on GaAs (or more generally III-V compound semiconductors) that was introduced in 1970's and was fully developed in 1980's with substantial help from the DoD research investment [6-10]. GaAs has enabled monolithic circuit concepts while improving the "toughness" of the previous generation technology based on silicon (Si).

What is common between these two success stories is that the substantial improvement in device performance and "toughness" originated from the intrinsic properties of the new material. More specifically, the increase in the semiconductor bandgap enabled significant new capabilities. Compared

to the relatively narrow bandgap of 1.1eV of the industry workhorse Si, GaAs and GaN have bandgaps of 1.43 and 3.4eV, respectively. Since many critical device parameters improve exponentially with the bandgap value, such improvements can be significant enough to justify the effort to fully develop a brand new technology.

Now comes another semiconductor with even larger bandgap than GaN. Recent improvements in the material synthesis technology has highlighted the availability of certain crystal orientations of Ga_2O_3 as a wide bandgap (WBG) semiconductor, which was originally developed for transparent conductive oxide (TCO) applications[11-16], for high voltage and temperature applications as well [17, 18]. The bandgap of Ga_2O_3 is 4.4 to 4.9eV depending on the crystal structure [12-14, 19-24], and this represents a major increase over GaN. Although there are other semiconductors with even wider bandgaps, such as AlN and diamond [25-35], the material synthesis maturity is too low for these advanced semiconductors to be considered for applications at this time. However, there is no reason why Ga_2O_3 cannot be further evaluated now for applications in high power electronics while we wait to see if the other technologies can overcome the current technology barriers.

The purpose of this assessment note is to critically examine the status and the prospects of the Ga_2O_3 technology based on the published data in the open literature. Another purpose is to bring this database up to date and expand it so that it may help in future technology benchmarking activities.

2. WHY GALLIUM OXIDE?

First, some historical perspective. Although gallium oxide is the subject of much recent research activity around the world for both optical and electrical applications, the interest in Ga_2O_3 goes back many years. It's wide bandgap and semiconducting characteristics attracted early attention for conductive windows for ultra-violet light [11, 19, 36]. Initial investigations, conducted mostly on polycrystalline films or small flakes of crystals revealed important information regarding the optical properties of Ga_2O_3. For example, Figure 2 shows the measured optical absorption edge for β-Ga_2O_3 in a U.S. Air Force sponsored study in 1965 [19]. These optical characteristics are consistent with more recent studies [37]. The electrical characteristics, however, were only recently analyzed since they are highly dependent on the crystal quality, and the initial crystals were full of defects [11].
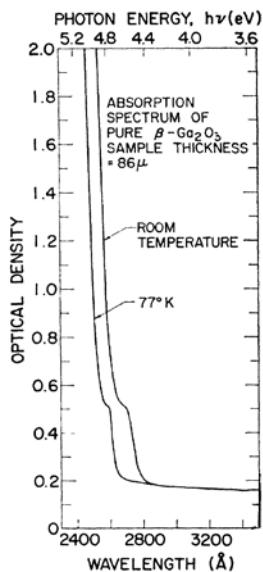
Figure 2: Absorption edge of pure β-Ga_2O_3 measured in 1965 [19].

For a while in 1970's, Ga_2O_3 was well known and used as an insulator on GaAs wafers. During the period of 1975 to 1985, which corresponds to high level of research activity for GaAs surface passivation (for C-MOS applications), thermal and anodic oxides were grown on GaAs at low temperatures [38-44]. These oxides contained mostly amorphous and α-polycrystalline forms of Ga_2O_3. Despite some success in passivating GaAs surfaces only when the oxides were grown in ultra-high vacuum systems (such as MBE) [45], this approach was abandoned. More recently, anodic oxides of GaAs grown at low temperatures were treated in oxygen plasma to increase their β-Ga_2O_3 content for an unsuccessful attempt to produce device quality films [41]. With a refractive index of n = 1.84- 1.88 at 980 nm wavelength, Ga_2O_3 has been used for anti-reflective coating on GaAs with reflectivity as low as 10^{-5} and a small absorption coefficient of about 100 cm^{-1} [22]. Ga_2O_3 remains to be an intrinsic part of the GaAs technology even today in a negative sense that it naturally forms on all free surfaces and must be carefully removed before every metallization step [46].

Today, gallium oxide is regarded as an important technology by itself mostly because it is a wide bandgap (WBG) semiconductor. But it is not unique in this respect. There are several other well-known WBG semiconductors in use today e.g. GaAs, GaN, SiC and ZnO. So, what makes Ga_2O_3 a special WBG semiconductor? To clarify this, we need to examine the intrinsic properties of WBG semiconductors in more detail.

All other parameters being equal, WBG semiconductors are preferred over narrow band semiconductors for electronics applications, because the large energy separation between the conduction and the valance bands allows the device to operate at elevated temperatures and at high voltages. This was one of the prime reasons for the success of silicon (Si) in replacing the original semiconductor germanium (Ge). At the time Si was regarded as the WBG semiconductor with its E_g = 1.1eV (compared to 0.65eV for Ge). However, since then many other semiconductor technologies have been developed to provide even wider bandgaps. The first wave of advanced WBG materials to be developed were compound semiconductors made from group III and V elements, such as GaAs and InP. Typical band gaps of these materials were in the 1.3-2.2eV range. Later, group III-N (e.g. GaN, AlN) and group IV materials (e.g. SiC, diamond) have been introduced extending the band gap range to well over 4eV. These are the traditional crystalline semiconductors with covalent bonding.

There are also other WBG semiconductors that have ionic bonding. These are mostly the oxides of post-transitional metals (e.g. ZnO, In_2O_3, CdO etc.) that offer wide bandgaps above 3eV [47-51]. Gallium oxide (Ga_2O_3), falls into this group of WBG semiconductors [16, 52].

Wider band gap semiconductors exhibit higher electrical breakdown strength. This is related to inverse relationship between the ionization coefficient and the bandgap. As it was the case for high temperature operation, where higher thermal energy is needed to create extra charge carriers, in WBG semiconductors higher electrical fields are needed to ionize charges. The relationship between the breakdown field strength and the band gap is exponential ($\varepsilon_c = a(E_G)^n$) with the index, *n*, in the range of $2.0 - 2.5$ [53-56]. Therefore, small increases in band gap values can significantly improve the field strength. Ga_2O_3, with its particularly large band gap is expected to be one of the major candidates for high breakdown voltage device applications.

WBG semiconductors find other applications due to their transparency to visible and near-UV light since for most semiconductors the optical and electrical bandgaps are identical. In this application, Ga_2O_3 offers the electrically conductive but optically transparent windows to visible and UV light up to 250nm wavelength. This wavelength is close to the wavelength of KrF laser and lower than the fourth-harmonic wave of Nd3:YAG laser. Applications in UV laser lithography [14] as well as solar-blind UV detector applications have been considered [57].

A. Is Gallium Oxide a Better Semiconductor?

Ga_2O_3 has a great potential for high electric field and high temperature applications, thanks to its ultra-wide bandgap. It is potentially an enabling technology for UV optoelectronics, also due its wide bandgap. In our "technology universe", as shown in Figure 3, β-Ga_2O_3 fits within the Ionic Semiconductor technologies group. This technology group also includes other metal-oxide semiconductors such as ZnO,

IGZO and ITO. The difference between Ga_2O_3 and the other ionic semiconductors in common use today is that all other metal-oxide semiconductors are useful as single crystal or thin film devices whereas β-Ga_2O_3 is only useful as a single crystal. This distinction precludes the use of Ga_2O_3 for thin film electronics. Its main applications will be in Power Electronics and Electro-optics (EO), as indicated by thick arrows in Figure 3. The high speed (meaning microwave) properties of Ga_2O_3 devices are not yet proven and therefore MMIC applications are not certain. The connection to this application group is shown with a thin arrow for now.
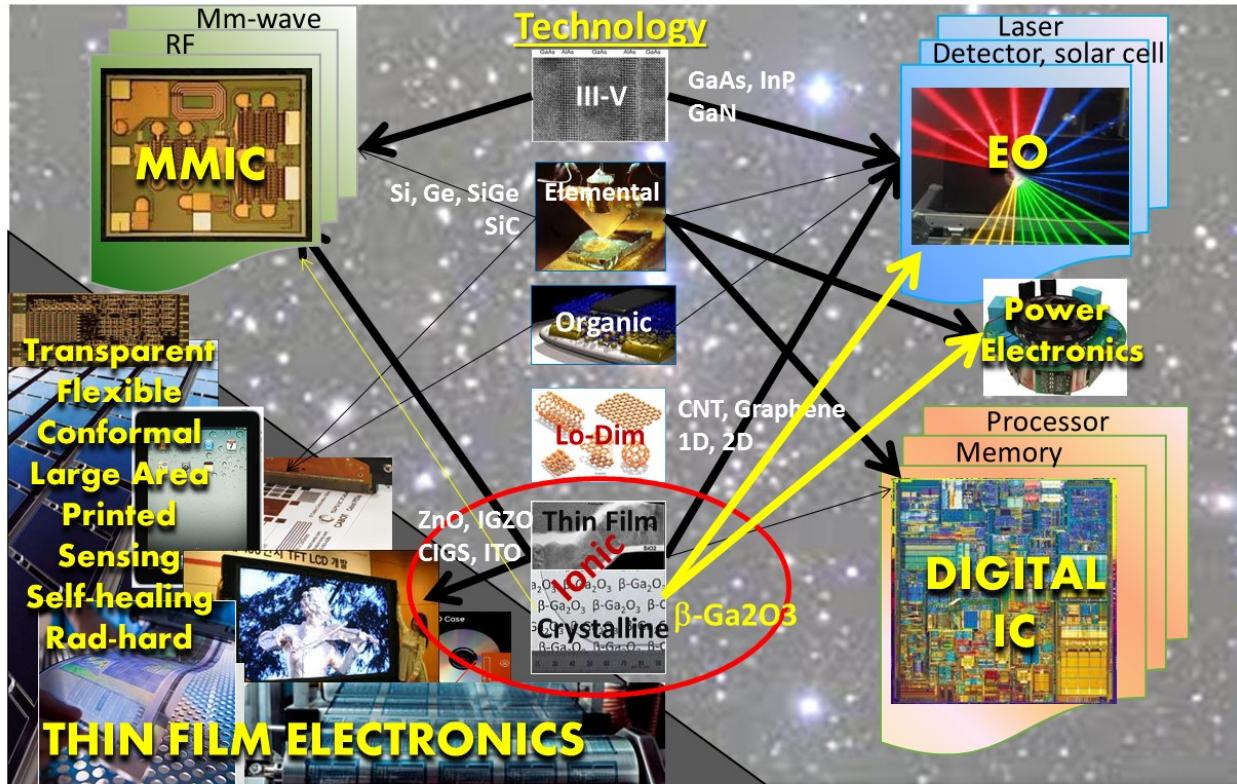
Figure 3: Initial assignment of β-Ga_2O_3 in the "Technology Universe". Thicker arrows indicate major application opportunities.

High efficiency power supplies and power converters are needed for aircraft electronics, radar and EW system power supplies, automobile electronics, electric motor controllers, and power conditioning for military electronics. The Air Force More-electric Aircraft (MEA) concept for example relies heavily on the availability of power converters, rectifiers, and uninterrupted power systems for backup [58-60]. Some or most of the sub-systems identified in the conceptual MAE system shown in Figure 4 can benefit from the availability of wide bandgap devices for reduction in size, cost and improved reliability at higher operating temperatures [61].

Power electronics applications range from on-chip power converters to high voltage rectifiers for electric power transmission lines. High-voltage switching transistors used in these applications are required to have small ON resistance while providing very high blocking voltages in the OFF state. The blocking voltage range can extend from 10's of volts to MV range. In general, high-voltage switching

transistors are used whenever transport, conversion and distribution of electric power are needed. Because of the requirement for high voltage, high current, and robustness in these applications, transistors for power electronic are large area devices. High voltage blocking requirement can only be met by the use of thicker layers of conventional semiconductor materials, which limit the miniaturization of power electronics systems. Similar systems implemented using WBG semiconductors with ultra-high breakdown voltages can provide orders of magnitude reduction in system size, cost and weight.
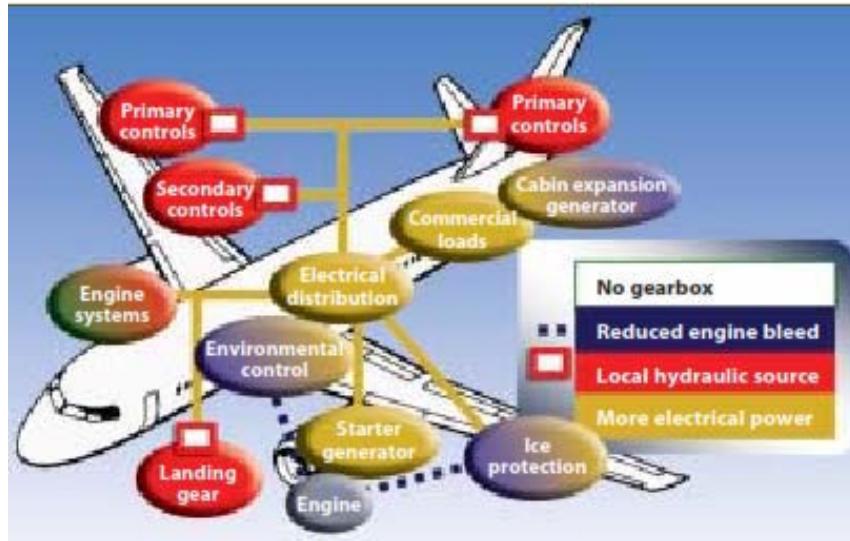
Figure 4: A More-Electric Aircraft (MEA) architecture [60].

B. How Does Ga_2O_3 Compare to Other Semiconductors?

We are paying attention to β-Ga_2O_3 because of its wide bandgap properties. But, there are existing other wide bandgap semiconductors in use today, such as GaN and ZnO, and indeed there are other semiconductors with even wider bandgaps. How do we select the right technology in which to invest?

There may be many ways to go about this selection process depending on our technology horizon. If we are choosing for near term applications, we may look for technology maturity, known reliability issues, availability, environmental impact etc. If our technology horizon is longer, we may assume that the near term technology issues can be addressed in time, and we choose a technology with the best overall promise in performance and/or cost. Occasionally, an unexpected breakthrough in science produces a technology that has an irresistible appeal (e.g. 2D-electron gas, graphene, low-dimensional materials). Some of these find immediate applications, such as 2D-electron gas resulting in high electron mobility transistors (HEMT) for high frequency applications [62]. Others require extensive R&D and may not live up to their initial promise [63]. Gallium oxide falls into the "long technology horizon" category with a sweetener regarding a recent breakthrough in materials science that enabled the fabrication of melt-grown ingots of high quality single crystals [14, 64-68]. Figure 5 shows a picture of 4-inch single crystal grown by edge-define film-fed growth (EFG) technique [17, 18]. The availability of large area substrates such as these very early in the development cycle is fortuitous and it will help accelerate all future R&D efforts.
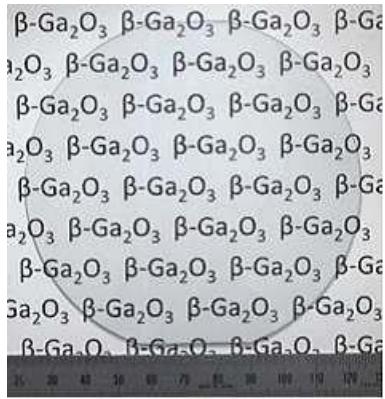
Figure 5: Photograph of 4-inch diameter Ga_2O_3 wafer [17].

Gallium oxide has a complex crystal structure, as we discuss later, and therefore it is too early to make theoretical predictions about all the performance details of future devices to be constructed using it. So far, the most prominent feature of Ga_2O_3 that is attracting attention is its potential for high electric field breakdown value, E_c. Again, because of its complex crystal structure, this parameter is difficult to pin down theoretically and may also have crystal orientation dependence. Since E_c is the current key feature of this technology, and the most future performance predictions are made based on this parameter, it is worth the effort to examine what we know about this parameter so far.

C. High Electric Field Breakdown

When electrical fields are applied to semiconductors across a potential barrier, the charge carriers are depleted in region of the semiconductor adjacent to the barrier. As the applied voltage increases, the depletion region width increases in some relationship to its charge density and electrical permittivity. This is similar to charging a capacitor except that the capacitor value is not fixed in this case. Eventually, when the applied voltage is high enough, the electrical field inside the semiconductor causes ionization of charges and a rapid breakdown of the electrical field. This is referred to as the avalanche breakdown and it is analogous to dielectric breakdown of insulators (no charge carriers) in ordinary capacitors. At exactly what electrical field value this avalanche mechanism start depends on material properties. Wide bandgap semiconductors have smaller intrinsic charge carriers and act more like insulators compared to small bandgap semiconductor that have high intrinsic carriers. The key metric that determines the onset of avalanche breakdown is the "impact ionization coefficient", which is the inverse of the distance an electron travels before being absorbed at a given electrical field. This parameter was recently calculated for Ga_2O_3 as $\alpha=a.exp(-b/E)$, with $a=2.5\times10^6$/cm and $b=3.96\times10^7$ V/cm [69]. Based on this, we can expect high electrical field values in Ga_2O_3 before impact ionization causes avalanche breakdown.

The electrical breakdown value is empirically related to the semiconductor bandgap. One of the often quoted value of 8MV/cm breakdown field value is obtained by curve fitting, as shown in Figure 6 [70]. In this figure, the breakdown field for diamond is assumed to be 10MV/cm and the bandgap of Ga_2O_3 was taken as 4.9eV.
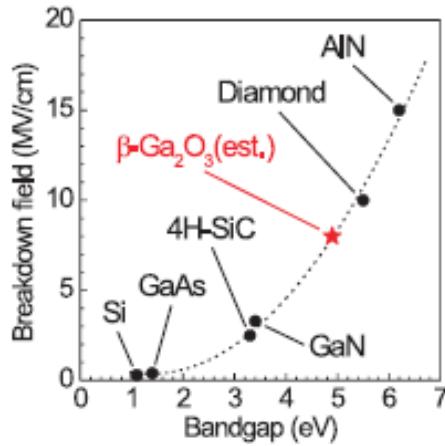
Figure 6: Breakdown field relationship with bandgap [70]

There are early indications that high electric fields can be achieved in transistors [71] with short channel lengths and this value (8MV/cm) may very well be valid. The exact value may be complex, however, given the complicated crystal structure and the uncertainty of the bandgap value [12-14, 19-24]. The electrical breakdown field strength may also have crystal orientation dependence (anisotropy) based on the observation that electron mobility, optical bandgap and thermal conductivity values are highly crystal orientation dependent [13, 72-75].

There have been several other attempts to correlated bandgap to breakdown field value for narrow and wide bandgap semiconductors [25, 53-56]. It was also suggested that a universal relationship can be used for direct and indirect bandgap materials in the form of $\varepsilon_c = a(E_G)^n$ with the coefficient, a, and the index ,n, values shown in Table 1 [56].

Table 1: Parameters used for curve fitting bandgap vs. E_c relationship [56].

Semiconductors	a	n
All	1.75E+05	2.359
Indirect	2.38E+05	1.995
Direct	1.73E+05	2.506

This relationship was developed using the known material parameters for a variety of narrower semiconductors and an attempt was made to predict the field breakdown value for wide bandgap materials such as SiC and GaN. Using the same approach, we can map the commonly accepted values of even wider bandgap materials (diamond, AlN), as shown in Figure 7.
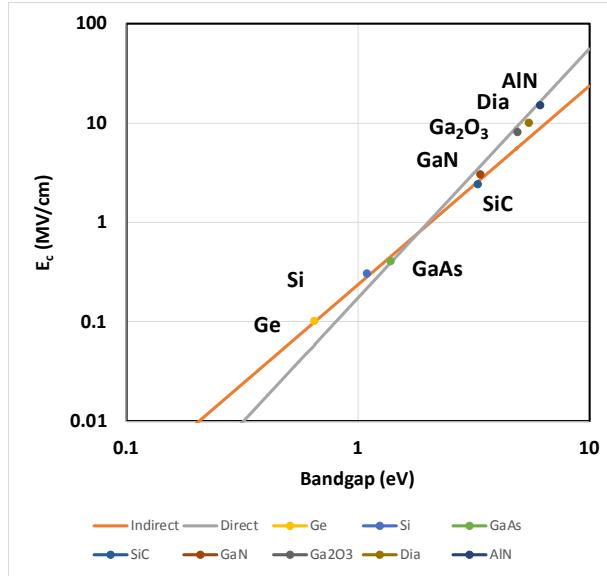
Figure 7: Breakdown field dependence on bandgap for direct and indirect bandgap semiconductors.

The fit between the prediction and the assumed values of E_c for ultra-wide bandgap materials (Ga_2O_3, diamond, AlN) is not very good in this chart. There is better fit to direct bandgap material relationship, although all 3 ultra-wide bandgap materials are regarded as indirect bandgap. A range of uncertainty in E_c for Ga_2O_3 may be identified by considering the bandgap to be in the range of 4.4-4.9eV and the material to be either direct or indirect bandgap. As shown Table 2 the estimated E_c values for Ga_2O_3 can range from 4.58 to 9.31 MV/cm. The lower end of this range makes the electrical breakdown strength of Ga_2O_3 comparable to GaN and the upper end makes it comparable or to better than the well-known insulators used for capacitors [56, 76-78]. We will continue to use 8MV/cm, which is close to the upper end of the range, for the rest of this note.

Table 2: The range of E_c values possible for Ga_2O_3

E_G (eV)	E_c Direct Bandgap MV/cm	E_c Indirect Bandgap MV/cm
4.4	7.11	4.58
4.9	9.31	6.17

D. Figure-of-Merit (FOM)

An assessment of the potential of new technologies with long horizons are traditionally made using figure-of-merit (FOM) numbers. FOM is a combination of several known technology parameters and it is used to predict the future performance of a class of devices that may be realized using a new technology. In the case of semiconductors for electronics applications, FOM numbers are sometimes normalized to the industry standard silicon (Si). Over the years, the next generation of semiconductor materials such as GaAs, GaN, SiGe etc. all have been justified initially due to their high FOM numbers.

This is a reasonable empirical approach to technology selection. But the predictions should not be taken literally. Even after full development of the "next" semiconductor technology with high FOM numbers, the Si technology still remains to be the most advanced and utilized semiconductor technology. In other words, high FOM numbers may justify making room for the new technology, but the incumbent technology may not be entirely displaced because of high FOM numbers of the new material.

There are several FOM methods used for power semiconductor devices. A list of the most commonly used FOMs and their brief description are given in Table 3.

Table 3: Some of the most commonly used power semiconductor device FOMs.

FOM	Definition	Description	Ref
JFOM	$\dfrac{E_c v_s}{2\pi}$	Maximize frequency and voltage	[79]
KFOM	$\sigma_{th} \cdot \left[\dfrac{c \cdot v_s}{4\pi\epsilon}\right]^{\frac{1}{2}}$	Minimize thermal limitations , σ_{th} = thermal conductivity	[80]
BFOM	$\epsilon \mu E_G^3$	Minimize conduction losses	[55]
BHFFOM	$\dfrac{1}{R_{on,sp} C_{in,sp}}$	Minimize high frequency switching loss, C_{in} = input capacitance	[54]
NHFFOM	$\dfrac{1}{R_{on,sp} C_{oss,sp}}$	Minimize high frequency switching loss C_{oss} = output capacitance	[81]
QF1	$\sigma_{th} \sigma_A$	Minimize thermal limitations $\sigma_A = \text{BFOM}$	[82]
QF2	$\sigma_{th} \cdot \sigma_A \cdot E_c$	Minimize thermal limitations $\sigma_A = \text{BFOM}$	[82]
HMFOM	$E_c \cdot \sqrt{\mu}$	Minimize power loss	[83]
HCAFOM	$\epsilon \cdot E_c^2 \cdot \sqrt{\mu}$	Minimize chip area	[83]
HTFOM	$\dfrac{\sigma_{th}}{\epsilon E_c^2}$	Minimize thermal impedance	[83]
PDFOM	$\dfrac{1}{\sqrt{R_{on} Q_{gd}} \cdot A_{pack} R_{th}}$	Maximize power density Q_{gd}= gate-grain charge, A_{pack} = Package area	[84]

JFOM is a materials based FOM introduced in 1965 by Johnson [79]. It highlights the high frequency and high voltage capability of a device. This was followed in 1972 by KFOM introduced by Keyes to take into account of the thermal limitations to the performance of transistors [80]. In 1982, Baliga introduced another FOM (BFOM) specifically for unipolar devices by minimizing conduction losses [55]. This is most commonly used FOM to compare the ultimate capabilities of devices based on different materials. Baliga later introduced BHFFOM to take into account of switching losses due to charging and discharging

of the input capacitance [54]. Another similar expression, NHFOM, was used by Il-Jung to emphasize the losses due to the output capacitance under some load conditions [81]. QF1 and QF2 are modifications of BFOM under different thermal heatsink conditions [82]. QF1 is for the case where the device and its heatsink have different thermal conductivities, whereas QF2 is specific to ideal heatsink conditions. There is actually a QF3, which eliminates the thermal restrictions and becomes identical to BFOM. Huang introduced a series of FOMs to compare the device performances based on materials, chip area and thermal properties [83]. These are designated HMFOM, HCAFOM, HTFOM, respectively. PDFOM is a figure-of-merit specifically for high power density converter and takes into account of switching losses and thermal limitations [84].

As mentioned above, the FOM most commonly used for comparing the ultimate potentials of unipolar devices fabricated on different semiconductor materials is BFOM. It only emphasizes the conduction losses, and therefore more applicable to low frequency devices, but nevertheless can be useful for new materials due to its simplicity. This is the expression most recently used for comparing the potential of Ga_2O_3 to other semiconductor technologies [18, 85, 86]. A BFOM (relative to Si) value of 3,443 was claimed in these comparisons meaning Ga_2O_3 is expected to yield that much improvement over Si from conduction losses point of view.

Table 4 lists some of the material parameters for Ga_2O_3 and compares them with other narrow and wide bandgap semiconductors using the FOM approach. Similar comparisons were provided by others [18, 72, 73] by normalizing BFOM to Si. Table 4 expands this list by adding Ge and AlN as semiconductors and also includes various other FOMs that are mostly material prameters dependent. **FOMs in this table were normalized to Ge rather than Si, because Ge is the original semiconductor.**

Table 4: Material properties and several FOM numbers (normalized to Ge) for major semiconductors [25, 29, 56, 86-88]

Material parameters and FOM	Ge	Si	GaAs	4H-SiC	GaN	AlN	Diamond	β-Ga_2O_3
Bandgap (eV)	0.67	1.1	1.4	3.3	3.4	6.2	5.5	4.9
Electron Mobility μ (cm^2 Vs^{-1})	3900	1400	8000	1000	1200	1000	2000	300
Breakdown Field E_c (MV/cm)	0.1	0.3	0.4	2.5	3.3	15	10	8
Relative dielectric constant ε	16	11.8	12.9	9.7	9.0	8.5	5.5	10
Thermal conductivity σ_{th} (W/°C)	0.64	1.5	0.55	2.7	2.1	7	10	0.27
Electron Velocity v_s (cm/s) x 10^7	0.6	0.9	1.0	1.5	1.5	1.5	1.0	1.5
JFOM	1	5	7	63	83	375	167	200
KFOM	1	3	1	7	5	17	20	1
BFOM	1	7	106	2429	6220	459736	176282	24615
QF1	1	17	91	10247	20409	5028358	2754407	10385
QF2	1	28	190	50470	103568	52535082	22610804	75947
HMFOM	1	2	6	13	18	76	72	22
HCAFOM	1	4	18	192	340	6053	2462	1109
HTFOM	1	0.35	0.07	0.01	0.01	0.00	0.00	0.00
BFOM normalized to Si	0.14	1.00	15	340	870	64316	24661	3444

The first thing to notice in this table is that most FOMs increase drastically with E_c (and hence with E_G). Some astronomically high FOM numbers can be obtained for the ultra-high bandgap semiconductors considered here. BFOM normalized to Ge for Ga_2O_3 is, for example, 24,615. Other FOM values are also high, except KFOM and HTFOM. These last FOMs include thermal conductivity, and the thermal conductivity of Ga_2O_3 is poor.

The second thing to notice is that the earliest FOMs (JFOM, KFOM and BFOM) for Si are not very high compared to Ge. A range of values from 3 to 7 is calculated. The transition from Ge to Si as the preferred semiconductor technology probably was not motivated by such FOM numbers. Yet, Si is a very capable technology and maintains its overwhelming dominance in the electronic industry to this day. One way to look at this is to argue that FOM numbers as low as 3 are sufficient to justify a technology change. Si is an indirect bandgap material (Ge is direct bandgap) with inferior electron and hole mobility values compared to Ge. Despite these disadvantages, the higher E_G value for Si (1.1 vs. 0.65eV) results in lower intrinsic carrier concentration for Si and allows devices made from Si to operate at higher temperatures than those made from Ge. For example, Si transistors were still functional at 100°C whereas Ge transistor gains dropped to unity. This line of argument is highly supportive of Ga_2O_3 with its BFOM value of 24,615.

Another way to look at it is to argue that Si displaced Ge due to its other relative technology merits despite low FOM numbers. For example, both n- and p-type Si could be passivated with thermal oxides (SiO_2) and therefore could be used for CMOS circuits. The native oxide of Ge is not very useful. Silicon is abundant as an element whereas Ge is scarcer. This line of argument is not very supportive of Ga_2O_3, which is made from rare-earth metals, has an indirect bandgap and lacks a p-type capability (thereby eliminating complementary devices and homo-junction bipolar transistors and various other minority carrier devices altogether).

When second- and third-wave electronic devices were introduced (III-V and III-N compound semiconductors), similar arguments took place in 1970's and 1990's. Despite the fact that none of the semiconductor technologies developed during this time period ever completely displaced Si as the most significant technology base, these new devices produced a range of new devices for high frequency, power, and high temperature applications. The military applications, in particular, have benefited significantly from the availability of these new technologies without having to give up Si-based electronics. Ga_2O_3 will probably have similar impact on military and specialized commercial applications side by side with the other existing technologies.

3. CRYSTAL STRUCTURE

Ga_2O_3 is a member of transparent oxide semiconductors (TOS) that include the oxides of In, Zn, Sn, Cd, Cu, Mg metals or the oxides of a combination of metals from this group. It is most related to In_2O_3 and ZnO within the metal-oxide group of $(In,Ga)_2O_3(ZnO)_n$ [50], the most common form of which is $InGaZnO_4$ (or IGZO). TOS materials are used in applications including solar cells, detectors, transistors and transparent conductive films. Although it is possible use single crystal TOS films, in most electronic applications [89], they are almost always amorphous. This is for better compatibility with flexible and non-conformal surfaces [49, 51, 90-94]. Ga_2O_3 is not one of those TOS materials that can be used in an amorphous or polycrystalline state for electronics, as will be discussed later. Only the *single crystal* form of Ga_2O_3 is of interest for these applications.

There appears to be 5 different crystal structures possible for Ga_2O_3 [36, 95], which are designated as $\alpha,\beta,\gamma,\delta$, and ε. The most common and the most stable crystal is β-Ga_2O_3, which is the main subject of this note and we will examine various aspects of this crystal below. The least well known of the 5 polymorphs is the ε- Ga_2O_3. The others have been studied for various applications, but no important electrical application has been identified, except α- Ga_2O_3, which may have even wider bandgap than β-Ga_2O_3. Before we concentrate on the β-Ga_2O_3 for the remainder of this note, we examine the other Ga_2O_3 crystals for completeness.

At first glance, we would expect the crystal structure of Ga_2O_3 to be the same as Al_2O_3 [96] because of the similarity between the aluminum and gallium ions. Indeed, α-Ga_2O_3 has a typical corundum structure, which is the natural state of Al_2O_3 ("corundum" is a Tamir word meaning ruby, the crystalline form of aluminum oxide). The α-Ga_2O_3 also has a corundum structure but it is not stable like its Al_2O_3 counterpart. On the other hand, β-Ga_2O_3 is a monoclinic crystal and stable, but β-Al_2O_3 is a solid ionic conductor with a different crystal structure. Only θ-Al_2O_3 resembles β-Ga_2O_3 [97]. Roy has indicated in 1952 that the other metastable forms of Ga_2O_3 can be all converted to β-Ga_2O_3 by various heat treatments [36], as shown in Figure 8.
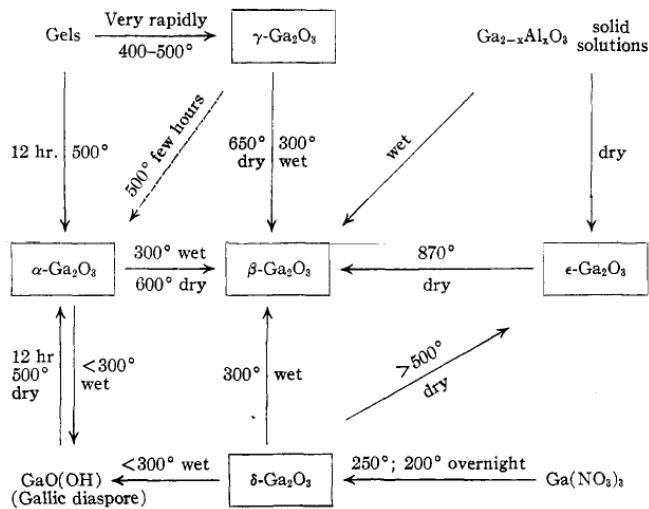
Figure 8: Transformation relationships among various forms of gallia and its hydrates[36].

Figure 5 lists the crystal structures of the 5 Ga_2O_3 polymorphs. We will discuss each polymorph separately in the sections that follow. However, it may be instructive first to remind ourselves the basic crystal types and how they relate to each other.

Table 5: Crystal structures of various Ga_2O_3 polymorphs

Polymorph	Crystal Structure
α-G_a2O_3	Corundum
β-G_a2O_3	Monoclinic
γ-G_a2O_3	Defective spinel
δ-G_a2O_3	Bixbyite
ε-G_a2O_3	Unclear (maybe similar to κ-Al_2O_3)

A. Crystal Systems

Crystalline solids contain repeating units of matter such as atoms, molecules or ions in 3-D. There are 7 basic crystal systems based on unique unit cells. Each unit cell is defined by cell parameters that describe edge lengths and the angles between them, as shown in the drawing of a basic unit cell in Figure 9. The edge lengths are a, b, and c, whereas the angles between planes are designated as α, β, and γ.
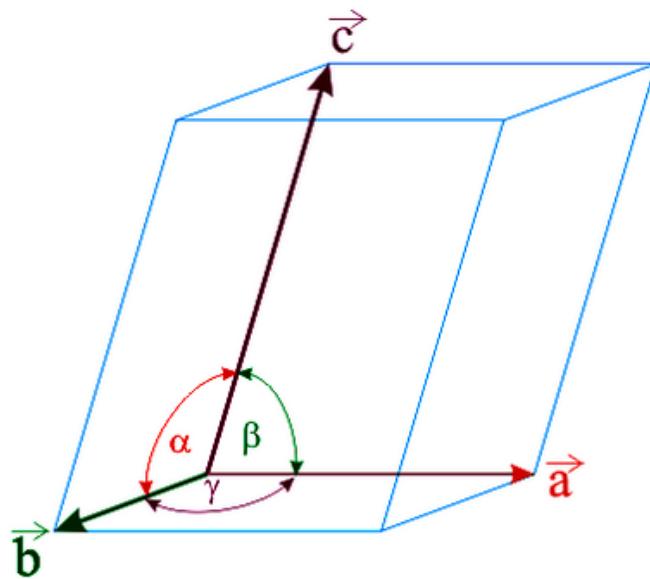
Figure 9: Basic unit cell of crystals.

Based on this definition of basic crystal unit cells, the 7 types of crystals can be identified as shown in Table 6.

Table 6: The basic crystal systems

Crystal System	Axial Length	Axial Angles
Cubic	$a = b = c$	$\alpha = \beta = \gamma = 90°$
Tetragonal	$a = b \neq c$	$\alpha = \beta = \gamma = 90°$
Monoclinic	$a \neq b \neq c$	$\alpha = \beta = 90° \neq \gamma$
Orthorhombic	$a \neq b \neq c$	$\alpha = \beta = \gamma = 90°$
Rhombohedral	$a = b = c$	$\alpha = \beta = \gamma < 120°, \neq 90°$
Hexagonal	$a = b \neq c$	$\alpha = \beta = 90°, \gamma = 120°$
Triclinic	$a \neq b \neq c$	$\alpha \neq \beta \neq \gamma \neq 90°$

In addition to grouping the crystal according to axial dimensions, they are also grouped according to how the edge of the unit cell connects equivalent points. These are called the Bravais unit cells. The 14 types of Bravais unit cells are shown in Figure 10. Based on these basic definitions, we can now examine different Ga_2O_3 polymorphs.
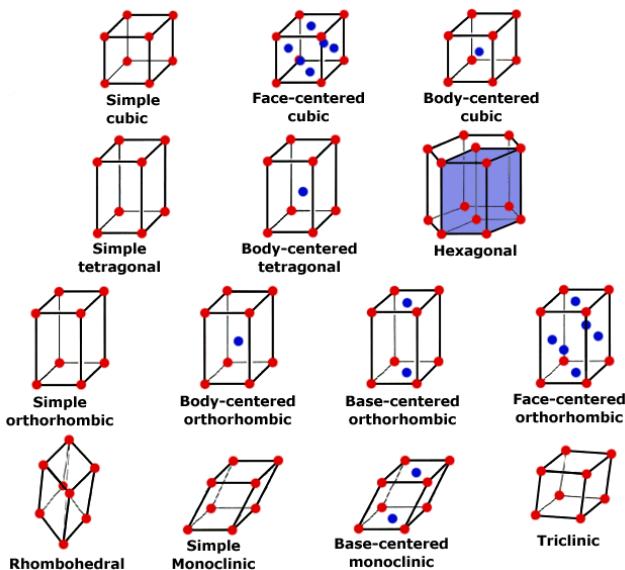
Figure 10: the 14 types of Bravais crystal unit cells.

B. α-Ga_2O_3

α-Ga_2O_3 has a corundum structure and is commonly known to be a hexagonal type crystal (although sometimes it is called a rhombohedral crystal [98]). There are 6 Ga_2O_3 formula units in each crystallographic cell with 2 independent lattice parameters "a" and "c" with values of 4.98Å and 13.43Å,

respectively [95, 99-101]. The oxygen ions are approximately hexagonal close packed and the Ga ions occupy two-thirds of the octahedral sites. A representation of α-Ga$_2$O$_3$ unit cell is shown in Figure 11.

One of the interesting properties of α-Ga$_2$O$_3$ is that its bandgap is measured to be even higher than other forms of Ga$_2$O$_3$. Several values were calculated [99, 100] or measured [102], all giving values around 5eV. Sn-doped thin films of α-Ga$_2$O$_3$ was shown to have even larger bandgap of 5.16eV [98]. As discussed above, wide bandgap properties of Ga$_2$O$_3$ is one of its most important feature and such large bandgap values should draw attention to this polymorph. Unfortunately, α-Ga$_2$O$_3$ is meta-stable and converts to more stable β-Ga$_2$O$_3$ at high temperatures, so that it is not possible to prepare bulk crystals of α-Ga$_2$O$_3$. However, several researchers have successfully prepared epitaxial layers of α-Ga$_2$O$_3$ on α-Al$_2$O$_3$ (sapphire). Because the lattice mismatch between these corundum type crystals is only about 4% (small value but still very large for good quality crystal growth), attempts were made to prepare such layers by ultrasonic mist chemical vapor deposition (CVD) [74, 103] and halide vapor epitaxy techniques [104]. Although the carrier concentrations were respectable (1e20 cm^{-3}) when doped with Sn, the electron mobility values were extremely poor (0.23 cm^{2}V^{-1}s^{-1}). When used for the fabrication of a MESFET, similarly poor mobility values were obtained as we will examine in detail below [103].
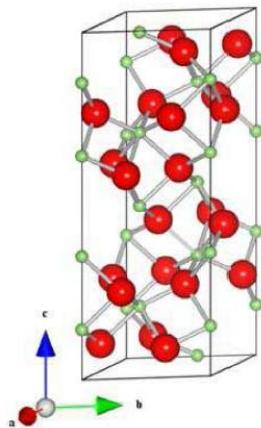
Figure 11: The crystal structure of α-Ga$_2$O$_3$ [98].

The large measured optical bandgap value (E$_G$= 5.16eV) is, at first glance, an important improvement. Based on the discussions above regarding E$_C$ vs. E$_G$ (e.g. see Figure 6 and Figure 7), the electrical breakdown field for this material should be higher than β-Ga$_2$O$_3$ and close to 9MV/cm. However, the results obtained with the first transistors fabricated with this material did not exhibit high breakdown voltages. Dang *et. al.* measured a maximum breakdown voltage of only 48V for a 5μm gate device, with approximately 5μm gate drain spacing [103]. This falls remarkably short of the expected breakdown voltage by a factor of 10. Schottky Barrier Diodes (SBD) made with mist-CVD grown α-Ga$_2$O$_3$ layers showed high breakdown strength for thinner layers (0.43μm) but not for thicker layers (2.58μm) [105]. There are 2 possibilities: a) the semiconductor material contains too many crystal defects due to lattice mismatch between α-Ga$_2$O$_3$ and α-Al$_2$O$_3$. These defective sites may have lower field breakdown strengths, b) the empirical relationship between E$_c$ and E$_G$ may not be valid at such ultra-high field regions. Most probably the reason is the first option, which points out the importance of the crystal

quality. Similar breakdown voltage reductions may be expected from β-Ga₂O₃ crystal depending on defect count. This, as is the case with all other single crystal semiconductor technologies, highlights the importance of the crystal quality for this technology also.

Because of the larger bandgap of α-Ga₂O₃ compared to β-Ga₂O₃, some researchers investigated the use of the heterojunction of the two crystal types for photocatalytic applications. Theoretically, these sister crystals make a Type II heterojunction with the α-Ga₂O₃ conduction band minima (CBM) and the valance band maxima (VBM) 0.07eV and 0.35eV higher [99]. It was concluded that the larger bandgap α-Ga₂O₃ is tantalizingly close to the energy values needed for water splitting process.

C. β-Ga₂O₃

This phase of Ga₂O₃ is main subject of this note and more details of its properties will be discussed in the sections that follow. Here we will only look at the crystal structure.

β-Ga₂O₃ has a base-centric monoclinic crystal structure, as shown in Figure 12, with a, b, c, and β values of 1.22nm, 0.3nm, 0.52nm and 104-degrees, respectively [106, 107]. There are 4 Ga₂O₃ formula units in each crystallographic cell, but unlike the case with α-Ga₂O₃ where Ga ions are only coordinated in octahedral geometry, there are 2 kinds of coordination of metal ions in β-Ga₂O₃, i.e. tetrahedral and octahedral. The coordination of Ga ions in the lattice has important impact on physical and electrical parameters as will be discussed throughout this note. Figure 12 indicates the location of both tetrahedral coordination of Ga(1) and octahedral coordination of Ga(2) ions in the unit cell. For clarity, these two coordination features are reproduced in Figure 13. Ga(1) is surrounded by 4 oxygen atoms, whereas Ga(2) is surrounded by 6 oxygen atoms.

The Ga-O and O-O interionic distances are different in these 2 coordination systems as listed in Table 7. Because of the reduced coordination of half the metal ions, the density of β-Ga₂O₃ is lower than the more compact α-Ga₂O₃. The closest approach between two Ga ions is 3.04Å, which is also considerable longer than α-Ga₂O₃ [101, 107].
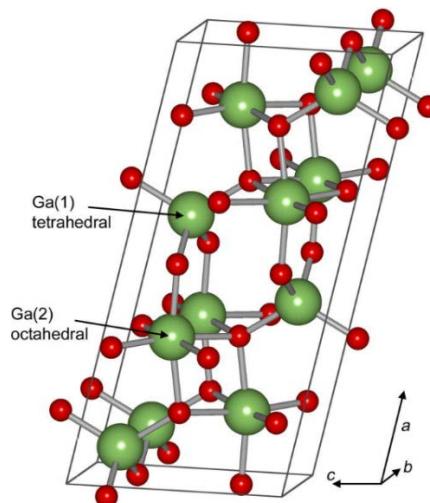
Figure 12: The crystal structure of β-Ga₂O₃ [106, 107].
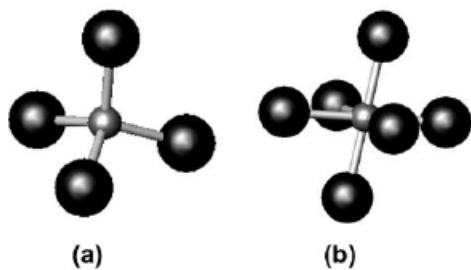
Figure 13: The coordination types for the Ga ion in β-Ga₂O₃. a) Tetrahedral coordination of Ga(1), and octahedral coordination of Ga(2).

Table 7: Average distances between ions in β-Ga₂O₃ [106, 107].

Coordination	Ga - O		O - O	
	Average (Å)	Range (Å)	Average (Å)	Range (Å)
Octahedral	2.00	1.95 - 2.08	2.84	2.67 – 2.90
Tetrahedral	1.83	1.80 – 1.85	3.02	2.93 – 3.13

D. γ-Ga₂O₃

Much less is known about γ-Ga₂O₃ structure except defect spinel-type structure of γ- Ga₂O₃ is similar to that of γ and η-Al₂O₃ [108]. The ideal spinel structure AB₂O₄ is represented by a 2 × 2 × 2 array of an fcc packed oxygen sub-cell, with the A and B cations occupying the 8a (of the 64 available) tetrahedrally and the 16d (of 32) octahedrally coordinated interstitial sites [96]. This is shown schematically in Figure 14. White balls in this figure represent oxygen ions. Larger dark balls represent octahedrally coordinated sites, and the smaller balls represent tetrahedrally coordinated positions. Presence of empty interstitial positions also can be observed. In the case of γ- Ga₂O₃, the unit cell edge length is 0.835nm [36] or 0.822nm [109].
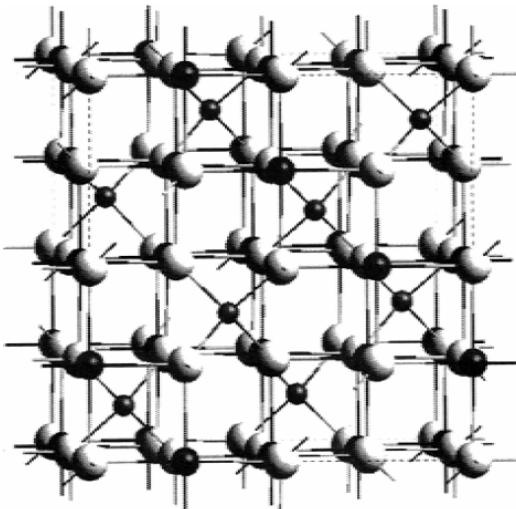
Figure 14: Three-dimensional view of the spinel structure [96].

First principles calculations were made on primitive cells containing 6 tetrahedral cationic sites, 12 octahedral cationic sites, and 24 oxygen sites by introducing Ga-ion defects and found that 14 inequivalent configurations are possible [95]. No clear preference of defect location (tetrahedral or octahedral sites) could be established.

Recently, γ- Ga_2O_3 epitaxial layers were grown on both c-cut sapphire and spinel substrates ($MgAl_2O_4$) using pulsed laser deposition technique [110-112]. It was found that the undoped crystals were defective whereas single domain crystal growth was possible by doping with Mn and by optimizing the growth conditions. Figure 15 shows a TEM image of a high quality Mn-doped γ- Ga_2O_3 layer on spinel substrate [112].
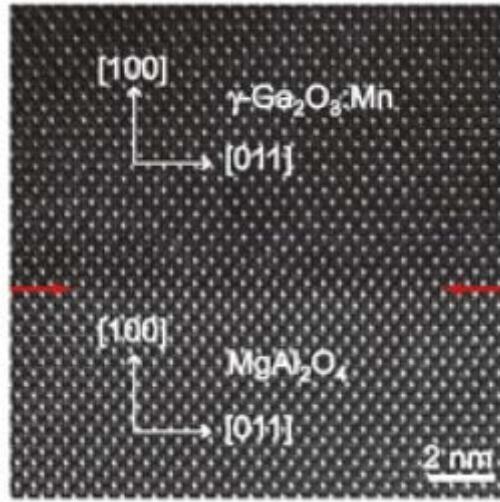
Figure 15: High resolution TEM image of Mn-doped γ-Ga_2O_3 layer on spinel $MgAl_2O_4$ substrate [112].

E. δ-Ga₂O₃

From the early studies of Roy *et. al.* δ- Ga$_2$O$_3$ is known as a body-centered cubic crystal with a unit edge length of a = 10.0 *Å* [36]. More recently this value was updated as 9.402 *Å* [95].The crystal structure is isomorphous with other bixbyite crystals such as In2O3, Mn$_2$O$_3$ and Tl$_2$O$_3$.

F. ε-Ga₂O₃

This is the most elusive polymorph Ga$_2$O$_3$, whose crystal structure is not well understood. Roy *et al* reported that a new phase of Ga$_2$O$_3$ can be obtained by heating δ-Ga$_2$O$_3$ above 500°C, which they designated as ε-Ga$_2$O$_3$ [36]. Similarly, Sn-doped, highly conductive Ga$_2$O$_3$ films deposited by PLD at temperatures above 475°C were found to have crystal structures similar to κ-Al$_2$O$_3$, and therefore suspected to be ε-Ga$_2$O$_3$ [113]. If that is the case, the crystal structure of ε-Ga$_2$O$_3$ would be orthorhombic. Later, Matsuzaki [114] confirmed that the PLD-grown structures are neither α-Ga$_2$O$_3$ nor β- Ga$_2$O$_3$, and most probably ε-Ga$_2$O$_3$ with orthorhombic lattice dimensions of a=0.504, b=0.873, and c=0.926 nm, which are close to the lattice parameters of a= 0.484nm, b= 0.833nm and c= 0.895nm of k- Al$_2$O$_3$ [115]. Using these films, this research group also fabricated transistors with modest performance.

First principles study undertaken by Yoshioka et al using κ-Al$_2$O$_3$ as the prototype concludes that the crystal structure is orthorhombic with the structural parameters shown in Table 8 [95]. The lattice parameters shown in this table are slightly smaller than the measured values [116].

Table 8: Structural parameters of ε- Ga₂O₃ [95].

ε-Ga₂O₃		
Lattice Parameter (nm)	*a*	b	c
	0.512	0.879	0.941
Volume (nm³)	0.423		
Z	8		
Crystal System	Orthorhombic		
Density (g.cm⁻³)	*5.88*		

4. ELECTRONIC STRUCTURE

As a member of the $(In,Ga)_2O_3(ZnO)_n$ family of TOS, the electronic structure of Ga_2O_3 can be first examined by the general characteristics of this family group [50]. This is a complex structure and its electrical characteristics strongly depend on the composition. In general, it was shown that the film conductivities trend lower as the Zn and Ga components decrease [117, 118]. This was thought to be due to the increase in the Indium content of the films which correlate with the increased density of octahedrally coordinated cations. This thinking was supported by the belief also that in transparent oxide films, the electrical conduction is mostly due to octahedral oxygen coordination [119-123] and the cations with tetrahedral coordination (i.e. Zn and Ga) do not contribute to conduction [124, 125]. However, this is not the current hypothesis since it was shown that the conduction band is formed from the *s*-states of all cations in this compound family and the *p*-states of their oxygen neighbors [50, 126].

Medvedeva *et al* make a general observation that the oxides of post-transition metals with $(n-1)d^{10}ns^2$ electronic configuration share similar electronic properties [50]. These oxides include In_2O_3, Ga_2O_3, ZnO and CdO, which all have tetrahedral and/or octahedral coordination of metal ions. The electronic band structure of these oxides are very similar and originate from the same strong interaction between the oxygen 2p and the metal ns orbitals. The Ms-Op interactions produce a gap between the valence and the conduction bands (as shown in Figure 16). The bandgap is direct in ZnO, but in indirect in In_2O_3 and Ga_2O_3.
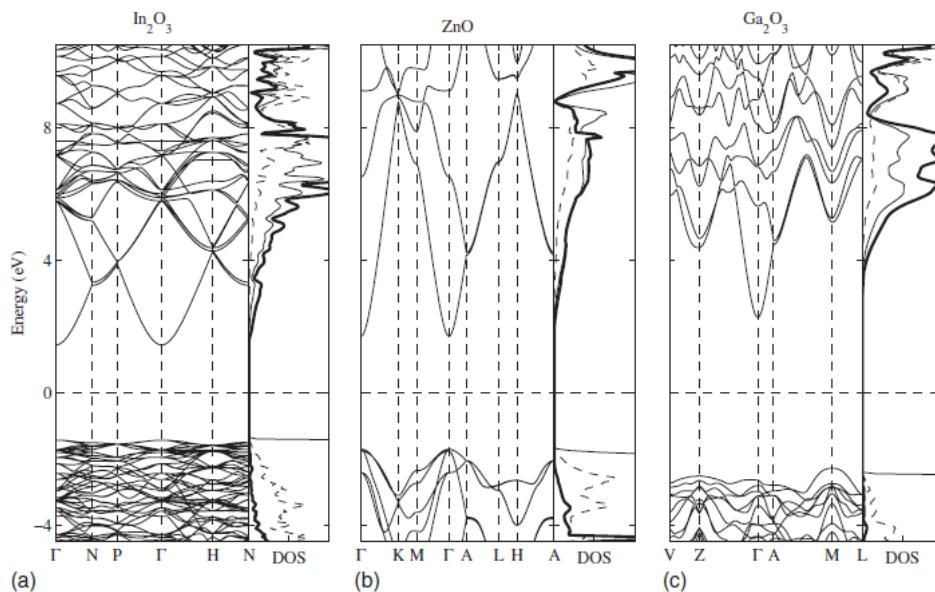
Figure 16: Electronic band structure and DOS of undoped stoichiometric a) bixbyite In2O3, b) wurtzite ZnO, c) monoclinic Ga2O3 [50].

The Ms-Op overlap also determines the energy dispersion of the conduction band which influences the effective electron mass and mobility. It was shown that the electron mass has a strong dependence on oxygen coordination with different crystals of the same oxide. This effect is more significant for ZnO, for example, where octahedral coordination on rock salt produces smaller effective mass than the tetrahedrally coordinated wurtzite crystal ($0.28m_o$ vs $0.35m_o$) [126]. In the case of Ga_2O_3, the difference

in effective mass is not expected to be large between α- Ga$_2$O$_3$ (corundum) and β- Ga$_2$O$_3$ (monoclinic) partly because β-Ga$_2$O$_3$ contains both tetrahedral and octahedral coordination of cations (i.e. mixed). However, the results reported by He *et al* (0.276m$_o$ and 0.342m$_o$) [100] are very similar to the case with ZnO and point to *significant differences between the phases*.

Figure 17 shows the band structures of β-Ga$_2$O$_3$ and α-Ga$_2$O$_3$. In general, the band structures of these two phases are very similar. For β-Ga$_2$O$_3$, the valance band maximum (VBM) is at M. The valance band energy level at Γ, where CBM occurs, is 0.03eV lower. Therefore, the direct bandgap is 4.69eV vs. a value of 4.66eV for indirect in this case. Similarly, α-Ga$_2$O$_3$ has a VBM at L or F **k** points and CBM is at Γ. The difference in the bandgap values between the direct and indirect is 0.05eV with a direct bandgap of 5.08eV. As mentioned before, the bandgap of α- Ga$_2$O$_3$ is larger than β- Ga$_2$O$_3$. The valance band is practically flat in both phases indicating low mobility for holes.
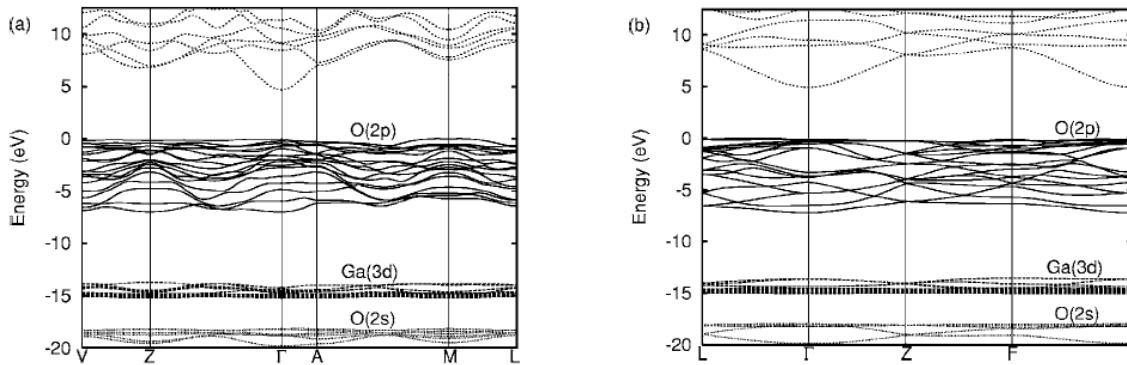
Figure 17: Band structures of β-Ga$_2$O$_3$ (a) and α-Ga$_2$O$_3$ (b) [100].

A. Doping

As we will see in the sections that follow, Ga$_2$O$_3$ layers can show significant n-type conductivity even without intentional doping. Based on the observations with other similar metal-oxide semiconductors, this conductivity was thought to be due to oxygen vacancies, V$_o$ [50]. This theory has been challenged by Varley *et al*, who using the density functional theory (DFT) showed that V$_o$ creates deep donors with ionization energies of more than 1 eV and cannot be responsible for the observed n-type conductivity [127]. It was proposed, instead, that several impurities including hydrogen, can be shallow donors. Hydrogen can occupy either interstitial (H$_i$) or substitutional sites (H$_O$) and in both configurations can act as shallow donor. In addition, Si, Ge, and Sn substituting on the Ga site, and F and Cl on the O site are shallow donors and can contribute to conductivity. Si and Ge prefer the tetrahedral coordination of the Ga(I) site, while Sn prefers the octahedral coordination of the Ga(II) site. F and Cl both prefer the threefold coordination of the O(I) site [127].

As easy as it is to achieve n-type conductivity with many metal-oxide wide bandgap semiconductors, such as Ga$_2$O$_3$, p-type conductivity is highly elusive. Despite some reports of achieving p-type conductivity (albeit at a very low mobility) using Zn as the dopant [128], it is argued that p-type doping is not favorable for many metal-oxides due to the nature of their valance band. In wide-band-gap oxides including ZnO, MgO, In$_2$O$_3$, Ga$_2$O$_3$, Al$_2$O$_3$, SnO$_2$, SiO$_2$, and TiO$_2$, conduction band states originate from

metal atoms, whereas the valence-band states are derived mainly from the O 2p orbitals and are characterized by small dispersion, large effective masses, and high density of states [129]. Holes tend to form localized small polarons i.e., localized holes trapped by local lattice distortions. These self-trapped holes (STHs) are energetically more favorable than delocalized, free holes in the valence band. Others argue that p-type doping may indeed be possible by substituting Ga atoms with Zn [130] or by N substituting O(1) atom [131] or both N-Zn [132]. There are some examples of the growth of Ga_2O_3 nanowires with p-type conductivity using N- or Zn-doping [128, 133].

If p-type conductivity in Ga_2O_3 is not possible, as it seems, this would be a major barrier for the Ga_2O_3 technology because without p-type conductivity p-n junctions will not be possible. P-n junctions are one of the fundamental building blocks of electronic devices. Without p-type conductivity all electronic devices become majority-carrier type leading to unipolar devices only. Minority-carrier devices are an important part of power electronics as in the Si and SiC technologies. Although high breakdown voltage devices can be fabricated using only majority carrier semiconductors, low on-resistance is difficult to achieve without minority carriers.

5. Electrical, Optical, Thermal Anisotropy

The electron effective mass values, although show phase dependence, as mentioned above, are nearly isotropic [134]. Holes, on the other hand, are significantly more anisotropic, as indicated in Table 9 Note the vert high effective mass of holes).

Table 9: Effective mass of CBM at Γ and VBM on the E line [134].

	CBM at Γ	VBM on E
m_{xx}	0.2315 ± 0.0003	6.14 ± 0.70
m_{yy}	0.2418 ± 0.0001	2.90 ± 0.15
m_{zz}	0.2270 ± 0.0001	4.19 ± 0.46

The calculated electron velocity in β-Ga_2O_3 seems to be significantly lower than that in α-Ga_2O_3 (0.96e5 vs. 2.35e5 m/s). This may be due to the highly anisotropic electronic nature of β-Ga_2O_3 when mobile charges are solely due to oxygen deficiencies [50]. As mentioned before, the conduction band of Ga_2O_3 is formed mostly by the *s* orbitals of the metal cations and the *p* orbitals of the oxygen atoms. Assuming that the material is highly doped (say by oxygen vacancy), these orbitals are responsible for charge transport. Asymmetry in conduction is dependent on the hybridization of these orbitals. Because the octahedral coordination produces larger overlap of s-p orbitals due to better symmetry, the energy dispersion of the conduction band is larger. This can be seen in Figure 17 where highly symmetric a-Ga_2O_3 with octahedral coordination have wider conduction bands. In the case of β-Ga_2O_3, the contribution from Ga p states to the bottom of the conduction band become significant. Unfortunately, due to weak hybridization of these highly anisotropic Ga p orbitals with the p orbitals of the oxygen atoms lead to localization of charges. As a result, the electron velocity and hence the conductivity is reduced in β-Ga_2O_3 compared to α-Ga_2O_3 [50].

The anisotropy of electrical and optical properties of β-Ga_2O_3 was demonstrated experimentally by Ueda *et al* using degenerately doped crystals grown by floating zone method [13]. The room temperature Hall mobility measured along the b and c axis of the crystal were 46 and 2.6 $cm^2V^{-1}s^{-1}$, respectively. Similarly, the conductivity along the same axes (also at room temperature) were 38 and 2.2 $ohm^{-1}cm^{-1}$, respectively. Based on the measured values, the electron mass values along the b and c axes were estimated as $0.44m_o$ and $1.24m_o$, respectively. The difference in electrical properties along these orthogonal directions is highly significant (more than an order of magnitude). These results point to higher curvature of the bottom of the conduction band along the b-axis, which is thought to be due to substantial interaction among Ga 4s orbitals in the octahedral sites [13]. This conclusion is consistent with the analysis of Medvedeva discussed above [50, 126].

The optical properties of β-Ga_2O_3 also show significant anisotropy as shown in Figure 18. Here φ is the angle between the c axis and the electric field vector E of the incident light. The fundamental absorption edges for **E//b** and **E//c** are 253 and 270 nm, respectively [13]. These values correspond to optical

bandgap of 4.79 and 4.52 eV for light polarized **E//b** and **E//c**, respectively. A summary of anisotropic electrical and optical parameters of β- Ga$_2$O$_3$ are shown in Table 10.
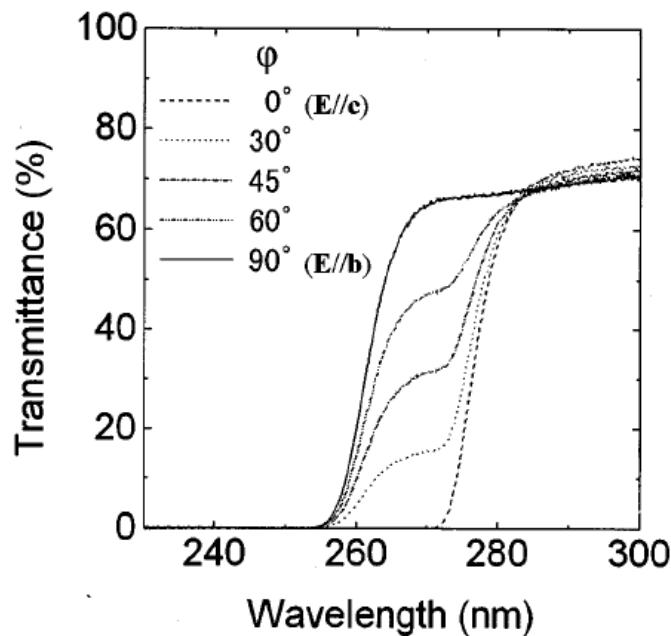
Figure 18: The optical transmission spectra of an insulating β-Ga$_2$O$_3$ single crystal for light polarized in several orientations [13].

Table 10: Summary of the orientation dependent electrical and optical parameters of β-Ga$_2$O$_3$.

Orientation	Mobility (cm^{-2}V^{-1}s^{-1})	Conductance (ohm^{-1}cm^{-1})	Electron Mass (m$_o$)	Absorption Edge (nm)	Optical Bandgap (eV)
E//b	46	38	0.44	253	4.79
E//c	2.6	2.2	1.24	270	4.52

The thermal conductivity of β- Ga$_2$O$_3$ is also highly anisotropic. At room temperature, the [010] direction has the highest thermal conductivity of 27.0 ±2.0 W/mK, while that along the [100] direction has the lowest value of 10.9 ±1.0 W/mK [72]. First-principals calculations confirmed that anisotropy in thermal conductivity is consistent with different speed of sound along each crystal direction. The calculated room temperature values 16.06 W/mK along the [100] direction, 21.54 W/mK along [010] direction, and 21.15 W/mK along the [001] direction [135]. Similar values were obtained for Mg- and Si-doped crystals [136, 137]. The temperature and orientation dependence of thermal conductivity is shown in Figure 19.
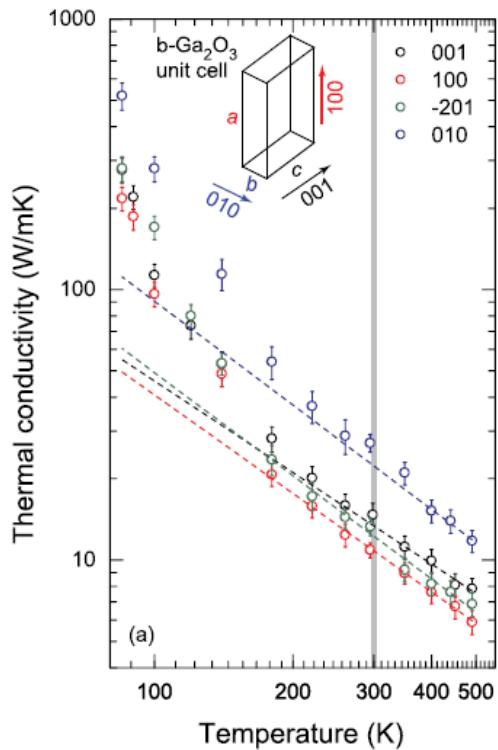
Figure 19: Temperature-dependent thermal conductivity of β-Ga₂O₃ measured along different crystal directions [72].

A fit to the experimental data can be made using the expression $\kappa(T) = AT^{-m}$, where A and m are fit parameters [72, 135]. Best fit is obtained separating the data into temperature zones of 80-200K and 200-495K as using the parameter values shown in Table 11.

Table 11: Fitting parameters for thermal conductivity of β-Ga₂O₃ for 2 temperature zones [72].

Crystallographic Orientation	A_1	m_1	A_2	m_2
[001]	1.06E10	3.93	8.14E3	1.12
[100]	1.85E9	3.59	1.06E4	1.21
[010]	7.99E8	3.21	3.28E4	1.27
[-201]	8.26E8	3.35	1.69E4	1.28

6. BULK CRYSTAL GROWTH

One of reasons for considering Ga_2O_3 for high voltage applications is the proven fact that high quality substrates can be prepared by conventional crystal growth techniques. Large area wafers cut from crystal boules are used to fabricate optical and electronic devices. Most electronic devices are "lateral devices" meaning that they are fabricated on the top surface of the wafer. Lateral devices make use of epitaxially grown thin layers on substrates. The quality of such layers depend strongly on the quality of the substrate. In the case of Ga_2O_3 with its wide bandgap properties, many future devices will be "vertical devices" to support extremely large voltages and conduct very high current densities. Such devices will likely use the whole substrate volume. In optical applications such as UV-transparent windows, thick wafers may also be needed.

The availability of high quality and large diameter substrates accelerates the development of electronic technologies based on the new semiconductor. Historically, after demonstrating the feasibility of interesting device characteristics on small wafers (typically a few sq. mm), large R&D efforts are required to increase the wafer size and quality (e.g. GaAs technology [10]). When suitable substrates are not available, the development of the even most promising new technologies can be stunted (e.g. graphene technology for electronics [63]).

As we discussed above, Ga_2O_3 crystals come in a variety of polymorphs, but the most stable one is β-Ga_2O_3. This crystal would not necessarily be everyone's first choice among others based on material properties. For example, α- Ga_2O_3 has a wider bandgap and may support higher electrical fields [98-100, 102]. As mentioned above, β- Ga_2O_3 has strong electrical, optical and thermal anisotropy due to its crystal structure. But, it is a stable crystal and can be prepared using traditional melt-grown crystal growth techniques. In this section we will survey the published data on bulk crystal growth of Ga_2O_3.

The following are the most common types of crystal growth for Ga_2O_3. We will review some of these methods in more detail below.

- Verneuil Method
- Floating Zone (FZ) Method
- Flux Method
- Czochralski Method
- Edge defined film-fed (EFG) Method
- Chemical Vapor Deposition

A. Verneuil Method

This is probably the earliest Ga_2O_3 crystal growth method, which was originally developed for growing synthetic ruby at the turn of the 20th Century and later adapted for the growth of single crystal metal oxides [138-140]. The Verneuil method, which is also called the "flame fusion method", involves melting a finely powdered substance using an oxyhydrogen flame, and crystallizing the melted droplets into a boule, as shown schematically in Figure 20. The ceramic material is fed into the reaction area in fine

powder form where it melts on the top surface of the seed crystal. By controlling the seed retraction rate and local temperature, relatively large crystals of Al_2O_3 (ruby) were grown with this technique [140].
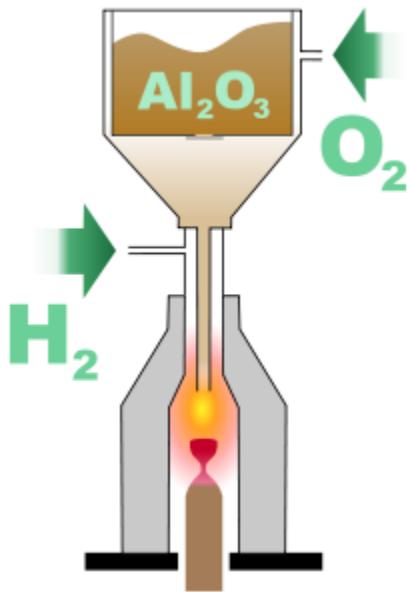
Figure 20: A schematic drawing of the Verneuil flame-fusion process apparatus [140].

This technique was used by Chase [141] Lorenz [11], Harwig [142, 143] and Binet [144] to prepare the first Ga_2O_3 single crystal boules. Chase originally used fine powders of ε- Ga_2O_3 but found it to be unstable. Using β- Ga_2O_3 powder, undoped and doped single crystals were prepared measuring 3/8-inch in diameter and 1-inch in length. The growth direction was parallel to the *b* crystallographic direction. The optical characterization of these early crystals was reported by Tippins (see Figure 2) [19].

Lorenz also used this method to prepare β-Ga_2O_3 crystals that were insulating when grown in an oxidizing atmosphere and had Hall mobility of about 100 cm^2/Vs. Crystals grown in reducing atmosphere conditions had a carrier concentration of about 1e18 cm^{-3} due to oxygen deficiencies.

The crystals grown by Harwig using essentially the same method [143]. Crystals were doped using Mg and Zr, which were introduced in the form of MgO and ZrO_2 into the power stream. They report that the undoped crystals were clear, Mg-doped crystals were light blue and the Zr-doped ones were blue. In a series of conductivity measuremets over a wide temperature range, it was concluded that nearly 40% of conductivity is due to ionic conduction, which may be enabled by cation vacancies. Mg-doped crystals had lower conductivity.

B. Floating Zone (FZ) Method

This method of preparing single crystals was favored in the early years of electronic technology for the production of oxygen-free Si crystals [145]. The method relies on a traveling melt zone for converting polycrystalline material into single crystal, as shown in Figure 21. Initially seed crystals were not used and the orientation of crystals were not well controlled [146]. This method is now highly refined and

good control in doping levels and crystal quality can be achieved. The initial limitation of diameter size has also been addressed using narrow growth necks.
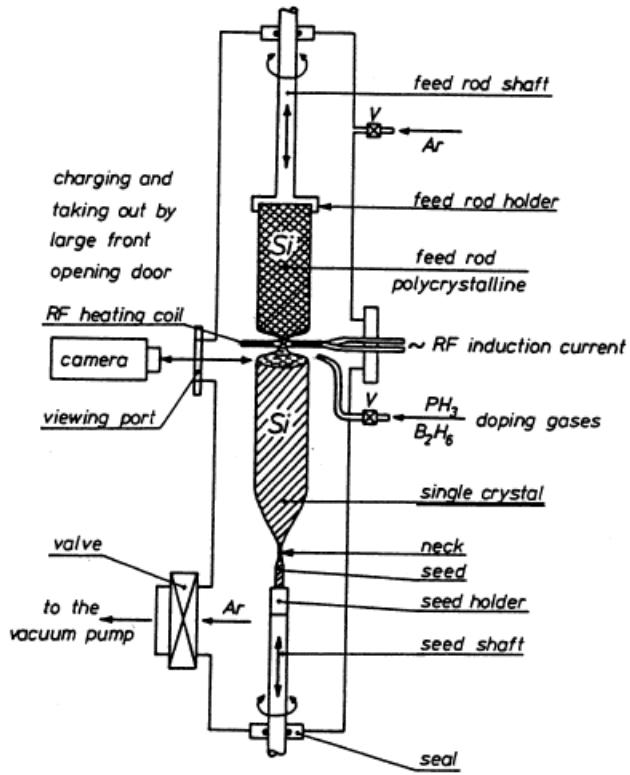
Figure 21: Schematic of a modern FZ-Si single-crystal puller for the growth of large crystals [145].

This method was used by several researchers to grow β-Ga$_2$O$_3$ crystals with different dopants. A wide range of conductivity values (< 1e9 to 38 Ω^{-1} cm^{-1}) could be obtained by changing the growth atmosphere for undoped crystals [14]. When Sn used as substitutional dopant, crystals grown even with high oxygen flow rates were highly conductive (0.96 Ω^{-1} cm^{-1}). The crystal size was small in this example measuring only 5mm in diameter and 60-70mm in length. Similar conductivity values were obtained by others when Sn is used as the dopant with this growth method [147]. The electron mobility was 80.4 cm^2/Vs for as-grown samples but increased to 82.9 cm^2/Vs after annealing at 1100°C for 3hr [67].

Crystal diameters of about 1-inch were grown by Villora *et al* by carefully selecting the growth axis [148]. It was found that stable growth proceeds only along the three crystallographic directions, the <100>, <010> and <001>. Figure 22 shows the crystals grown in these growth axes. The electrical characteristics of the samples from these crystals, as shown in Table 12, exhibit some anisotropy but in general are similar to each other. Higher Hall mobility was obtained (μ_H = 172 cm^2/Vs) for unintentionally Si-doped crystals also grown by this method [21]. Zhang et al also found that the preferred crystal growth axis is <100> and crystals with 6mm in diameter and 20mm in length can be grown with this method [15]. Attempts were made to dope Ga$_2$O$_3$ with Ti and Ge using this growth method, but the results were not promising since both Ti and Ge produced deep donor (or acceptor) level that contributed very little to conduction [149].
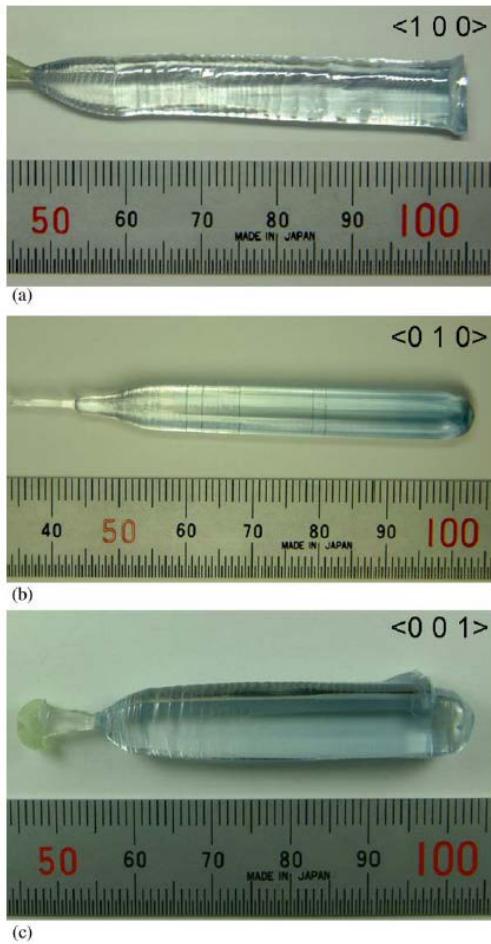
Figure 22: As-grown crystals along the crystallographic axis (a) <100>, (b) <010> and (c) <001> [148].

Table 12: Electrical properties measured by the bar method on three different oriented samples [148].

Direction	Resistivity (Ω.cm)	Mobility (cm²/Vs)	Carrier Conc. (cm⁻³)
<100>	0.11	83	7E17
<010>	0.19	78	4E17
<001>	0.08	98	9E17

C. Czochralski Method (CZ)

This is a mainstream crystal growth method applied to the growth of many semiconductors. The method is now well refined for the growth of very large diameter single crystal boules. Its first use for semiconductors is attributed to Teal [150] for the growth of Ge crystals, but the technique itself was known long before that date. Some historians regard the Czochralski Method to be a part of the family

of growth techniques that are the "inverse" of the Verneuil technique discussed above. For example, Scheel [151] connects these growth method as shown in Figure 23. To make this generalization, the Verneuil technique is credited for the invention of the nucleation, growth rate, and diameter control so that the growth techniques that followed, including Bridgman Method [152], vertical-gradient-freeze growth method of Ramsperger and Malvin, Czochralski method are regarded to be of the same technology family [151].
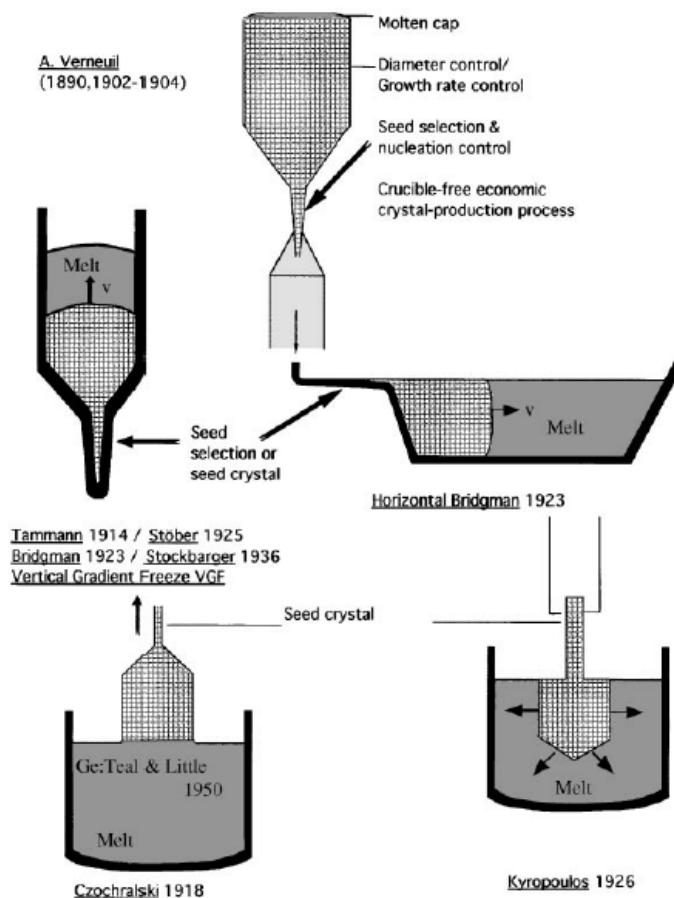
Figure 23: Modification of Verneuil's principles of nucleation control and increased crystal diameters in other crystal growth techniques [151].

The most famous of these melt-grown methods is the Czochralski Method, which has 2 critical dates attached to it i.e. 1918 and 1950. The work of Czochralski essentially involved the measurement of the maximum crystallization rates of metals [153]. Metal wires of about 0.8mm diameter were pulled from melts with increasing velocity. In the process, he discovered that some parts of the pulled wires were single crystal and that the crystal content can be improved by using single crystal seeds. This method did not find much practical use until 1950 when Teal and Little modified it to grow Ge crystals [154]. It was later refined by Ernest [155]. This method is now known as the Czochralski Method. However, several historians dispute this attribution and point out that crystal pulling from melt were already known due to the work of Gernez who also made the initial crystallization velocities [156]. It was pointed out that Czochralski's work follows Tammann's work on glass crystallization [157] and the title of his paper was "

Ein neues Verfahren zur Messung der Kristallisations geschwindigkeit der Metalle" (a new method for measurement of the crystallization velocity of metals) and had nothing to do with actual crystal preparation [158]. The details of the procedure he described in his patent application many years later cannot be readily accepted as a proof that he was working with a melt-grown crystal from a heated crucible [159]. Accordingly, some historians argue that this now famous growth method should indeed be called the "Teal and Little" method [150, 158].This view was later disputed by Tomaszewski [160] who provide an interesting anecdote regarding the accidental discovery of induced crystallization on molten Sn when Czochralski accidently dipped his pen into it instead of the ink well. Different accounts of this historical event are given by others that provide credibility for Czochralski's efforts in the crystal growth and not just the growth rate measurement techniques [161].

Regardless of what the method should actually be called today, it is a suitable method for the growth of β-Ga_2O_3 crystals. To date, most of the work on single crystal β-Ga_2O_3 by this method is done by Leibniz Institute for Crystal Growth. The report by Tomm *et al* in 2000 [64], who utilized 10% CO_2 in Ar to provide sufficient oxygen to prevent Ga-rich crystal growth, is the first report on this subject. Undoped crystals grown by Tomm *et al* showed some dimensional control problems in the form of "corkscrews" which were thought to be due to circulation pattern in the melt and the radial temperature gradient. Similar growth conditions were used later by Galazka to obtain crystals unintentionally doped to 2-6e17 cm^{-3} and had Hall electron mobility as high as 150 cm^2/Vs [162, 163]. More detailed electrical measurements by the same group later established that the ionization energy for the shallow donors was 36meV and that at least 2 donor levels were found; one due to oxygen vacancy and another due to unintentional Si doping [65].

As the diameter of crystal is increased to about 2-inch and the doping level is maintained above 1e18 cm^{-3}, the boule dimension control has shown some instabilities. As shown in Figure 24, higher doped crystals had corkscrew instability due to infrared absorption in the crystal during growth [65]. Reducing the doping level produced better dimension control and insulating crystals with Mg doping also had excellent dimension control.

Figure 24: β-Ga_2O_3 single crystals obtained by the Czochralski method. Carrier concentration 2e18 cm^{-3} (left), 4e16 cm^{-3} (middle) and insulating with Mg doping (right) [65].

D. Edge Defined Film-fed (EFG) Method

This is also a melt-type crystal growth and has many similarities to the CZ Method. The major difference is that the crystal growth is carefully shaped by the use of special fixtures located at the top of the melt zone and where the crystal growth actually takes place. The origin of this method is attributed to LaBelle and Mylavski [164-166], who replaced the previously used floating shaping disks (Floating Orifice Technique [167]) on the top surface of the melt with capillary tubes. Because the inlet of the capillary is closer to the bottom of the melt than the top, a constant flow of molten material could be drawn out and crystallized at the other end of the tube in a controlled manner, as shown in Figure 25. This simple innovation has allowed the design of many interesting growth systems to fabricate not only filaments but also complex shape crystals. Some examples of these are shown in Figure 26. This method also known to produce crystals at a much higher rate than the other techniques. For examples, hundreds of feet long alumina filaments were prepared at growth rates of 5cm/min [168].
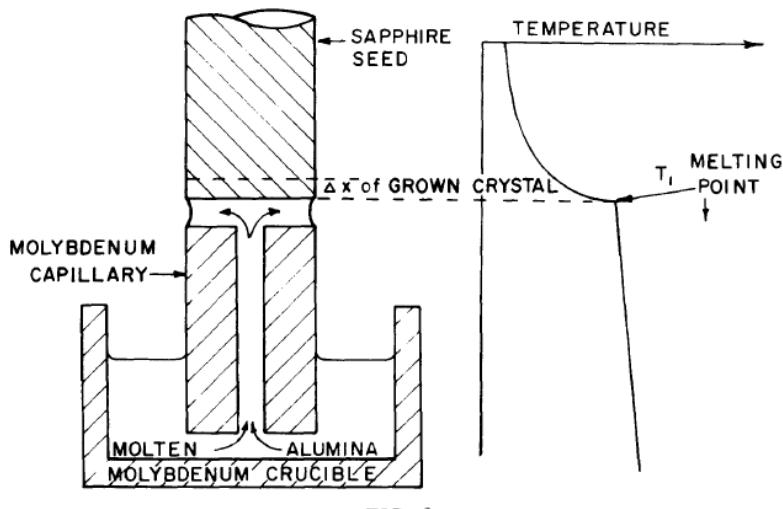
Figure 25: Schematic of the EFG system used for alumina [166].

This now well-established crystal growth method for Al_2O_3 is a natural fit for the growth of β-Ga_2O_3 crystals because of the similarities between Al_2O_3 and β-Ga_2O_3. Aida [68] *et al* reported the first successful growth of β-Ga_2O_3 single crystals with EFG method. A growth rate of 10mm/hr was reported for crystal ribbons of about 50mm in width, 70cm in length and only 3mm in thickness (see Figure 27).

The EFG method is one of the ways to overcome the problems associated with large diameter crystal growth using the Czochralski Method. It was estimated that to increase the crystal size beyond 2-inch already demonstrated with the Czochralski method [65], the oxygen content must be increased to 35-100% [163]. However, this results in the oxidation of the Ir crucible and causes mixing of Ga-Ir oxides. The EFG method may be one way to overcome this problem since the width of the crystal ribbon can be tailored during growth [169]. A number of patents were issued to the Tamura Corporation for the dimensional control of Ga_2O_3 ribbons grown by EFG method [170-175]. The photograph of a 4-inch Ga_2O_3 wafer shown in Figure 5 was grown by EFG. According to some of these patent applications, the main surface of the crystal ribbons are (-201), (001) or (110). The crystal quality seems to be excellent

with the reported full-width at half-maximum (FWHM) values of the X-ray diffraction rocking curve (XRC) ranging from 75 to 17 arcsec [17, 68, 175].
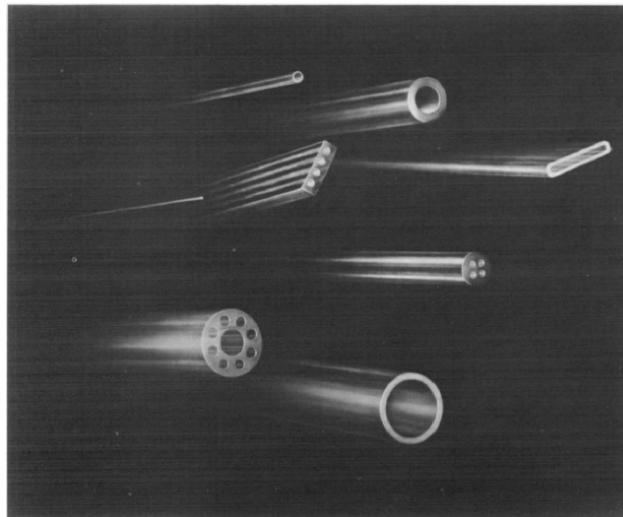
Figure 26: Sapphire shapes produced by EFG [166].

The electrical characteristics of EFG-grown Ga_2O_3 ribbons with (-201) surfaces are also very promising. Hall effect mobility values of 153 and 886 cm^2/Vs was measured at room temperature and at 85K, respectively [176].
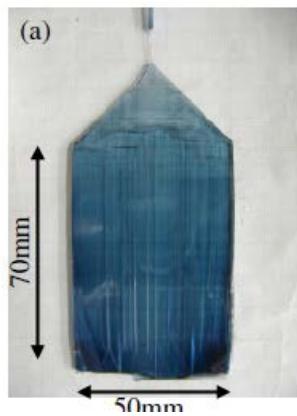
Figure 27: As-grown β-Ga_2O_3 ribbons prepared by EFG method [68] .

Some of the remaining issue to be addressed with EFG-grown β-Ga_2O_3 crystals are the thickness of the crystals (ribbons) and unintentional doping with Si. It is desirable to grow insulating substrates for electronics application to minimize substrate leakage currents. Currently, insulating substrates are grown with Mg-doping to achieve higher resistivity at the expense of reduced electron mobility [177].

The major limitation of this growth method is the limited thickness of the crystals, which are essentially ribbons. The crystal shown in Figure 27 has the dimensions of a credit card. More recently grown crystals have the dimensions of iPad mini, but thinner. Such substrates are not entirely flat and it is questionable how many wafers can be cut out of such boules. It may be possible to grow very long ribbons by taking advantage of the fast growth rates and cut out wafers from these ribbons like cutting out cookies.

Other single crystal growth methods used for β-Ga$_2$O$_3$ substrate growth include The Flux Method [178-180], Chemical Vapor Transport [181], Bridgman Method [182] and free crystallization [183]. These method will not be reviewed in more detail here.

E. Vertical Bridgman Method

This melt-grown crystal growth technology is related to both the Czochralski and the FZ methods. As described above, the original Bridgeman method refers to a horizontal growth system where a temperature gradient exists. The melt is in the zone with the higher temperature zone and the crystallized solid is in the lower temperature zone. Controlled crystallization occurs at the boundary of these zones [152]. The same approach has been successfully applied to the growth of sapphire and piezoelectric crystals in a vertical system [184, 185].

Figure 28 shows schematically the vertical Bridgman (VB) system used for the growth of β-Ga$_2$O$_3$ crystals. The diameter control in this system us achieved by the crucible dimensions. RF coils provide the energy for heating the crucible to a temperature around the melting point of β-Ga$_2$O$_3$. The small temperature gradient in the furnace is the key aspects of the system. The crucible is rotated and lowered during the growth so that melting starts at the bottom of the crucible and the melt zone travels upwards as the crucible is lowered, as shown in Figure 29. This aspect of the growth has similarities with the FZ growth.
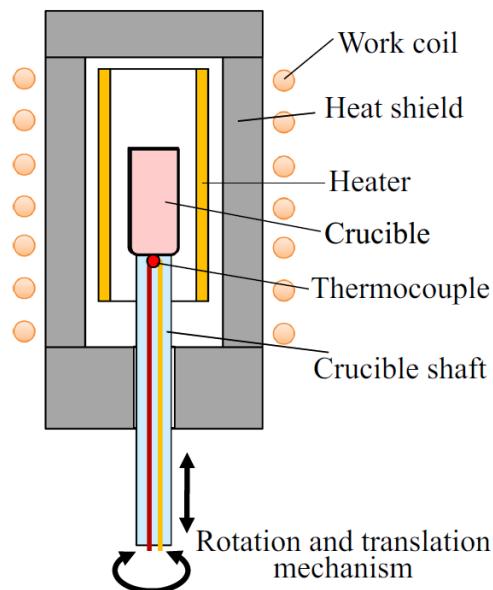
Figure 28: Schematic diagram of the VB growth furnace [182].
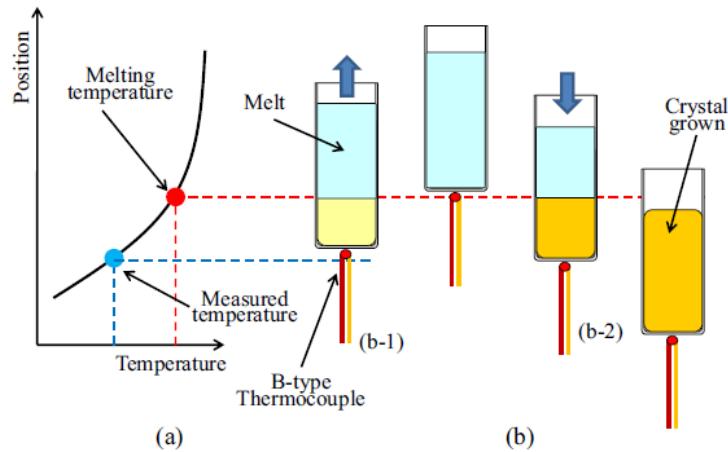
Figure 29: Schematics of (a) the temperature distribution in the furnace, and (b) the growth processes [182].

In this method, one of the key technology innovation was the use of a platinum–rhodium crucible rather than an Ir crucible used for the Czochralski (CZ) method. As mentioned above, Ir crucibles introduce a limitation on the amount of oxygen that can be present during growth to avoid the oxidation of the crucible itself. However, higher oxygen content is needed for the growth of larger diameter boules. With the use of platinum–rhodium crucible, this limitation was overcome. The adhesion of the grown crystal to the crucible was poor so that they could be easily removed. However, significant impurities were introduced in the grown crystal from this type of crucible.

When growing sapphire crystals with this method, several types of seed crystal was used [186]. In the case of β-Ga$_2$O$_3$, seed crystal was used in connection with the conical crucibles. Unseeded growth in flat bottomed crucibles also yielded single crystals with smooth top surfaces. The crystal growth orientation was perpendicular to the (100) surface. This growth orientation was explained in terms of growth anisotropy. It is known that the growth rate of β-Ga$_2$O$_3$ is orders of magnitude higher in [010] and [0-10] directions than the [100] direction [187]. The (100) is the major cleavage plane for β-Ga$_2$O$_3$, which means that the bonding strength on this surface is weaker. The growth in [100] direction is therefore slower. In addition, in VB growth, there is a temperature gradient along [100] direction whereas the temperature is constant along [010] and [0-10]. The net result of these growth rate variations is the growth in [100] direction with flat top in crystals grown without seed layers. No electrical characteristics of the crystal were published.

F. Substrate Growth Summary

All the substrate growth methods described above are mature technologies by themselves in the sense that some or all of them have been around for a long time. The Verneuil technique, for example, has been around for more than a century for the growth of crystals similar to β-Ga$_2$O$_3$. The application of these techniques to the growth of single crystal β-Ga$_2$O$_3$ boules is, however, relatively new with the exception of the Verneuil method. The results obtained in the short time since their first use is highly encouraging and further refinements will bring better capabilities in the future if interest in this area continues at its current pace.

Based on what we know now, can we make a prediction on the best growth method for the future mass production of substrates? At present, the Czochralski method has a limitation in the crystal dimension control beyond 2-inch because larger diameter growth requires higher oxygen content growth conditions [163]. The current Ir-based crucibles are not compatible with higher oxygen environment at the growth temperatures. Because no crucibles are required, FZ method may offer a better path to large diameter crystal growth. On the other hand, EFG method already offers the possibility of large wafers to be manufactured from the ribbon-type crystal that result from this method. EFG is not a standard bulk growth technique for semiconductors but with its fast growth rates (linear growth rate because of thin ribbons) it may still offer an immediate solution.

Clearly, the availability of large area, low defect density, high crystal quality substrates with high electrical/optical parameters will accelerate the development of devices and circuits. On the other hand, the intrinsic thermal conductivity limitations of Ga_2O_3 may place an upper ceiling to the power levels that can be achieved. If that limitation becomes apparent as more and more powerful devices are fabricated, we may be forced to use other types of substrates with better thermal conductivity.

A top-level comparison of the substrate growth technologies reviewed here is shown in Table 13.

Table 13: Comparison of substrate growth methods for Ga_2O_3.

Growth Method	Advantages	Limitations	Notes
Veneuil	• Versatile growth system. • Inexpensive. • Highly customizable. • Crucible-free growth.	• Small boule sizes. •	Research only.
Floating Zone (FZ)	• Mature technology base. • Crucible-free crystal growth; less contamination. • Growth in high oxygen atmosphere possible. • Excellent doping control with Sn and Si. • High electron mobility for doped crystals. • Large diameter crystal growth is possible.	• Limited crystal orientation have been demonstrated. • Technology base is narrowly located in Japan.	Mainstream technology.
Czochralski	• Mature technology base. • Crucible-free crystal growth; less	• Crucible based technology. • Limited oxygen concentration allowed	Mainstream technology base.

	contamination. • Growth in high oxygen atmosphere possible. • Excellent doping control with Sn and Si. • High electron mobility for doped crystals. • Large diameter crystal growth is possible.	during growth. • Technology base is narrowly located in a single institution in Germany. • Higher doping causes corkscrew type dimensional instabilities.	
EFG	• Fast growth rate. • High quality substrates. • Excellent doping control. • Large area growth. Suitable for large diameter substrate production.	• Technology base is narrowly located in Japan. • Ribbon-type crystals.	Ribbons only.
Vertical Bridgman	• Excellent dimensional control. • High oxygen atmosphere growth. • Seeded or no-seed growth. • Low adhesion to crucible.	• Slow growth rate in [100] direction. • Large diameter crystals are not yet demonstrated.	Established technology base for sapphire growth that can be modified for Ga_2O_3.

G. Contributing Research Groups in Bulk Crystal Growth

Table 14 lists the active research groups in bulk β-Ga_2O_3 crystal growth. This field is dominated by Japanese and German research groups. Private Japanese corporations' contributions are highly significant indicating near term commercial interest in this technology. Germany has a significant foothold in the Czochralski method, which is one of the most promising technical approach to large crystal growth for commercialization. If some of the technical difficulties associated with large diameter boule growth with the Czochralski method cannot be not resolved, FZ method may be used commercially. This field, and the new emerging field of EFG method are dominated by the Japanese companies.

Table 14: Active research groups in bulk Ga_2O_3 crystal growth.

Epitaxy Method	Research Organization	Country	Notes
Verneuil	• Aerospace Corporation • IBM Watson Research Center • State University • Ecole Nationale Paris	• USA • USA • The Netherlands • France	Old technology. Not likely to be commercialized.
Floating Zone (FZ)	• Tokyo Institute of Technology • Institute for Molecular Science • National Institute for Material Science • Waseda University • Chinese Academy of Sciences • Tohoku University	• Japan • Japan • Japan • Japan • China • Japan	Japan dominated. Highly significant technology for large crystals.
Czochralski (CZ)	• Leibniz Inst. For Crystal Growth	• Germany	Germany dominated. Classical method to grow large crystals.
EFG	• Tamura Corp. • Namiki Precision Jewel • National Inst. Of Information and Comm. • Saga University	• Japan • Japan • Japan • Japan	Entirely Japanese. Emerging technology with promising results.
Vertical Bridgman	• Shinsu University • Fujikoshi Machine Corporation	• Japan • Japan	Crucible based technology with good dimensional control.

7. EPITAXIAL GROWTH

Epitaxial layers are the thin layers of semiconductor prepared over wafer substrates. These layers are used to fabricate electronic or optical devices. When epitaxy layers are grown on substrates that are of the same material composition, the crystal defect levels can be low. If a native substrate is not available, epitaxial layers can still be fabricated on lattice mismatched substrates but the epitaxial growth is more challenging and the resulting layers can contain significantly more defects. One of the major advantages of the Ga_2O_3 technology is that high quality substrates can be prepared by a number of methods, as reviewed above. Typically, the epitaxial layer provides the sole conduction path within various devices of electronic circuits fabricated on wafers. The substrate is only used to support these circuits and provide a thermal conduction path for the excess heat generated in devices. In these typical cases, the substrate is as insulating as possible to avoid crosstalk between circuit elements. However, high power electronic circuits make use of very high voltage and current transistors and diodes, which are produced in a way that the electrical current flows dominantly in the vertical direction. In these devices, the substrate can be an intrinsic part of the device. Even in these cases, epitaxial layers are needed on top of the substrates to fabricate the critical parts of devices where electrical contacts are made.

Currently all transistors fabricated with Ga_2O_3 are lateral devices, meaning all electrical contacts are on top of the substrate. Such devices have much in common with high speed GaAs and GaN devices. As it is the case with the GaAs and GaN technologies, epitaxial layers with good crystal quality (minimum defects) and high electrical parameters (mobility, conductivity, breakdown strength etc.) will be needed. As the technology matures and very high power devices are fabricated, the Ga_2O_3 transistors will resemble Si vertical transistors. A different set of material requirements will be identified for those future devices. Here, we will only review the epitaxial layer techniques developed for the current devices.

Many of the techniques developed for Si, GaAs, and GaN epitaxy are directly applicable to Ga_2O_3. These techniques include Molecular Beam Epitaxy (MBE), halide vapor phase epitaxy (HVPE), metal-organic chemical vapor deposition (MOCVD), and mist chemical vapor deposition. Epitaxial layers of Ga_2O_3 of various polymorphs were grown on both Ga_2O_3 substrates (homo-epitaxy) or on other substrates such as sapphire (hetero-epitaxy). Polycrystalline films were grown on sapphire substrates at various substrate temperatures, but these films have low conductivities and are not yet suitable for electronic devices [20, 113]. We will review the current status of epitaxy growth techniques in this section.

A. MBE

In MBE, the epitaxial layers are grown in ultra-high vacuum systems. The atoms that make up the epitaxial layer (including dopants) are brought together on the heated wafer surface in correct proportions. The challenge in Ga_2O_3 epitaxy is the source of ionized oxygen in the chamber. Currently, this is accomplished by either ionizing oxygen using radio frequency (RF) plasma [23, 188-190] or by the use of ozone [187, 191].

Regardless of the source of oxygen, the growth of epitaxial layers of metal oxides require the optimization of several growth parameters such as metal/oxygen flux ratios and substrate temperature.

In general, more oxygen is provided than that can be incorporated during the growth (i.e. oxygen rich growth). Sometimes, it is advantageous to grow in metal-rich environment. If no oxygen is present, the surface of the substrate may be etched due to the formation of volatile oxide compounds. This is illustrated in Figure 30 [190]. The growth rate is expected to be lower when grown in metal-rich environment but the experimental evidence show that the growth rate is influenced more strongly by other factors and the growth rate can be independent of Ga-O ratio under some growth conditions [192].
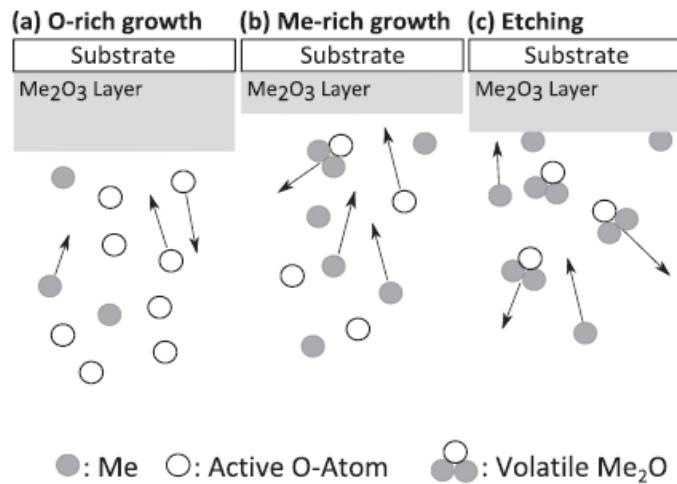
Figure 30: Schematic of Ga$_2$O$_3$ growth in metal- or oxygen-rich environments [190].

The growth rates of β-Ga$_2$O$_3$ epitaxial films grown with this method are typically in the 0.5-1.0nm/min range. In a systematic study of film growth in an ozone MBE, the growth rate of films on (010) surface first increased with substrate temperature and then decreased above 750C [191, 192]. The maximum growth rate was 1.0nm/min at 750°C. Much higher growth rate of 3.0nm/min growth rate was obtained with a similar growth system at 700°C on the same orientation substrates grown by the same company (Tamura) [70]. The maximum growth rate for plasma assisted MBE at 700°C is 2.1nm/min, again on (010) surface [192].

The film growth rate is similar to each other for most available surface orientations including (010), (101), (001) and (310), but a factor of ten lower for (100) [187]. Figure 31 shows the growth rate dependence on substrate orientation. The lower growth rate on (100) surface is thought to be due to lower adhesion energy and the higher re-evaporation of impinging atoms. A small change in the surface orientation had a significant impact on the layer growth rate.
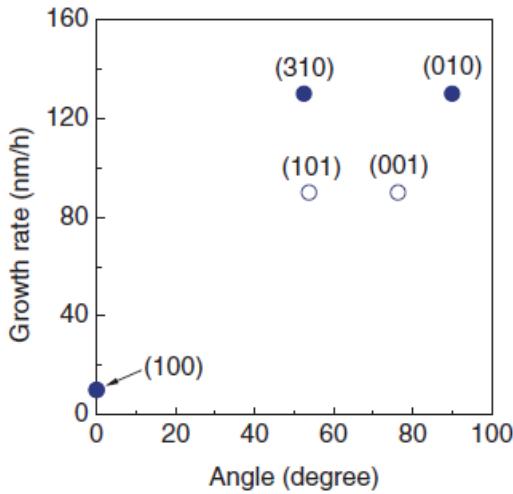
Figure 31: Relationship between surface orientation of β-Ga₂O₃ substrate and homo-epitaxial growth rate. The horizontal axis is the angle between the substrate surface and (100) plane [187].

Sn is the current preferred dopant for the MBE epitaxial films. Carrier concentrations as high as 2e19 cm⁻³ were demonstrated with ozone MBE systems, whereas 1e18 cm⁻³ is the highest reported for plasma-assisted MBE. Figure 32 shows the carrier concentration and Hall mobility values for epitaxial layers fabricated on both types of MBE reactors. In both cases, the mobility drops to 10-30 cm²/Vs level at the maximum carrier concentration levels. For reference, the doping and the mobility of Si-doped substrates are shown in Figure 32a.

(a)   (b)
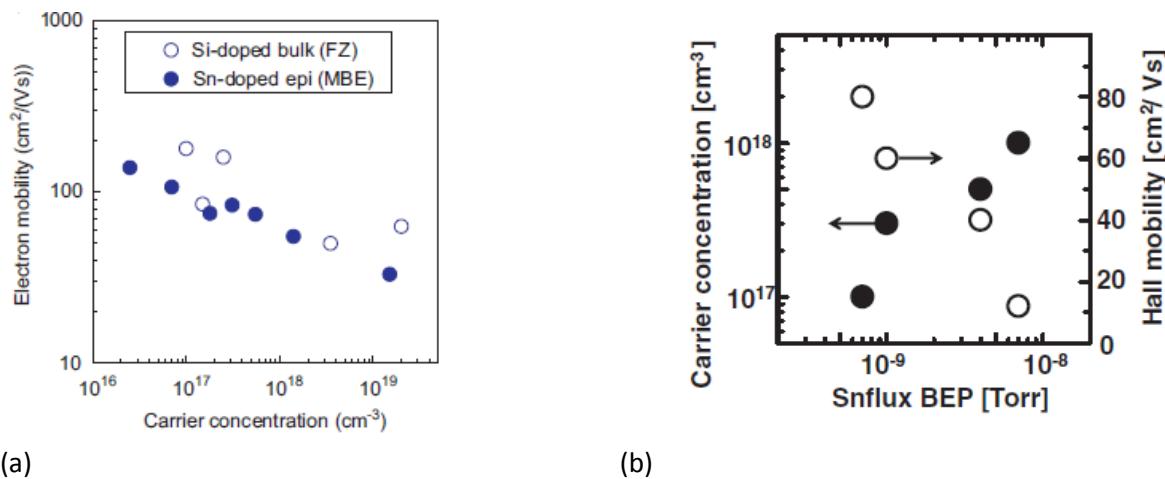
Figure 32: Carrier concentration and Hall mobility for Sn-doped epitaxial layers. (a) Ozone MBE [86, 187], (b) Plasma-assisted MBE [192].

The epitaxial films grown in plasma-assisted MBE on substrates other than β-Ga₂O₃ typically had poorer crystal quality and contained multiple crystal orientations. Films grown on c-plane (0001) sapphire had predominantly (-201) crystal orientation but also contained α-Ga₂O₃ when the growth temperature was low[24]. The growth of α-Ga₂O₃ is probably encouraged by the crystal structure similarities (corundum) with sapphire. Only above 800°C, where α-Ga₂O₃ is not stable, the films became predominantly β-Ga₂O₃.

Films grown on (001) sapphire and (100) also had (-201) orientation and did not show α-Ga$_2$O$_3$ phase, perhaps because the growth temperature was kept constant at 820°C [23]. On the other hand, the Nd-doped α-Ga$_2$O$_3$epitaxial layers could be grown intentionally on some sapphire surfaces at temperatures below 800°C. Films grown on R-, A-, and M-plane sapphire substrates were α-Ga$_2$O$_3$, whereas those grown on C-plane were β-Ga$_2$O$_3$ [193]. Because of the similarities in the crystal structure of Al$_2$O$_3$ and β-Ga$_2$O$_3$, continuous films of single crystal α-(Al$_{1-x}$Ga$_x$)$_2$O$_3$ could be prepared with this approach.

B. Halide Vapor Phase Epitaxy (HVPE)

This is an old epitaxy growth method that was previously used for the growth of III-V compound semiconductors [194]. It was originally known simply as Vapor Phase Epitaxy (VPE), which was for a long time the only way to prepare ultra-pure GaAs layers[195]. This approach was later used for the growth of thick layers of GaN, which could be separated from the original substrate and used as substrates themselves[196]. Several features of this technique stand out: high purity materials, high growth rate, and simplicity. These particular features may be very important when applied to the growth of Ga$_2$O$_3$ epitaxial layers for power devices with thick layers that need to sustain high electric fields. The drawback of this technique, as applied to the growth of thin epitaxial layers for transistors, is that the thickness control across the wafer is problematic. Most halide systems are horizontal systems and the precursor concentration is not constant across large wafers.

A simple HVPE system is shown in Figure 33 [197]. In this example, the Ga source is maintained at 850°C for the generation of GaCl with the use of Cl$_2$ or HCl carried in N$_2$. The O$_2$ precursor is introduced into the system further downstream. The sample is held at a temperature higher than the source temperature, although in simpler constructions, the sample and the source temperatures were the same [12]. Since diluted precursors arrive at the substrate, which is held at high temperature, the reaction occurs rapidly in equilibrium conditions. This make the growth mass-transport limited and the growth rate is directly proportional to the input partial pressure of the precursors.
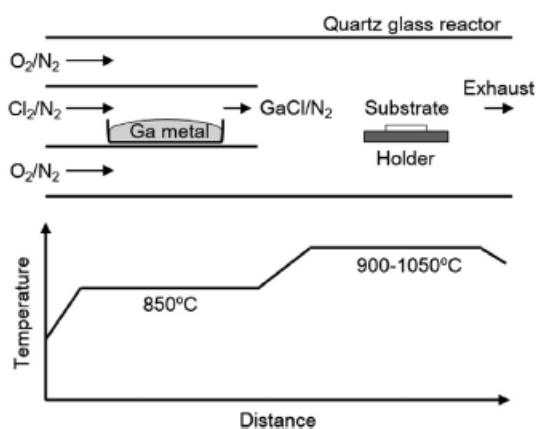
Figure 33: Schematic drawing of a HVPE system for Ga$_2$O$_3$ growth [197].

Initial films were grown without substrates, although these early films were not continuous and nor were they single phase [12]. Later this growth approach was used successfully to prepare α-Ga$_2$O$_3$ and β- Ga$_2$O$_3$ films on both β-Ga$_2$O$_3$ and sapphire substrates. In all cases, the striking feature of this growth

technique was the highly elevated substrate temperatures; typically above 800°C and sometimes above 1000°C. The other important feature is the capability to keep the residual donor concentration low; typically below 1e14 cm^{-3}.

The first straightforward application of this technique is for the homoepitaxial growth of β-Ga2O3 using the system shown in Figure 33. Films were grown on Sn-doped (001) β-Ga2O3 substrates with GaCl and O$_2$ precursors in N$_2$ carrier gas [198]. The source material (Ga) was kept at 850°C and the substrate temperature was varied from 800°C to 1050°C to investigate the growth rate and crystal quality dependence on the growth temperature. As would be expected from mass transport limited growth conditions, the growth rate was nearly temperature independent at 5μm/hr. This growth rate is higher than those obtained with MBE. The crystal quality and surface morphology improved with the growth temperature. Figure 34 show the surface quality of films grown at 800°C and 1000°C. The microstep arrays parallel to the [010] direction are thought to be due to slight misalignment of the substrate and the different growth rates on (100) and (001) planes [187]. Schottky diodes fabricated on the top surface had a reverse breakdown voltage of about 1000V indicating that the electrical breakdown strength is at about 0.83MV/cm. This is far short of the expected 8MV/cm value used in the FOM calculations. But the absolute value of breakdown is impressive. This is the first kV level blocking voltage resorted with Ga$_2$O$_3$. The doping level (N$_D$-N$_A$) was estimated to be 1e13 cm^{-3}.
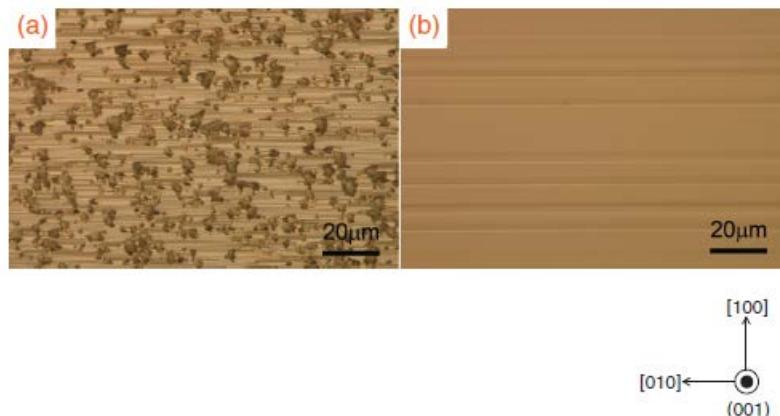
Figure 34: Images of 5 μm thick HVPE-grown β-Ga$_2$O$_3$ films on (001) substrates. Growth temperature (a) 800°C, (b) 1000°C [198].

Perhaps the most significant advantage of this growth method is the growth of high quality single crystals on substrates other than Ga$_2$O$_3$. Both α- and β-Ga$_2$O$_3$ layers were grown on sapphire. Because of the similarity in the arrangement of the oxygen atoms on the surface of (0001) sapphire and (-201) β-Ga$_2$O$_3$, the grown layers exhibited this crystal orientation with some other in-plane rotational domains [199]. Using slightly off-axis substrates were useful in suppressing some of these domains. But the most impressive feature of this growth method was highlighted by the achievement of extremely fast growth **rates of 250μm/hr**. This is nearly 2 orders of magnitude higher than the growth rate achieved with MBE. The growth rate could be controlled almost linearly by the precursor flow rates due to mass transport growth behavior, as shown in Figure 35.
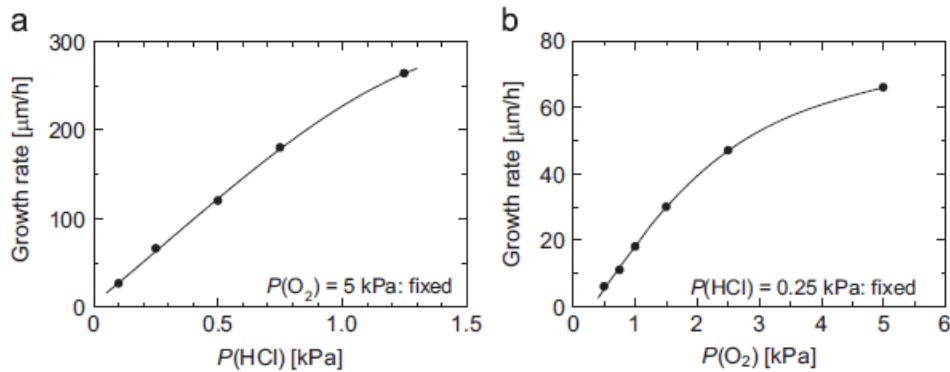
Figure 35: Growth rate of β-Ga₂O₃ as a function of (a) HCl partial pressure, (b) O₂ partial pressure [199].

Although this growth method normally employs very high growth temperatures (around 1000°C), and proven to be particularly suitable for the growth of β-Ga₂O₃, which is stable at such high temperatures, it is also used successfully to prepare α-Ga₂O₃ epitaxial layers at lower temperatures. As mentioned before, α-Ga₂O₃ is metastable and cannot be prepared from melts. But it can be grown epitaxially on sapphire, which has a similar crystal structure. It was shown that high quality α-Ga₂O₃ layers can be grown on (0001) sapphire at a growth temperature of 520-580°C [104] using essentially the same system shown in Figure 33. Above 580°C, films contained β-Ga₂O₃ phases. The film growth rate was impressive with a maximum of 150 mm/hr growth at 550°C, as shown in Figure 36. With its simpler crystal structure and wider bandgap, α-Ga₂O₃ may become an important material for ultrahigh power device fabrication and this method may allow the fabrication of layers needed for that application.
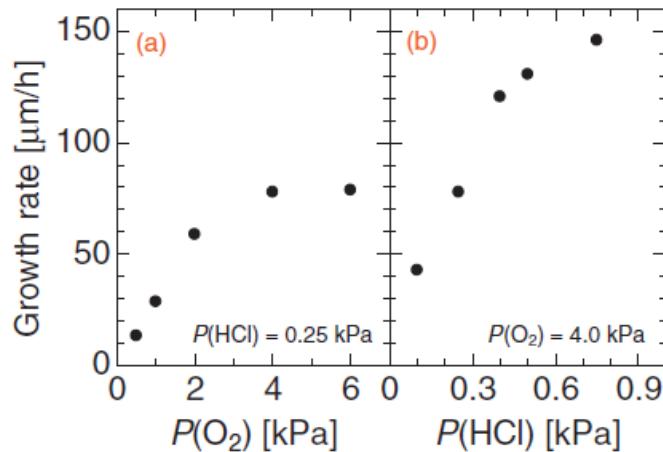
Figure 36: Growth rate of α-Ga₂O₃ as a function of (a) O₂ partial pressure, (b) HCl partial pressure [104].

C. Metal-Organic Chemical Vapor Deposition (MOCVD)

This epitaxial growth technique is also very mature and has been around since the early days of GaAs research. Its use peaked when MOCVD replaced MBE as the main grown technique for the InGaP/GaAs

heterojunction bipolar transistors (HBT) used in the fabrication of RF circuits of nearly all cell phones. Today, multi-wafer MOCVD reactors are used to grow these layers on 6-inch wafers.

MOCVD is in essence a CVD system that uses metal-organic compound for some or all its precursors. It is typically a vertical system with substrates resting on heated and rotating platforms, as shown schematically in Figure 37. Films grown in these reactors can have excellent uniformity in thickness, doping and composition, but the growth rates are as slow as MBE.
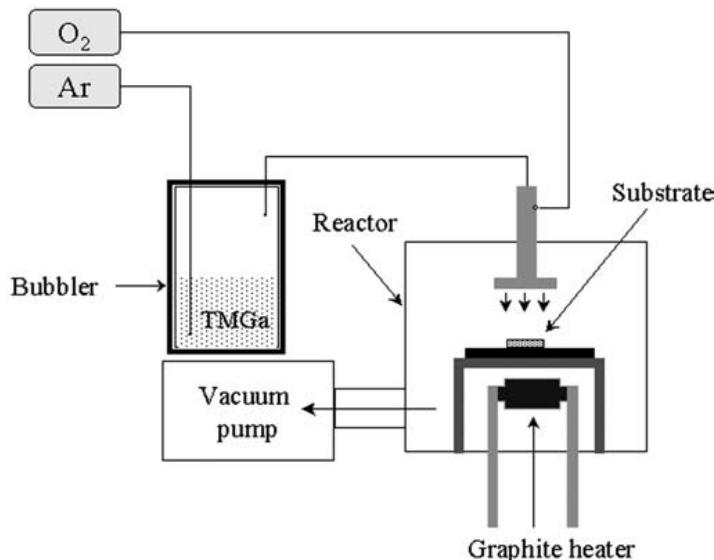
Figure 37: Schematic drawing of a typical Ga$_2$O$_3$ MOCVD reactor [200].

For the growth of Ga$_2$O$_3$ films, only the Ga precursor needs to be a metal-organic source since oxygen can be supplied from inorganic source, either as O$_2$ directly or in the form of water. In Atomic Layer Deposition (ALD), a deposition method related to MOCVD, ozone is also used as the oxygen source [201]. Various Ga precursors have been used for Ga$_2$O$_3$ deposition, including gallium tris-hexafluoroacetylacetonate (Ga(hfac)$_3$) [202], (Ga[OCH(CF$_3$)$_2$]$_3$·HNMe$_2$) [203], [Ga(μ-O-t-Bu)(O-t-Bu)$_2$]$_2$ [204]. The most common precursor for Ga in use currently is trimethylgallium (TMGa) [37, 200, 205-211]. Many different growth conditions were reported with correspondingly different crystal qualities. Here, we will only concentrate on some of the important growth parameters and will highlight e few of the common observations made by several groups.

The first observation to be made is that the films grown at lower temperatures (<700°C) seems to be all amorphous or polycrystalline, even when they are grown on β-Ga$_2$O$_3$ crystals. The crystallinity of grown layers could be improved by thermal annealing after growth.

The second observation is that the use of oxygen as the precursor seems to result in polycrystalline films even at elevated temperatures, such as 800°C. When water vapor is used, however, under similar growth conditions, the films had crystalline structures [211]. Figure 38 shows images of layers grown by MOCVD on (100) β-Ga$_2$O$_3$ substrates at 800°C using oxygen and H$_2$O as precursors. It was suggested that the presence of hydrogen has a positive effect on the kinetic conditions of the substrate surface and

enhance the growth. Similar polycrystalline results were observed by others when oxygen was used as the precursor on (100) Ga₂O₃ [206], (110) MgO [208], and Si [205] substrates. However, when triethylgallium (TEGa) is as the Ga precursor, epitaxial layers could be grown even with oxygen (i.e. no water) [212].
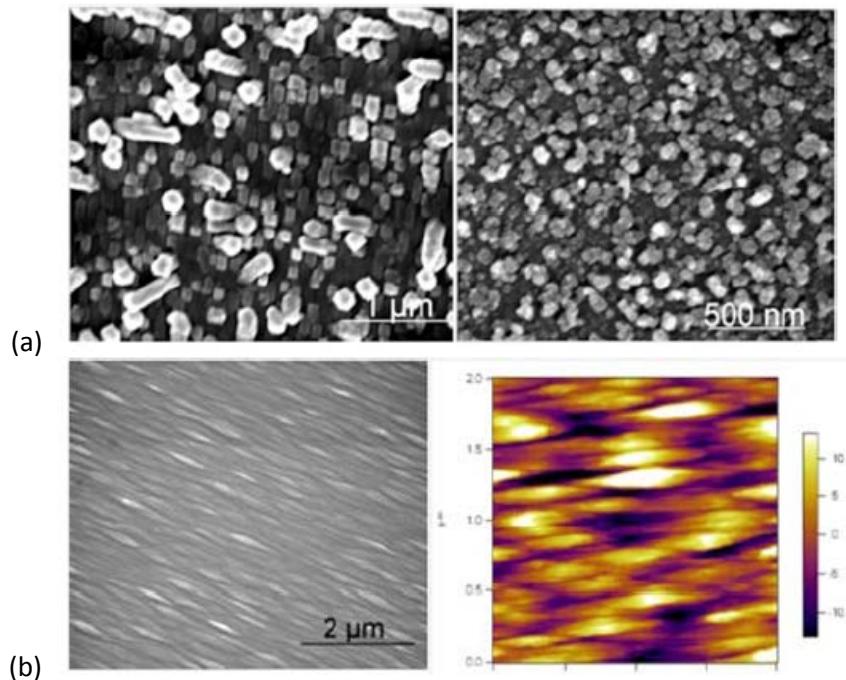
Figure 38: SEM and AFM pictures of Ga₂O₃ epitaxial layer surfaces grown by MOCVD with (a) Oxygen and (b) Water [213].

A controlled doping of the grown films is a requirement for device applications. Some initial studies suggest that this may not be easily achieved in MOCVD. Dopants successfully used for substrates, Si and Sn, have been considered for MOCVD epitaxial layers also. Si dopants were introduced using tetra-ethyl-ortho-silicate (TEOS) [210]. Although the films were grown using water and high temperature for high crystal quality on (0001) sapphire substrates, the incorporation of Si into Ga₂O₃ crystal was not effective. The dopant concentration was limited at 5e19 cm⁻³, beyond which films became polycrystalline. Even at such high Si concentration, the films were highly resistive indicating that donors are not incorporated into the structure. Sn-doping seems to have the opposite effect on the crystal quality, at least up to 10% concentration. MOCVD films grown with oxygen as the precursor on (100) Ga₂O₃ substrates at 700°C used Sn from tetraethyltin (Sn(C₂H₅)₄) source [206]. It was found that Sn-doping prevented the polycrystalline formation normally associated with oxygen precursors. The crystal quality increased and the layer resistivity decreased monotonically up to 10% Sn concentration. At this Sn concentration, the carrier density was 9.54e17 cm⁻³, resistivity was 1.2e⁻¹ ohm.cm and the Hall mobility was 12.03 cm²/Vs [206]. Higher mobility values of up to 41 cm²/Vs were obtained with Sn-doped MOCVD layers when TEGa was used as the Ga precursor [212].

D. Mist Chemical Vapor Deposition

This is a relatively simple and inexpensive deposition technique that has been extensively used for the deposition of metal-oxide thin films including ZnO [214-217], SnO_2 [218-221] and ZnMgO [222] in the past. The term "mist CVD" was coined by researchers at the Kyoto University to distinguish their technique from others. This is the term now used for the deposition of Ga_2O_3 epitaxial layers. This technique is a variation on the well-known spray pyrolysis technique where droplets of solvents are deposited directly on a heated substrate. Pyrolytic reaction on the surface leads to the formation of films. But this approach suffers from large non-uniformity and porosity. An improvement on this initial method was made using fine mist of precursors in a vapor phase reaction on the substrate [222]. This process was then called Ultrasonic Spray CVD (USCVD). At Kyoto University, this method was improved by transporting the precursor mist horizontally to the reactor where it is vaporized and deposited on the substrate. It was first applied to the growth of ZnO films and the process was called "mist-CVD" [215]. A picture and the schematic drawing of the first system is shown in Figure 39. It was later modified for Ga_2O_3 growth. Another research group from the FLOSFIA Inc. of Japan, developed another variation of this technique, which is trademarked as MIST EPITAXY© [105, 223].
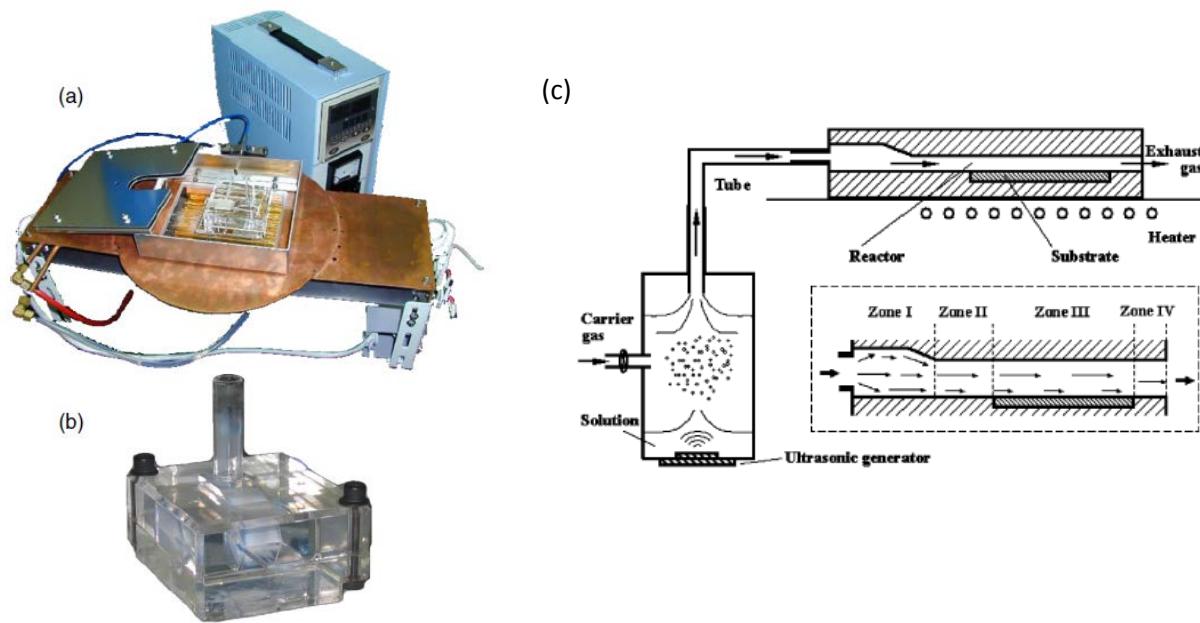
Figure 39: Photographs of the growth system which enables the growth at high temperatures up to 800°C. (a) Total view and (b) the reaction chamber and susceptor, c) Schematic drawing of the system [217].

If we ignore the trademarks and the current labels attached to this deposition method, we find that similar methods had been used elsewhere before including Argentina [218], Korea [220], and France [214, 224] for the growth of SnO_2 thin films. The process was then simply called "pyrosol" meaning the pyrolysis of an aerosol. The pyrosol technique is described in simple terms in Figure 40. The precursors of the material to be deposited are dissolved in an appropriate solvent, which can be water, an alcohol

or a ketone. A mist of the solution is produced by an ultrasonic generator and it is transported by a gas at atmospheric pressure toward a heated substrate pyrolysis occurs [224]. The deposition mechanism is nucleation followed by a growth process.
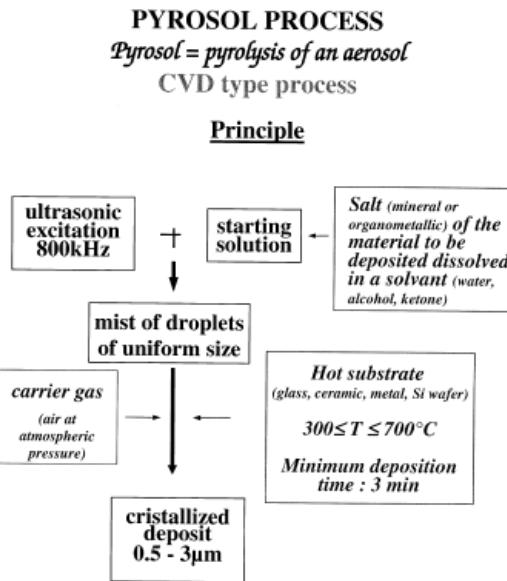
Figure 40: Schematic description of the pyrosol process [224].

Now we turn to the use of the pyrosol method for the deposition of Ga_2O_3 layers on various substrates. When the pyrosol method is used for Ga_2O_3, it will be referred to as the mist-CVD in this note.

There are 2 general observations on mist-CVD growth of Ga_2O_3. First, the growth system looks remarkably like the other pyrosol systems (see Figure 41 [225]). The gas flow is horizontal and the sample is tilted toward the gas flow. Second, almost all reported results are for the growth of Ga_2O_3 phase other than the β-phase. Third, most or all reported results are for layers grown on non-native substrates. The second and the third observations are related in the sense that α-$Ga_2O_3$and γ-Ga2O3 have crystal structures that are similar to sapphire and $MgAl_2O_4$, because of their corundum and defective spinel structures, respectively. β-Ga_2O_3 substrates, on the other hand, are monoclinic type. Fourth, all reports on this subject originate from a few institutions in Japan.
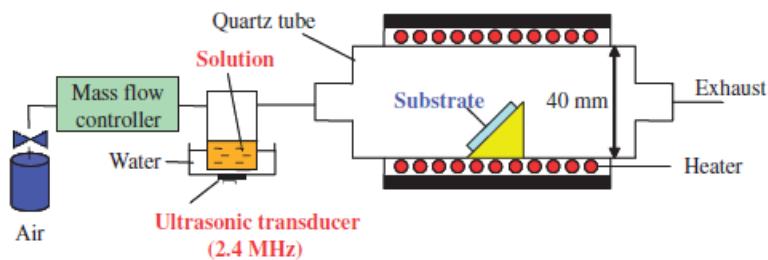
Figure 41: Schematic drawing of a typical mist-CVD system [225].

The Kyoto University group have grown α-Ga$_2$O$_3$, α-(Ga$_{1-x}$Fe$_x$)$_2$O$_3$, α-(GaAl)$_2$O$_3$ and Sn-doped α-Ga$_2$O$_3$ all on c-plane sapphire (α-Al$_2$O$_3$). The following chemicals dissolved in water and HCl were used as the metal source: gallium acetylacetonate [(C$_5$H$_8$O$_2$)$_3$Ga], iron acetylacetonate [(C$_5$H$_8$O$_2$)$_3$Fe], aluminum acetylacetonate [(C$_5$H$_8$O$_2$)$_3$Al], and tin chloride dehydrate [SnCl$_2$.2H$_2$O] were used for Ga, Fe, Al and Sn, respectively. The amount of each precursor was adjusted to change the film composition. Typical film growth rate was "a few" nm/min. The initial experiments were directed toward establishing a stable substrate temperature for α-Ga$_2$O$_3$ growth. Films grown from 350 to 390°C were amorphous, from 550 to 630°C contained β-Ga$_2$O$_3$, and those grown in the temperature range of 430 to 470°C were deemed to be pure α-Ga$_2$O$_3$ [74]. However, all subsequent report state that the growth temperature was kept constant at 500°C [225-228]. Undoped films were highly insulating and Sn-doping was used to reduce resistivity from 1e10 to 1e-2 ohm.cm (nearly 12 orders of magnitude reduction in resistivity) by changing the carrier concentration from 1e17 to 2e19 cm^{-3} [98, 228]. The Hall mobility of doped films were rather poor (2.8 cm^2/Vs).

The research group at the Kochi University of Technology employed a home-built system very similar to that used by the Kyoto University group. The Ga and Sn sources were the same as were the substrates (c-plane sapphire). The only difference is that the growth temperature was somewhat lower i.e. 350 – 425°C. The carrier concentration of Sn-doped films were also lower (7e18 cm^{-3}), which resulted in more resistive films [229]. Nevertheless, they used these films to fabricate field effect transistors with modest performance levels [103].

The group at the Tokyo Institute of Technology has grown γ-Ga$_2$O$_3$ films in their own mist-CVD system, which looks practically the same as others [75]. They also used gallium acetylacetonate [(C$_5$H$_8$O$_2$)$_3$Ga] dissolved in 2% HCl. To induce γ-Ga$_2$O$_3$ growth, the substrate was chosen to be (100) MgAl$_2$O$_4$, which has spinel crystal structure. It was found that the crystal growth was only successful in a very narrow substrate temperature window of 390-400°C.

Recently, a major deviation was made in this technology by the researchers at FLOSFIA Inc. with the use of all-inorganic precursors [105, 223]. Instead of using the usual gallium acetylacetonate [(C$_5$H$_8$O$_2$)$_3$Ga], which contains C, they used halide sources such as gallium chloride, gallium bromide, or gallium iodide. Similarly tin halides (presumably SnCl$_2$) was used to controllably dope the grown films to achieve a carrier concentration of 1e17 to 3e19 cm^{-3}. No other details of their growth method is reported except that substrates were 4-inch in diameter. These films showed high purity as expected from a halide process and the devices fabricated using these films also showed record performance levels (we will review these in the following sections). This approach seems highly encouraging for the growth of α-Ga$_2$O$_3$ epitaxial films that may find electronic applications.

E. Ion Implantation

Strictly speaking, ion implantation is not an epitaxial growth method. But, it is included in this section because the layers produced by this technique behave electrically like the epitaxial layers for device applications. Ion implantation is commonly used for the Si and GaAs technologies. For narrow bandgap materials like Si, ion implantation is used to increase conductivity. For wide bandgap materials like GaAs, it can be used for both increasing and decreasing conductivity. The increase in conductivity is simply due

to the addition of extra donors (thermally activated), whereas the decrease in conductivity can be accomplished due to ion implant damage to the crystal (not activated) [230-232].

Ion implantation method was applied to produce thin n-type layers on β-Ga_2O_3 using Si ions. Both UID FZ-grown substrates and MBE-grown UID epi-layers were implanted with doses ranging from 2e14 to 2e15 cm^{-2} and at implantation energies of 10-175keV [233]. These implantations mostly produced high carrier concentrations of 1e19 to 1e20 cm^{-3} (the aim of implantation was to produce highly conductive surface layers for ohmic contacts). After implantation, it was necessary to anneal samples at 900-1000°C in nitrogen for 30minutes. In this temperature range, the activation energy was typically 60%. However, as shown in Figure 42, samples annealed at such high temperatures showed changes in surface morphology with or without implantation. Ohmic contacts were made to these implanted layers using Ti/Au metallization and a minimum specific contact resistivity of 4.6e-6 $\Omega.cm^2$ was demonstrated.
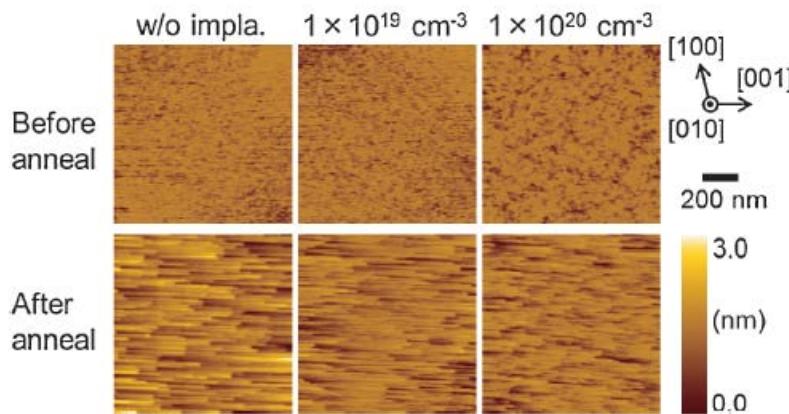
Figure 42: Surface AFM images of UID Ga$_2$O$_3$ substrates before and after annealing at 1000 C: without implantation, with Si = 1e19 cm^{-3}, and with Si = 1e20 cm^{-3} [233].

F. Summary of Epitaxial Growth

The epitaxial growth techniques currently used for the growth of Ga$_2$O$_3$ films are modifications of already existing techniques. In other words, no new method was introduced specifically for the growth of these layers. This should be taken as a positive sign since the development of new techniques is expensive and takes a long time. The methods that are currently used for the high volume manufacturing of III-V and III-N compound semiconductor wafers, i.e. MBE and MOCVD are also suitable for the fabrication of Ga$_2$O$_3$ epitaxial layers for electronic devices. Although the growth rate is low, high uniformity films can be fabricated using these techniques. Scaling for production should not be difficult since that kind of transition was already made for other material systems.

The other growth systems are basically horizontal tube systems, whose transition to manufacturing will need to be engineered. Both of these systems are atmospheric systems and can be implemented with small capital expenditure (for research and manufacturing). HVPE is a very high temperature growth that can produce extremely high purity material and very high growth rates. This method should be kept in mind when developing power electronic devices. Mist-CVD system is relatively new and the films

grown in such systems have inferior properties. However, this growth system and HVPE are both suitable for the growth of hetero-epitaxial growth. The use of readily available substrates is highly appealing from cost point of view and also because of low thermal conductivity of Ga_2O_3 native substrates.

Table 15 summarizes the advantages and disadvantages of each growth method.

Table 15: Summary of Epitaxy Growth Methods

Epitaxy Method	Advantages	Disadvantages	Notes
MBE	• Uniform layer doping and thickness. • Large wafer sizes. • Scalable for production • Good control of doping density using Sn. • Electron mobility as good as the substrates.	• Requires ultra-high vacuum. • Expensive equipment. • Slow growth rates (typically 1nm/min).	• Two choices for oxygen source; ozone or rf-plasma. • Homo-epitaxy or hetero-epitaxy. •
HVPE	• Very rapid growth. • High purity layers. • Suitable for α-Ga_2O_3 and β-Ga_2O_3 layers. • Relatively inexpensive. • Good control of growth rate. • Relatively inexpensive.	• High growth temperature. • Layer thickness uniformity is uncertain. • Small wafer sizes at present.	• Atmospheric pressure system. • Inorganic precursors. • Mass transport limited growth. • Horizontal system.
MOCVD	• Uniform layer doping and thickness. • Large wafer sizes. • Scalable for production. • Vertical system with multi-wafer capability.	• Poor electrical parameters. • Marginally stable growth parameters. • Requires much more work. • Relatively expensive.	• Vacuum system. • Organic precursors for Ga. • Water works better than pure oxygen as O_2 precursor.
Mist-CVD	• Simple and inexpensive. • Suitable for α-Ga_2O_3 layers. • Medium growth rates. • Inorganic precursors allow the growth of highly pure layers. • Good doping control. • High carrier concentration demonstrated.	• Organic Ga precursors cause unacceptable levels of impurities. • Large wafer sizes. • Scalable for production. •	• Currently all horizontal systems. • Vertical system designs are possible. • Organic or inorganic precursors.

Ion Implantation	• Large wafer sizes possible. • Scalable for production. • Wide doping range. • Selective area. • Planar technology.	• High temperature activation causes surface morphology change. • Low mobility so far. • Surface dopant depletion during activation. • Only useful for β-Ga_2O_3 because of high temperature activation requirement.	Used for ohmic contact formation. Also used for FET channels.

.

G. Contributing Research Groups in Epitaxial Growth

Table 16 lists the active researchers in epitaxial growth of Ga_2O_3. This field is also dominated by Japanese research groups that include universities and corporations. Private Japanese corporations' contributions are highly significant indicating near term commercial interest in this technology.

Table 16: Active research groups in epitaxial growth of Ga_2O_3.

Epitaxy Method	Research Organization	Country	Notes
MBE	• Tamura Corporation • National Institute for Materials Science • National Inst. For Information and Comm. • Koha Corporation • Toyama National College of Technology • UCSB • Paul-Drude Institut Festkorperelektronik	• Japan • Japan • Japan • Japan • Japan • USA • Germany	Japan dominated. Most likely method to be used in fabricating epi-layers for lateral transistors in production.
HVPE	• National Institute of Materials Science • University of Tokyo	• Japan • Japan	All Japanese. Most likely technology to be used for vertical devices for power applications. Can be scaled up for production rapidly.
MOCVD	• Shandong University • Leibniz Inst. For Crystal Growth • Nat. Chung Hsing University • Inha University • Universita di Padova • CNR-IMEM	• China • Germany • Taiwan • S. Korea • Italy • Italy	Many participants except Japan. Possible alternative to MBE for production of lateral transistors.

	• Argonne National Laboratory	• USA	
Mist-CVD	• Kyoto University	• Japan	All Japanese.
	• Kochi University of Technology	• Japan	Suitable for hetero-
	• Tokyo Institute of Technology	• Japan	epitaxy of α- Ga_2O_3
	• FLOSFIA Inc.	• Japan	layers.
			May scale up to large wafer sizes rapidly for production.
Ion Implantation	• Tamura Corporation	• Japan	Limited activity so far.
	• National Inst. For Information and Comm.	• Japan	
	• Koha Corporation	• Japan	

8. ELECTRONIC DEVICES

With the availability of high quality substrates and epitaxial layers, electronic devices were fabricated using both α- and β-Ga$_2$O$_3$ semiconductors. This field is moving fast as better quality materials are made available and the doping mechanisms are perfected. For power devices, both lightly and highly doped layers are needed. Both of these are now available with undoped crystal background carrier concentrations of as low as 1e-13 cm^{-3} and highly doped crystals with N$_D$-N$_A$ > 1e19 cm^{-3}. Unfortunately, no reliable p-type doping is available. This will limit the type of devices that can be made with the existing materials to majority carrier devices. This is a major limitation at present but there may be a technical breakthroughs in the future using heterojunction to implement p-n junctions. This would bring a large number of new device types into play, especially for power electronics where Ga$_2$O$_3$ is competitive. In this section we will only review the majority carrier devices that have two or three terminals.

A. Two Terminal Devices

The only two terminal devices reported so far are the UV detectors and Schottky Barrier Diodes (SBD). The first device type takes advantage of the ultra-wide bandgap properties of Ga$_2$O$_3$ to detect short wavelength UV light. The second device type makes use of the high electrical breakdown strength to achieve high blocking voltage diodes.

a. UV Detectors

Solar-blind UV detectors find use in missile guidance systems and have been the subject of intensive research about a decade ago with the availability of wide bandgap semiconductors based on AlGaN. The function of these simple devices is to detect low wavelength UV light (shorter than 280nm) while being insensitive to visible and infrared radiation. Currently, high sensitivity UV detectors and detector arrays can be made from Al$_x$Ga$_{1-x}$N semiconductor. Various device types have been fabricated with varying detector sensitivities. The device types include photoconductors, metal-semiconductor-metal (MSM) photodetectors, Schottky barrier photodiodes, p-i-n (PIN) photodiodes, avalanche photodiodes, and focal plane arrays [234]. While some of these devices require good ohmic contacts (e.g. photoconductors, PIN diodes) others can be implemented using rectifying Schottky contacts only. In all cases, the device structure is simple but the materials quality requirements are stringent to minimize dark currents and visible light response.

With the availability of high quality Ga$_2$O$_3$ substrates and epitaxial layers, there has been an interest to implement UV detectors with this semiconductor. Currently, due to the lack of good p-n junctions, only photoconductors and MSM detectors can be fabricated.

The initial UV detectors were made from nanocrystals of Ga$_2$O$_3$ [235-237]. These early devices were mostly photoconductive type and suffered from materials quality variations and large dark currents. Thin films were made using sol-gel and PLD (it was referred to as laser MBE) were also used with varying levels of success [57, 238]. Both photoconductors with ohmic contacts and photodetectors with Schottky contacts were demonstrated on the same film. When Ti/Au ohmic contacts were converted to Schottky contacts by annealing, an increase in responsivity was detected [239]. In another examples of

using thin film Ga_2O_3 for UV detection, evaporated films on SiC were employed [240]. The response of photoconductors made on thin film Ga_2O_3 is shown in Figure 43. Although the reverse bias current increased nearly 5 orders of magnitude when exposed to UV compared to dark conditions, the overall responsivity was less than 0.1A/W. This is similar to the low responsivity obtained with Ga_2O_3 thin films grown on sapphire by MBE [24].
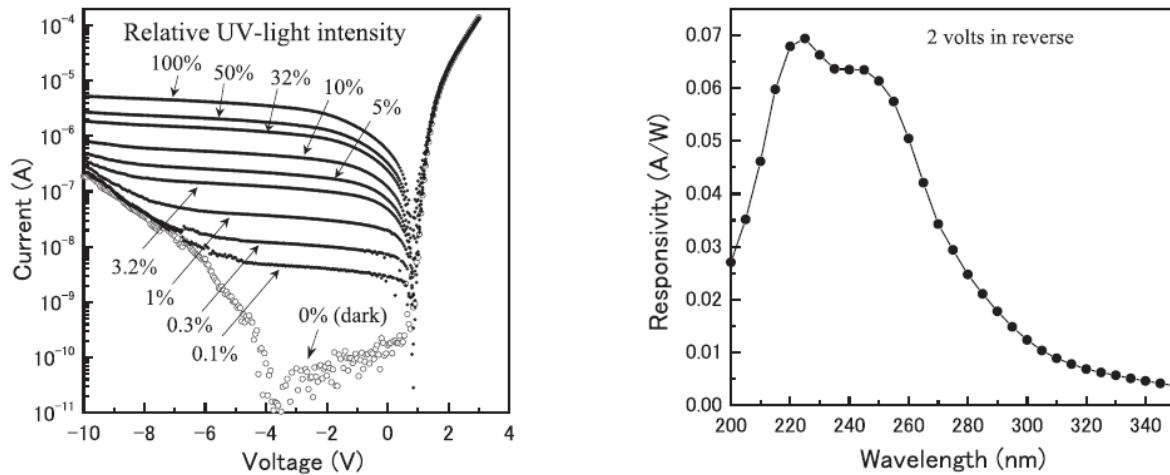
Figure 43: Response of Ga$_2$O$_3$ thin film photodiodes to UV radiation a) light intensity response b) spectral response [240].

UV detectors fabricated on single crystal Ga_2O_3 exhibited similar characteristics to thin film devices. A similar increase in responsivity was also observed with photodetectors made on single crystals when the ohmic contacts were annealed to turn them into Schottky contacts [241]. Responsivity was higher but still under 1A/W. Although, it was claimed that responsivity values as high as 1000 A/W were achieved with annealed samples, this value is much higher than 100% conversion and implies that there is an internal gain in the device. The physical origin of this gain is not clear.

In summary, only simple MSM type photodiodes and photodetectors were fabricated so far on various Ga_2O_3 crystals (mostly nanocrystals and thin films). These initial examples demonstrate that Ga_2O_3 can be used for this application, but the electrical performance levels are inadequate at present to challenge the incumbent technology based on $Al_xG_{1-x}N$ semiconductor. This application probably is not a major driver for this technology.

b. Schottky Barrier Diodes

Schottky Barrier Diodes (SBD) are simple rectifying devices made from non-ohmic metal contacts on semiconductors. They are used as blocking devices with fast switching times. The advantage of SBD over the regular p-n diode is that minority carriers are not involved and therefore diode recovery times are shorter. They have, however, a great disadvantage in R_{on} values. As the doping density is reduced and the layer thickness is increased to achieve higher blocking voltages, R_{on} also increases. Because R_{on} does not benefit from minority carrier injections, as in PIN diodes, its value can be high. Other technologies, such as Si and SiC, use a combination of p-n junction and SBD to benefit from the strengths of both technologies. This option is not available with Ga_2O_3 at present.

The current SBDs made on Ga_2O_3 are not tailored for any particular application. They are simply used to assess the material properties. For example, the prime strength of Ga_2O_3, high breakdown voltage, can be assessed using these simple devices. Although SBDs can be made on planar surfaces, R_{on} values for these type of devices are much higher than their vertical counterparts. The assessment of material parameters using planar devices are more complicated, especially for β-Ga_2O_3, which as many anisotropic parameters. We will only survey the vertical SBDs here.

There are only a few critical technological components of a SBD; Schottky metal for rectification and ohmic metal for backside contact. SBDs can be fabricated directly on suitably doped substrates, or on lightly doped epitaxial layers on highly doped substrates. The first approach yield better blocking voltages whereas the second approach yield better R_{on}. A third approach is to remove the substrate entirely and make ohmic contact to the opposite side of the film. This approach yields the lowest R_{on}.

The most critical part of the technology is the Schottky metal, which must produce a rectifying contact. The Fermi Level difference between the metal and the semiconductor plus interface states produce an energy barrier. This barrier height is small with narrow bandgap semiconductors, but easier to achieve with wide bandgap semiconductors. In the case of Ga_2O_3, several metals have been shown to be suitable for this purpose. Ti seems to be a good ohmic contact. A typical SBD cross section is shown in Figure 44.
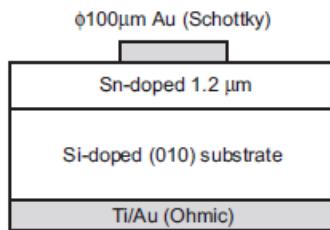
Figure 44: Schematic drawing of a typical vertical SBD [86].

A survey of SBDs fabricated on α- and β-Ga_2O_3 substrates and/or epitaxial layers are shown in Table 17. At this early stage in the device development, there is no consistency in the preferred approach to making these devices. Substrates grown by CZ, FZ and EFG have been used either directly or as support for the epitaxial layers. Epitaxial layers have been grown by almost all available techniques including MBE, HVPE, and mist CVD. No results are available with MOCVD epitaxial layers.

Several interesting observations can be made from the results in this table. First, the Schottky barrier heights all seem to be about 1eV. This is a large value compared to what can be obtained with narrower bandgap semiconductors. Second, the ideality factor seems to be almost unity. Third, Schottky contacts are made using noble metals such as Au and Pt. Ti, which is normally used to make rectifying contacts to other semiconductors such as GaAs, is used as ohmic contact. Fourth, several crystal orientations were used. The impact of crystal orientation on device performance is not clear from the data.

PARAMETER

PARAMETER									
Substrate	β-Ga_2O_3	β-Ga_2O_3	Sapphire	Sapphire	Sapphire	β-Ga_2O_3	β-Ga_2O_3	β-Ga_2O_3	β-Ga_2O_3
Substrate Growth Method	FZ and EFG	CZ	c-plane	c-plane	c-plane	EFG	FZ	FZ/EFG	EFG
Substrate Orientation	(010)	(100)	N/A	N/A	N/A	(-201)	(010)	(010)	(001)
Substrate Thickness (µm)	600		N/A	N/A	N/A	606		600	600
Substrate Doping (cm^{-3})	1.00E+19	0.6-8e17	N/A	N/A	N/A	1.40E+17	0.3-1e17	1.00E+19	6.00E+18
Epi-layer	β-Ga_2O_3	N/A	α-Ga_2O_3	α-Ga_2O_3	α-Ga_2O_3	N/A	N/A	β-Ga_2O_3	β-Ga_2O_3
Epi-layer Growth Method	MBE (ozone)	N/A	Mist	Mist	Mist	N/A	N/A	MBE (ozone)	HVPE
Epi-layer Orientation	(010)	N/A	(0001)	(0001)	(0001)	N/A	N/A	(010)	(001)
Epi-layer Thickness (µm)	1.4	N/A	3	0.43	2.58	N/A	N/A	1.2	12
Epi-layer Dopant	Sn	N/A	Sn	Sn	Sn	N/A	N/A	Sn	Sn
Epi-layer Carrier Conc. (cm^{-3})	4.00E+16	N/A	2-7e17	2-7e17	2-7e17	N/A	N/A	6.00E+16	<1e13
Ohmic Metal	Ti/Au	Ga/In	Ti/Au	Ti/Au	Ti/Au	N/A	Ti/Au	Ti/Au	Ti/Au
Schottky Metal	Pt/Au	Au	Au	Pt/Ti/Au	Pt/Ti/Au	Ni/Au	Pt/Ti/Au	Au	Pt/Ti/Au
Barrier Height (eV)		1.04	1.7-2.0	N/A	N/A	1.25	1.3-1.5		
Ideality Factor			1.1	N/A	N/A	1.01	1.04-1.06	1.13	
Turn-on Voltage (V)	1.7								
Current Density (A/cm^2)	250			3000	3000	70.3	200		
Ron (mΩ-cm^2)	2			0.1	0.4	11	4.30-7.85		
V$_{br}$ (V)	100		270	531	855	40	115-150	125	1000
E$_c$ (MV/cm)	0.71		0.90	12.35	3.31			1.04	0.83
Reference	[187]	[242]	[223]	[105]	[105]	[176]	[243]	[86]	[198]

Based on this small database, we can observe that the on-current density is not correlated to the carrier concentration, although R_{on} shows strong dependence on carrier concentration. R_{on} also shows dependence on the layer thickness, as expected. The highest current density in this table is 3,000A/cm^2. Other results are in the 70-250A/cm^2 range. The most important parameters are the breakdown voltage and R_{on}. Both of these parameters are highly scattered. The highest breakdown voltage is obtained with 12µm thick HVPE epitaxial layers. All other β-Ga_2O_3 epi-layers showed moderate breakdown voltages even for several micron thick layers.

The most interesting, and perhaps the controversial results are obtained with α-Ga_2O_3 epitaxial layers grown by mist-CVD. Both the breakdown voltage and the R_{on} values are particularly low with devices fabricated on these films. Part of the reason for low R_{on} is the removal of the substrate, which eliminates substantial series resistance. R_{on} values of 0.1 and 0.4 mΩ-cm^2 were obtained with 0.43 and 2.58 µm thick layers. The corresponding breakdown voltages were 531 and 855V, respectively. These voltages translate to breakdown electrical filed strengths of 12.35 and 3.31 MV/cm. The first value is extremely high; even higher than the maximum predicted value of 8MV/cm for Ga_2O_3 and it stands out among other E_c values, which are about 1MV/cm for β-Ga_2O_3. It is possible that α-Ga_2O_3, with its larger bandgap value compared to β-Ga_2O_3 is producing extremely high breakdown strength. But the difference in Eg values is very small (<0.3eV) and such a large difference cannot be explained based on this difference. The second though is that the crystal structures are different and the corundum structure of α-Ga_2O_3 is favoring higher breakdown strength. Third, the high E_c value is obtained only with very thin layers. The

breakdown strength of thicker layers was much lower. As the layers get thicker, maybe due to higher lattice imperfections, E_c is reduced. If indeed, E_c is thickness dependent, we can expect much effort to be spent on epi-layer quality improvements.

For a vertical unipolar device, the R_{on} and V_b are related through the following equation [54].

$$R_{on} = \frac{4V_b^2}{\varepsilon \mu E_c^3}$$

Where ε is the dielectric constant, μ is the mobility, E_c is the breakdown field, V_b is the breakdown voltage and R_{on} is the on-resistance.

Using the material parameters from Table 4 and the device results from Table 17, we can chart the results so far on to what is expected ultimately expected from perfect crystals, as shown in Figure 45.
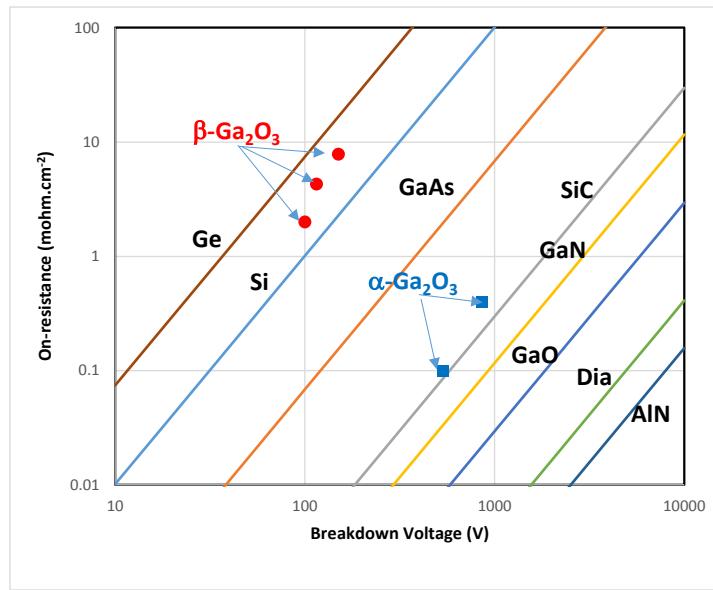
Figure 45: On resistance vs. breakdown voltage expected from material properties for several important semiconductors. Actual results obtained with α- and β-Ga$_2$O$_3$ SBDs are superimposed.

It can be seen immediately that, within these limited results, the SBDs on The α-Ga$_2$O$_3$ epitaxial layers are significantly better. As a snapshot in time, the current β-Ga$_2$O$_3$ results are similar to what can be expected from Si devices. The α-Ga$_2$O$_3$ results seem to be comparable to SiC devices. As more results become available, the actual results will probably get closer to the GaO line on this figure.

B. Three-Terminal Devices (Transistors)

Transistors are three-terminal devices that can be used as high power switches and amplifiers. There are many types of transistors but the ones applicable to the Ga$_2$O$_3$ technology, at present, are unipolar types. Within this narrow group of devices, we are confined further down to mostly depletion type of devices (some enhancement mode operation possible). The first Ga$_2$O$_3$ transistor appeared in 2012 and since then several other groups fabricated transistors using α- and β-Ga$_2$O$_3$ layers fabricated by different

growth methods. Additionally, thin film transistors were also fabricated on Si-substrates using additive techniques such as spray pyrolysis and exfoliation and film transfer.

Table 18 summarizes the characteristics and the performance of transistors reported so far.

Table 18: Reported Ga$_2$O$_3$ transistor characteristics and electrical parameters.

PARAMETER

	MESFET	D-MOSFET	D-MOSFET	MESFET	FP-MOSFET	D-MOSFET	Nano-crys.	TF	Nano-crys.
Transistor type									
Substrate	β-Ga$_2$O$_3$	β-Ga$_2$O$_3$	β-Ga$_2$O$_3$	Sapphire	β-Ga$_2$O$_3$	β-Ga$_2$O$_3$	Si/SiO2	Si/SiO2	Si/SiO2
Substrate Growth Method	FZ	FZ	FZ	N/A	FZ	CZ	N/A	N/A	N/A
Substrate Orientation	(010)	(010)	(010)	c-plane	(010)	(100)	N/A	N/A	N/A
Substrate Thickness (μm)	600			N/A	N/A	N/A	N/A	N/A	N/A
Substrate Doping (cm^{-3})	Mg: Insulating	Fe: Insulating	Fe: Insulating	Insulating	Fe: Insulating	Mg: Insulating	p+	p+	p+
Epi-layer	β-Ga$_2$O$_3$	β-Ga$_2$O$_3$	β-Ga$_2$O$_3$	α-Ga$_2$O$_3$	β-Ga$_2$O$_3$	β-Ga$_2$O$_3$	β-Ga$_2$O$_3$	poly-Ga$_2$O$_3$	β-Ga$_2$O$_3$
Epi-layer Growth Method	MBE (ozone)	MBE (ozone)	MBE (ozone)	Mist-CVD	MBE (ozone)	MOCVD	Exfoliated CZ	Pyrolysis	HVPE
Epi-layer Orientation	(010)	(010)	(010)	(0001)	(010)	(100)	(100)	N/A	(001)
Epi-layer Thickness (μm)	0.3	0.3	0.3	0.21	0.3	0.2	0.020-0.100		0.3
Epi-layer Dopant	Sn	Sn	Si implant	Sn	Si implant	Sn	N/A		UID
Epi-layer Carrier Conc. (cm^{-3})	7.00E+17	7.00E+17	3.00E+17	3.00E+17	3.00E+17	4.80E+17	5.50E+17		3.00E+17
Contact Layer Fabrication	BCl3 RIE	Ion Implant	Ion Implant	N/A	Ion Implant				
Contact Layer Carrier Conc. (cm^{-3})	N/A	5.00E+19	5.00E+19	N/A	5.00E+19				
Ohmic Metal	Ti/Au	Ti/Au	Ti/Au	Ti/Au	Ti/Au	Ti/Al/Ni/Au	Ti/Au	Al or Ca	Ti/Au
Gate Metal	Pt/Ti	Pt/Ti/Au	Au	AgO$_x$	Ti/Pt/Au	Ti/Au	Si	Si	Ni/Au
Passivation	None	ALD Al$_2$O$_3$	ALD Al$_2$O$_3$	N/A	ALD Al$_2$O$_3$	ALD Al$_2$O$_3$	N/A	N/A	HfO$_2$
Gate dielectric	None	ALD Al$_2$O$_3$	ALD Al$_2$O$_3$	N/A	ALD Al$_2$O$_3$	ALD Al$_2$O$_3$	N/A	N/A	HfO2
Gate dielectric thickness (nm)	N/A	30	30		20	20	N/A	N/A	42
Gate Length (μm)	4	2	4	5 and 10	2	2	3	30-120	3
S-D spacing (μm)	20	20	20		22	3.6	3	30-120	10
S-G spacing (μm)	8	9	8		5	0.8			2
G-D spacing (μm)	8	9	8		15	0.60			5
Gate Width (μm)	628	500	500	40 and 262	200		1	500-1500	11.7
I$_{dmax}$ (mA/mm)	26	39	65		78	60	0.002		11
V$_{br}$ (V)	250	370	415	48	755	230	70		~80
Breakdown Field (MV/cm)	0.313	0.411	0.519		0.503	3.833			
Pinch-off Voltage (V)	-30.0	-20.0	-30.0	-0.8	-55.0	-30.0	-14.0	130.0	0.1-2.9
Max. Transconductance (mS/mm)	2.30	1.50	3.60		3.40	3.50	0.40		0.18
On-off ratio	1.E+04	>1e10	>1e10	3.E+07	>1e9	1.E+07	1.E+07		>1e4
Field effect mobility (cm$_2$/Vs)				1.3	95	19.7	70	2	0.17
Reference	[70]	[244]	[18]	[103]	[245]	[71]	[246]	[247]	[248]

The first set of transistor results came from Japanese researchers at the National Institute for Information and Communication Technology and Tamura Corporation. Working with other researcher at Japanese universities, this group fabricated the first transistor with large breakdown voltage. It is not surprising that they were the first to fabricate devices because they have been previously very active in developing bulk crystal and epitaxial layer fabrication method. Therefore they had access to this new material before others. Their first transistor was a simple Metal Semiconductor Field Effect Transistor

(MESFET). Using the same metallization schemes for ohmic and Schottky contacts as previously used for SBDs (i.e. Ti/Au and Pt/Ti, respectively, they have fabricated circular pattern FETs with gate lengths of a modest 4μm [70]. Figure 46 shows cross-sectional and top views of this transistor. Circular FET geometries are not typically how these transistors are produced, but it provides a simplicity to device fabrication by eliminating a difficult mesa isolation step.
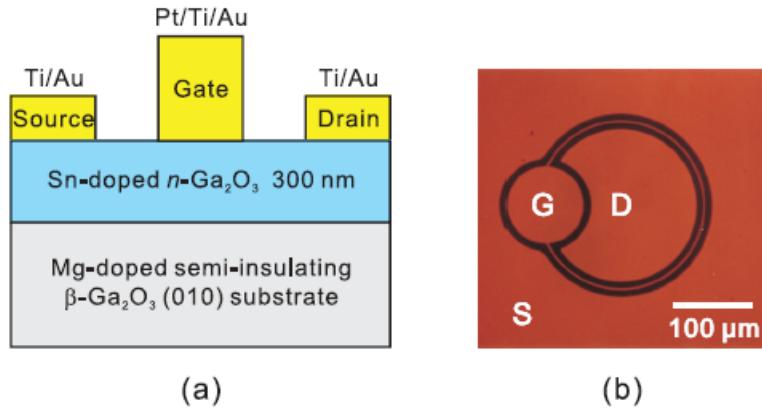
Figure 46: Cross-sectional schematic illustration and (b) optical microscope micrograph of Ga_2O_3 MESFET [70].

This transistor suffered from technological deficiencies in almost all aspects of transistor fabrication. Source and drain contacts were barely ohmic even though the researchers went through great pains to treat the wafer surface with BCl_3 RIE to create charges at the interface. The gate contact was also barely a Schottky contact evidenced by large gate leakage current. The pinch-off was soft due to poor charge confinement at the semi-insulating substrate and the epitaxial layer. But, it served to highlight the fact that transistors can be fabricated using Ga_2O_3 and that reasonably high breakdown voltages can be obtained. The maximum electrical field in this transistor is estimated to be 0.33 MV/cm, which is even lower than the values obtained with SBDs (see above).

The same group later improved this device by addressing the issues highlighted above. First, to reduce the gate leakage current, a thin layer of gate insulator (ALD Al_2O_3), was used. Second, the ohmic contacts were improved by local ion implantation at the location of source and drain contacts [233]. A contact resistivity of 8.1e-6 $\Omega.cm^2$ was obtained. This is reasonably low value for an ohmic contact for now, but other technologies can achieve better values. Third, a different substrate doping was used (Fe doped) to improve pinch-off characteristics. All these first order improvements are in the right direction and better results were obtained. The transistor layout has not changed, which is still not suitable for any purpose other than materials evaluation. The breakdown voltage and electrical field strength values were improved as shown in Table 18. The Sn-doped epitaxial layer used for this transistor had doping density variations across the wafer, which will impact almost all transistor parameters. It is assumed that the results presented are the best values measured, and do not represent typical values.

In another iteration of their transistor, the problems associated with Sn doping uniformity was addressed by eliminating this dopant during epitaxial layer growth. The transistor channel and the ohmic contact regions were formed by different doses of Si ion implantation. This approach also solves the

mesa isolation issue, since ion implantation is applied to selective areas. The device performance was improved with respect to current levels and breakdown voltage. The maximum electric filed value was marginally improved to 0.519 MV/cm.

Although not mentioned as an issue with the latest transistor version from this group at the time of publication, they later reported that ion implantation damage causes migration of Fe dopants from the substrate into the active region of the device. Similar problems were observed at the early stages of the GaAs technology. The solution to this problem was to have a undoped epitaxial buffer layer between the ion implanted region and the substrate [249]. This innovation was applied to making even better transistors a few years later [245]. A cross-sectional drawing and a top view of their latest transistor is shown in Figure 47. In addition to the improvements to layer structure, this transistor also has a field plate structure to reduce the electrical fields near the drain side of the gate electrode. Also note that the transistor is now in more conventional rectangular shape. Because the active device area is defined by ion implantation, mesa isolation was not needed. Although higher breakdown voltages were obtained with this transistor (755V), the electrical field value was not improved over their previous device. Note that the electrical field profile across the channel is not linear and the maximum field value may be higher in some localized areas. Nevertheless, the object of this transistor was to suppress these localized high field using field plates and demonstrate high breakdown voltages across multi-micron channel distance. If 8MV/cm field strength could be maintained uniformly across the channel between the gate and the drain contacts, the expected breakdown voltage would have been 12,000V. The demonstrated value of 755V is only a small fraction of this expected value.
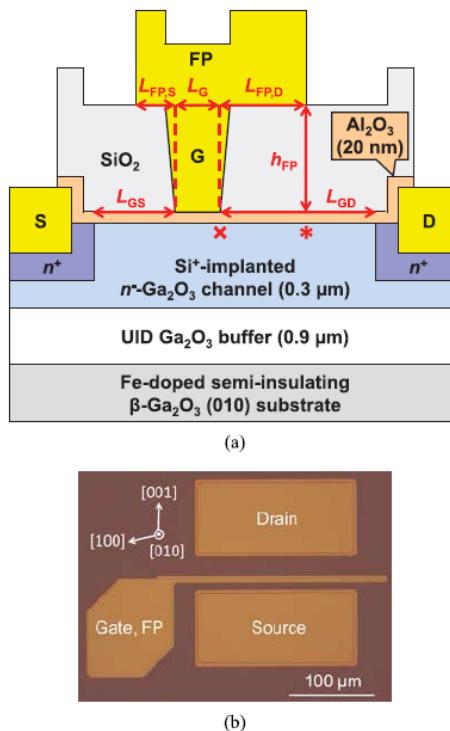
Figure 47: Field Plated MOSFET a) cross sectional drawing, b) top view of the rectangular transistor [245].

The first Ga$_2$O$_3$ transistor that looks more like the modern transistors was demonstrated at AFRL [71]. This transistor makes use of mesa isolation, for the first time, using BCl$_3$ ICP/RIE. The gate length is small but not yet at the sub-micron dimensions of modern power transistors. In contrast to previous transistors, this device makes use of MOCVD grown (100) layers on Mg-doped CZ substrates. The device parameters are comparable to previous devices in terms of saturated current level, on/off ratios, transconductance and pinch-off voltage. The significant parameter highlighted with this transistor is the high electrical breakdown strength of 3.8MV/cm. Although this demonstration was for sub-micron gate-drain spacing of 0.6μm, it still provides a useful benchmark. Scaling of this high breakdown strength was not provided by making longer channel transistors with uniform electrical fields.
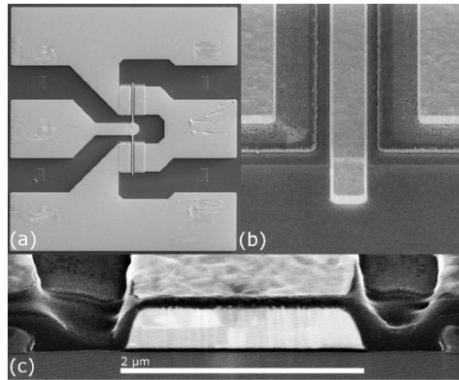
Figure 48: SEM images of β-Ga$_2$O$_3$ MOSFET. a) top view, b) close up of the channel area, c) cross section [71].

Recently, there also have been reports of transistors fabricated on less conventional Ga$_2$O$_3$ materials. A group of researchers from New Zealand and Japan have used mist-CVD grown α-Ga$_2$O$_3$ epitaxial layers to fabricate MESFETs [103]. Sapphire was used as the substrate. Circular transistor layout was used to avoid mesa isolation, as it was the case with earlier β-Ga$_2$O$_3$ FETs. Although the ohmic contact metals were similar to other transistors, a special Schottky contact based on AgO$_x$ was used. This rectifying contact method was originally developed for ZnO- based materials [250, 251] and have shown similar improvements in Schottky diode characteristics for Ga$_2$O$_3$. Although the transistors showed reasonable on/off ratios, all other parameters were worse than those obtained with β-Ga$_2$O$_3$ FETs. Part of the reason for poor performance was the quality of the epitaxial layer, which only had a mobility of 0.23 cm^2/Vs.

Similarly poor performance was obtained with Ga$_2$O$_3$ transistors when the epitaxial layer was prepared in a technique similar to the one described above. Using spray pyrolysis technique, researchers in England and Greece fabricated bottom-gated MOSFETs using highly doped Si and the gate electrode. Not only was the electrical performance of this transistor was very poor, but also it exhibited strong hysteresis in transfer characteristics.

More recently, some researchers in the USA used nano-membranes of Ga$_2$O$_3$ to fabricate transistors [246, 248]. In construction, these transistors resemble 2D transistors made with graphene or MoS$_2$ and therefore their characteristics cannot be directly compared to more conventional devices made with epitaxial layers. The surprising aspect of this approach is that almost 2D layers (flakes) can be peeled off

β-Ga$_2$O$_3$ crystals using scotch tapes. Ga$_2$O$_3$ is not known as layered crystal, but it has strong cleavage planes where the bonds are weaker. Figure 49 shows cross-sectional views of these unconventional transistors. Unlike other thin film transistors, these type of transistors can preserve high crystal quality of substrates, as evidenced by the high measured field-effect mobility of 70 cm^2/Vs [246]. This is the highest mobility value obtained with Ga$_2$O$_3$ transistors so far. Although a similar approach was employed by Tadjer [248], field-effect mobility of only 0.17 cm^2/Vs was demonstrated.
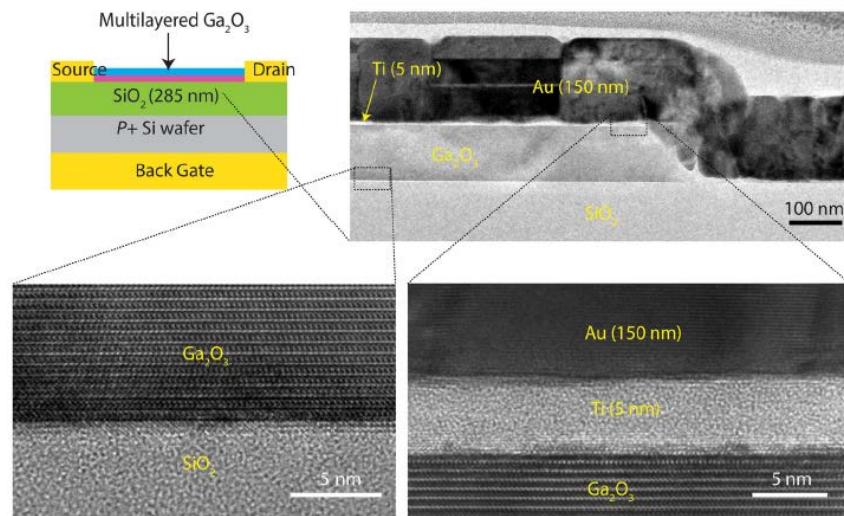
Figure 49: Cross-sectional TEM image of β- Ga$_2$O$_3$ FETs, showing a flat interface between β-Ga2O3 and the SiO$_2$ dielectrics as well as between the β-Ga2O$_3$ and the Ti/Au electrode [246].

C. Summary of Electronic Devices

Only a limited number of electronic devices have been demonstrated using Ga$_2$O$_3$ as the semiconductor so far. Because of its doping limitations, all devices are majority carrier type. As 2-terminal devices, photoconductors and photodetectors were fabricated. Three-terminal device include MESFETs and MOSFETs, both operating mostly in depletion mode.

Photodetectors are some of the simplest devices to fabricate since they need only Schottky or ohmic contacts, and not necessarily both at the same time. The main application of these devices are solar-blind UV radiation detection. Because of its ultra-wide bandgap, Ga$_2$O$_3$ offer a unique opportunity for the detection of UV with wavelengths shorter than 280nm. Indeed, the fabricated devices show the expected wavelength response, but the responsivity values are not yet competitive with other detectors made from Al$_x$Ga$_{1-x}$N.

Schottky Barrier Diodes (SBD) are also simple 2-terminal devices that can highlight the expected high breakdown voltage characteristics of this material. Although the initial results are highly encouraging, the breakdown strength values obtained so far with β-Ga$_2$O$_3$ crystals are about 1MV/cm, far short of the expected 8MV/cm theoretical value. Results with α-Ga$_2$O$_3$ SBDs, on the other hand, showed results that

are as high as 12 MV/cm. This is 50% higher than the theoretical value. There are 2 concerns with this spectacular results. First, it only comes from a single source. No one else repeated these results. Second, the best performance was obtained only with sub-micron thickness films. When the film thickness was increased to about 2.5µm, the breakdown strength was reduced to about 3.3MV/cm. Such thickness (distance) dependent field strength values were noticed with the three terminal devices also as discussed below. The R_{on} vs V_{br} relationship with the fabricated devices so far indicate that β-Ga_2O_3 devices have the performance levels that are expected of the current Si devices, whereas α-Ga_2O_3 devices have performance levels similar to SiC devices. Obviously, the performance of these simple devices rely heavily on the crystal quality, and any improvements in the material quality will also improve the device performance in the future.

Three-terminal devices require more fabrication sophistication and their performance can be impacted by both the material properties and the fabrication steps. A systematic improvement is device performance was undertaken by the Japanese group, who started with a simple MESFET on single epitaxy layer. In 4 iterations, they have developed devices with selectively implanted contact layers and field plates. Although they have demonstrated a three-terminal breakdown voltage of 755V, the maximum electrical field strength over a 15µm channel device was only about 0.5MV/cm. The MOSFET fabricated at AFRL demonstrated higher field strength of 3.8MV/cm but only for short channel devices (0.65µm). These devices together represent the current published status of the mainstream Ga_2O_3 transistor technology.

Other transistors were fabricated using α-Ga_2O_3 layers grown by mist-CVD technique, β-Ga_2O_3 layers grown by spray pyrolysis and layer transfer. The overall performance of these devices were worse that the mainstream devices. On the other hand, transistors fabricated using exfoliated β-Ga_2O_3 nano-membranes showed the highest field effect mobility of all Ga_2O_3 transistors. This last results underscores the importance of crystal quality in device performance.

D. Contributing Research Groups in Device Technology

Table 19 lists the active researchers in Ga_2O_3 device technology. This field is also dominated by the Japanese research groups that include universities and corporations. Since the Japanese are leaders in crystal growth technologies, their early leadership in device technology is not surprising. Other research groups rely on the Japanese supply of materials for their research, except some Chinese groups are growing their own material. Private Japanese corporations' contributions are highly significant indicating near term commercial interest in this technology. A short corporate profiles of 2 prominent Japanese commercial companies engaged in Ga_2O_3 technology is shown in the Appendix.

Table 19: List of research groups active in Ga₂O₃ device fabrication.

Device Type	Research Organization	Country	Notes
Photodetectors	• National Institute for Information and	• Japan	Chinese are very active in this field.

	Communication		Material requirements are not severe.
	• Ishinomaki Senshu University	• Japan	
	• Nippon Light Metal Co., Ltd	• Japan	
	• International Center for Materials Nanoarchitectonics	• Japan	
	• Vienna University of Technology	• Austria	Mostly nanocrystals-based detectors.
	• Sensor Materials Center, NIMS	• Japan	
	• Hunan University	• China	
	• Chinese Academy of Science	• China	
	• Beijing University of Posts and Telecommunications	• China	
	• Beijing University of Posts and Telecommunications	• China	
	• Zhejiang Sci-Tech University	• China	
	• The State University of New York at Potsdam	• USA	
SBD	• FLOSFIA Inc.	• Japan	Mostly Japanese.
	• Tokyo University	• Japan	
	• Tamura Corporation	• Japan	All α-Ga$_2$O$_3$ SBD results are from FLOSFIA Inc.
	• National Institute for Information and Communication	• Japan	
	• Linkoping University	• Sweden	
	• Koha Company Limited	• Japan	
	• Japan Science and Tech Agency	• Japan	
	• Saga University	• Japan	
	• Rutsumeikan University	• Japan	
	• Kyoto University	• Japan	
	• Humboldt Universitat zu Berlin	• Germany	
	• Leipniz-Institut fur Kristallzuchtung	• Germany	
β-Ga$_2$O$_3$ FET	• National Institute for Information and Communication	• Japan	Many participants and highly cooperative work between institutions.
	• Koha Company Limited	• Japan	
	• Japan Science and Tech Agency	• Japan	
	• Tamura Corporation	• Japan	
	• Tokyo University	• Japan	Majority of work concentrated in a few research centers in Japan.
	• Air Force Research Laboratory	• USA	
	• Naval Research Laboratory	• USA	
	• Leipniz-Institut fur Kristallzuchtung	• Germany	
	• Imperial College	• England	
	• ICEHT	• Greece	USA is competitive.
	• University of Crete	• Greece	
	• Thessalonika University	• Greece	
	• Korea Aerospace University	• S. Korea	
	• University of Notre Dame	• USA	

	• UCSB	• USA	
	• IBM Watson RC	• USA	
	• University of Parma	• Italy	
α-Ga$_2$O$_3$	• University of Canterbury	• New Zealand	Poor performance
	• Kochi University of Technology	• Japan	compared to β-Ga$_2$O$_3$

9. SUMMARY

Ga₂O₃ is a member of the ultra-wide bandgap semiconductor family. Because of its wide bandgap, it finds applications in UV-transparent conductive films, UV detectors, and high power electronics and possibly in microwave switching and amplification. Power electronics applications range from on-chip power converters to high voltage rectifiers for electric power transmission lines. High-voltage switching transistors used in these applications are required to have small ON resistance while providing very high blocking voltages in the OFF state. There are already kV-range power switches today. The target for the Ga_2O_3 devices will be in the 100's of kV to MV range.

The empirical relationship between the bandgap and the maximum electrical field that can be sustained in semiconductors predicts a critical breakdown field strength of 8MV/cm for Ga_2O_3. This number is not etched in stone. Based on the variation in the bandgap value from 4.4 to 4.9eV for various crystal forms, and models for direct and indirect bandgap semiconductors, a range of values from 4.6 to 9.3 MV/cm can be expected. As stated before, **all other parameters being equal**, wide bandgap semiconductors are preferred over narrow band semiconductors for electronics applications, because the large energy separation between the conduction and the valance bands allows the device to operate at elevated temperatures and at high voltages. When the relative advantages of Ga_2O_3 are examined using various figure-of-merit methods, extremely high merit numbers are obtained. One of the most commonly used FOM, Baliga FOM, indicates 3443 fold advantage over Si.

Ga₂O₃ belongs to the ionic metal-oxide semiconductor family, which also includes ZnO. Unlike other members of this semiconductor family, Ga_2O_3 is only useful as a single crystal i.e. amorphous or poly-crystalline films are not useful for electronics. Therefore, there is an added emphasis to the material quality to ensure proper device operation. Single crystal substrates are essential for this technology.

There are 5 possible polymorphs of Ga₂O₃. In many respects Ga_2O_3 resembles Al_2O_3 because of the similarities between the Ga and Al ions. But, in crystalline form, Ga_2O_3 and Al_2O_3 have drastic differences. The alpha polymorph is the most common and stable form of Al_2O_3, whereas only the beta-polymorph of Ga_2O_3 is thermally stable. That means, melt-grown Ga_2O_3 crystals are all β-Ga_2O_3. The well-known crystal growth methods such as Veneuil, Czochralski, floating zone and edge fed film growth can be used. On the other hand, the crystal structure of β-Ga_2O_3 is monoclinic and gives rise to anisotropic electrical, optical and thermal properties. This makes the growth of large diameter crystals challenging. Further, β-Ga_2O_3 has 2 strong cleavage planes that must be considered in choosing the substrate orientation for wafers. Other polymorphs can be grown epitaxially on various other substrates, and perhaps on β-Ga_2O_3 substrates.

Ga₂O₃ is basically an n-type semiconductor with no p-type counterpart. Initially, the conduction was thought to be due to oxygen deficiencies, but this theory is not challenged. Several n-type dopants were used in practice including Si and Sn. In theory n-type conduction is possible with other dopants. Si, Ge, and Sn substituting on the Ga site, and F and Cl on the O site are shallow donors and can contribute to conductivity. Si and Ge prefer the tetrahedral coordination of the Ga(I) site, while Sn prefers the octahedral coordination of the Ga(II) site. F and Cl both prefer the threefold coordination of the O(I) site.

In Ga$_2$O$_3$, metal ions provide electrons for conduction but only electrons associated with octahedral coordinated Ga(II) are free. Electrons from tetrahedral coordinated Ga(I) are thought to be localized and do not contribute to n-type conduction. Valence-band states are derived mainly from the O 2p orbitals and are characterized by small dispersion, large effective masses, and high density of states. Holes tend to form localized small polarons i.e., localized holes trapped by local lattice distortions. Therefore, as is the case with many other ionic metal-oxide semiconductors, p-type conduction in Ga$_2$O$_3$ is not likely.

Because of the lack of p-type doping in Ga$_2$O$_3$, it is not clear what can be done to make ultra-high breakdown devices that also have low turn on voltages. The use of minority carrier assisted turn on mechanisms are an intrinsic part of the current power electronics [252-254]. The Ga$_2$O$_3$-based power device could also benefit from the availability of minority carrier so that PIN type diodes and IGBT (insulated gate bipolar transistor) type transistors can be fabricated. These devices preserve the high voltage blocking capacity while lowering the on-state resistance. Such devices exceed the theoretical limits of unipolar devices (limits that were used in the FOM discussions in Chapter D). If p-type Ga$_2$O$_3$ continues to be a challenge in the future, the projected performance of this new semiconductor must be compared not only to unipolar devices made with other materials but to the performance of bipolar devices made from semiconductors such as SiC and GaN. This apples vs. oranges type comparison was not made in this document.

Anisotropy of electrical and optical parameters need to be fully understood. An often overlooked aspect of the Ga$_2$O$_3$ performance is the crystal structure dependent optical and electrical characteristics. The difference in the hybridization of electrons for Ga(I) and Ga(II) lead to highly different electrical and optical characteristics not only between the polymorphs of Ga$_2$O$_3$ but also in the crystal orientations of β-Ga$_2$O$_3$. It is expected that α-Ga$_2$O$_3$ will have significantly higher electron velocity compared to β-Ga$_2$O$_3$. Since β-Ga$_2$O$_3$ has a highly asymmetric crystal structure, important electrical and optical parameters (mobility, electron mass, conductivity, optical bandgap) are highly orientation dependent, as shown in Table 10. If β-Ga$_2$O$_3$ is chosen as the preferred polymorph, great deal of attention will need to be paid to choosing the correct orientation for devices. Anisotropy issues are not currently the top concerns for crystal growers at present due to other more fundamental issues being navigated.

Most of the well-known melt-grown crystal growth techniques can be used for β-Ga$_2$O$_3$. The techniques that have been successful include, Verneuil, Czochralski, vertical Bridgman, floating zone, and EFG. Crucible-based growth techniques such as Czochralski and Bridgman have some limitations in growing large diameter crystals because higher oxygen atmosphere needed for large crystals tend to react with the crucible. FZ growth technique does not need crucibles and may be more suitable for large crystals. The current limit in crystal size is about 2 inches with these techniques. EFG method produces ribbons rather than cylindrical boules. Wide ribbons can be used for producing up to 4-inch diameter wafers. Some of the current issues involved in crystal growth are related to the complex crystal structure of β-Ga$_2$O$_3$. Different growth rate along different crystal orientations sometimes give rise to growth defects. As would be expected, there are no bulk growth approaches for other polymorphs of Ga$_2$O$_3$.

Epitaxial layers of both α- and β-Ga$_2$O$_3$ can be grown by well-known growth methods. These methods include MBE, MOCVD, HVPE, and mist-CVD. Ion implantation is also possible for β-Ga$_2$O$_3$. MBE and MOCVD are mature technologies and used for volume production of other semiconductor wafers. There is no reason why similar transition from research to production cannot be made for Ga$_2$O$_3$. When MBE is used, the oxygen source is either ozone or ionized oxygen using RF plasma. The preferred oxygen source for MOCVD seems to be water. HVPE is suitable for very fast rate growth of ultra-pure materials. It was shown to be suitable for the growth of α-Ga$_2$O$_3$ on sapphire substrates. Mist-CVD is a low cost system that is similar to spray pyrolysis. This system can use organic or all inorganic precursors. One company in Japan has demonstrated α-Ga$_2$O$_3$ results that are excellent in terms of material quality and device performance. No confirmation of these results are available from another source.

UV detectors and Schottky Barrier Diodes (SBD) are the only two-terminal devices fabricated so far. Both device types are simple constructions and the device performance is mostly a function of the material quality. Although the performance of photodetectors do not offer much advantage over other technologies such as Al$_x$Ga$_{1-x}$N, the performance of SBDs are being monitored as a clue to proving the ultra-wide bandgap advantages of Ga$_2$O$_3$. So far, results with β-Ga$_2$O$_3$ do not exhibit a breakthrough. Most results are around 1MV/cm benchmark level. One company in Japan, using their unique mist-CVD growth technique, has demonstrated very good results with α- Ga$_2$O$_3$. The highest breakdown voltage values were above 12MV/cm, which is 50% higher than the empirically expected value for Ga$_2$O$_3$. The only hesitation here is that this result was obtained with thin layers (0.43 μm). Similarly, reasonably high breakdown field values were also obtained with three-terminal devices (transistors) that have short channel lengths (0.65 μm).

Three-terminal devices demonstrated so far are MESFETs and MOSFETs. Both MBE and MOCVD grown epi-layers were used to fabricate devices with gate lengths of 2-4 μm. These initial devices show that gate modulation of the channel current is possible (i.e. field effect). Most devices show reasonable turn-off characteristics and on/off ratios. Other device parameters such as field effect mobility, transconductance and current density are rather poor at this stage. No high frequency results were reported. Three-terminal breakdown voltages as high as 755V were reported, but the breakdown strength values are still low in the 0.5MV/cm range. The exception to this is the transistor fabricated at AFRL, which showed 3.8MV/cm breakdown strength. The channel length of this transistor was sub-micron (0.65μm). High breakdown strength results with multi-micron channel lengths are not yet found in open literature. Transistors made on α-Ga$_2$O$_3$ films showed much worse performance than β- Ga$_2$O$_3$ counterparts.

In summary, the Ga$_2$O$_3$ technology development is making good progress on many technology fronts. Customized material growth techniques are being developed after the initial stages of using conventional growth systems. The Japanese appear to be highly active in all aspects of materials technologies and therefore they will continue to set the pace for the development of devices, since the device performance is highly dependent on material quality at this stage. The progress in Ga$_2$O$_3$ technology will probably accelerate as more resources are devoted. The absence of p-type doping may be an issue in the future if alternative means of producing p-n junctions cannot be implemented.

10.   OUTLOOK

The initial device results obtained at AFRL with MOCVD-grown layers on β-Ga$_2$O$_3$ substrates goes a long way toward proving the high voltage potential of this technology. These initial devices are lateral geometry devices that may not be ultimately the right choices for very high power devices. Sooner or later, very high power devices (high voltage and low R$_{on}$) will require vertical structures and large geometries. However, lateral devices may prove to be useful as RF devices if contact resistance can be kept low and the electron mobility is improved. If efficient RF power amplification can be demonstrated, there may be application opportunities at L/S-band radar and communication systems.

With that future in mind, and using the survey of the technology status discussed in above sections, we can identify several technology development opportunities. This is not to say that all unknowns are identified and that we only need a development roadmap. There are still many outstanding questions regarding the issues that may seriously derail this effort. But we also know quite a lot about the choices that are open to us regarding these issues, so that educated guesses can be made about their potential solutions.

At present, the technology development activities are paced by the availability of good quality substrates and epitaxial layers. The matter is made worse by the fact that the desirable type of materials are available from a few Japanese sources and that the available wafers are small in size. This problem may disappear rapidly if a high volume commercial application is identified. In the past, the materials development efforts for GaAs and GaN were highly aided by the high volume commercial optical device applications. This is much less likely to happen with Ga$_2$O$_3$ because of its electronic structure, i.e. it is an indirect bandgap material and has no viable p-type doping. High power electronics application is the only driver for the technology at present. This type of electronics have a large commercial market, but there are several current viable alternative solutions. If Ga$_2$O$_3$ lives up to its potential and delivers MV-class devices, then there may be high value product opportunities. The devices fabricated so far fall considerably short of these goals. The device fabrication itself is not the technology barrier since reasonable devices were fabricated rapidly using marginal quality materials.

The real technology breakthrough opportunities lie in the material preparation in the near future timeframe. As we examined above, substrate technologies are in flux at present and the availability of large wafers is limited. Substrates with 3- and 4-inch diameter prepared by Czochralski and FZ methods needs to be available for epitaxial layers. Currently, both of these technologies are fighting the dimensional control issues and wafers larger than 2-inch in diameter are not common. EFG method has demonstrated 4-inch diameter substrates and this may be the preferred way, but it is not the mainstream technology. Crystals fabricated in this technique are ribbons rather than boules, and fabricating large diameter wafers from such ribbons may or may not be economically viable.

All considered, HVPE technique may be the way forward for both substrates and epitaxial layers for vertical devices. The growth rates are so high in this method that layers thick enough to be wafers themselves can be grown. Making use of high purity and good crystal quality of layers, impressive power level can be demonstrated with vertical devices. Already the highest breakdown device (1kV) was demonstrated with this material prepared by this technique.

The current overall Ga$_2$O$_3$ technology development vector follow the development path of the β- Ga$_2$O$_3$ material system. This is understandable since it is the most stable polymorph and it is compatible with conventional melt growth techniques. Some of the best device results have been obtained using this material option. However, it has a complex crystal structure with many anisotropies. Some groups are seriously considering the use of α-Ga$_2$O$_3$ as an alternative. From all perspectives (crystal structure, electronic configuration, optical and thermal), α- Ga$_2$O$_3$ is a better polymorph. Unfortunately, it cannot be melt grown and substrates made of this crystal are not possible.

A top-level technology status comparison of all Ga$_2$O$_3$ polymorphs is shown in Figure 50. The status of technology components in this figure are qualitatively judged to a maturity levels between 0 and 1. For example, β- Ga$_2$O$_3$ is given a 0.9 for substrate technology whereas α- Ga$_2$O$_3$ is assigned a small (but not a zero) value because quasi-substrates are possible with HVPE epitaxy. The doping technology is assigned a value of 0.5 because only n-type doping has been demonstrated. Clearly, β- Ga$_2$O$_3$ technology is further along the evolution path (a wider circle in Figure 50), but α- Ga$_2$O$_3$ has a lead in at least one technology component i.e. diodes. Very high breakdown strength (12MV/cm) has been demonstrated with thin layers (0.43μm).
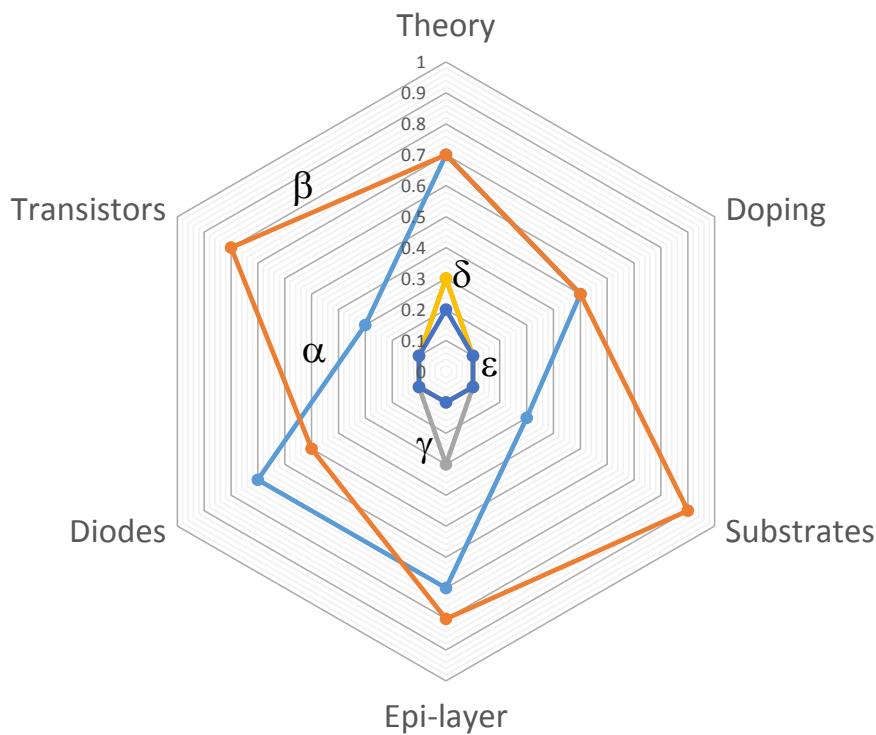
Figure 50: Qualitative representation of the technology development status of all 5 polymorphs of Ga$_2$O$_3$.

Epitaxial growth of α- Ga$_2$O$_3$ layers is possible, however, and this may be good enough to pay attention to this technology. First, higher quality layers can be prepared using HVPE. Second, vertical devices can be fabricated in the form of diodes first and transistors later. Lateral transistors require thin epitaxial

films on insulating substrates and may not be best implemented with α- Ga_2O_3. Ion implantation is also not a good option for β- Ga_2O_3 because of the high temperature annealing step.

Whether the development path of α-Ga_2O_3 or β-Ga_2O_3 is chosen going forward, there are still many critical issues that must be addressed. The thickness dependent electrical breakdown strength is the most pressing issue. We need to understand why thicker layers are not able to sustain high fields. If this is a materials uniformity issue, the material quality must be improved accordingly. To maintain emphasis on this issue, a new metric is required. The current critical metric, E_c, is thickness independent. We may instead want to measure the minimum layer thickness that can sustain a given voltage. Table 20 shows some critical metrics that can be used for development purposes. Since Ga_2O_3 is regarded as a potentially MV-class technology, the inclusion of a MV milestone in this table is appropriate.

Table 20: Suggested metrics for thickness dependent breakdown strength for diodes and FETs.

Breakdown Voltage	Layer Thickness (μm)	Layer Thickness (μm)	R_{on} ($m\Omega.cm^{-2}$)	R_{on} ($m\Omega.cm^{-2}$)
	GOAL	ACHIEVED	GOAL	ACHIEVED
1kV	< 1.25	12 [198]	<0.03	--
10kV	< 12.5	--	< 3.0	--
100kV	< 125	--	< 300	--
1MV	< 1250	--	<30000	--

11. ACKNOWLEDGEMENTS

12.   APPENDIX I: Profile of Japanese Ga$_2$O$_3$ Companies

A. FLOSFIA Inc.

FLOSFIA INC. is pioneering the development of next generation wide band gap power devices. Utilizing its proprietary Mist-CVD and all corundum structured Gallium Oxide based single crystal on sapphire, FLOSFIA will achieve industry-first, high breakdown voltage, high efficiency power devices with functional cost parity with silicon power devices.

FLOSFIA is a University of Tokyo venture capital (UTEC) financed start-up company. UTEC is a seed/early stage technology focused venture capital firm associated with The University of Tokyo. UTEC manages $300 million in venture capital funds, investing in world-class high technology start-up companies having synergy with the University. UTEC works closely with researchers and engineers to co-found companies which will contribute to the global society through innovation. UTEC has invested in 65 companies with 9 IPO and 8 M&A exits to date (as of December 2015).

COMPANY PROFILE

Name:	FLOSFIA Co., Ltd. (Furosufia)
President & CEO:	HitoRa ShunMinoru
Establishment:	31, 2011
Location:	Kyoto, Kyoto Prefecture Nishikyo Ku tomb Ohara No. 1 No. 36 Kyoto Katsura Venture Plaza North Building
TEL / FAX :	075-963-5202 / 075-320-1712
Joint research:	Kyoto University, Shizuo Fujita Professor
Capitalization:	¥ 613,685,840 (including capital reserves)
Patent Portfolio:	11 Patents

B. TAMURA CORPORATION (Including Koha Corp)

TAMURA CORPORATION is a Japan-based company engaged in the manufacture and sale of electronic components, electronic chemicals and soldering systems, and information equipment. The Company operates in four business segments. The Electronic Components segment manufactures and sells transformers, alternate current (AC) adaptors, switching supply units and piezo-ceramic products. The Electronic chemicals and Soldering Equipment segment provides fluxes, solder pastes, solder resisting equipment and thermosetting conductive adhesive pastes. The Information Equipment segment manufactures and sells communications network equipment, broadcast equipment, wireless microphones and information application equipment. The others segment is engaged in transportation and warehousing business.

Name:	TAMURA CORPORATION
President & CEO:	Naoki Tamura
Establishment:	May 11, 1924
Headquarters:	1-19-43, Higashi-Oizumi, Nerima-ku, Tokyo, Japan 178-8511
No of Employees:	5,634
Capitalization:	¥11,829 million
Merger:	In August 2011, Koha Co., Ltd. became a wholly owned subsidiary of the Tamura Corporation through a share exchange.

13.   REFERENCES

[1]   L. F. Eastman and U. K. Mishra, "The toughest transistor yet [GaN transistors]," *IEEE Spectrum,* vol. 39, pp. 28-33, 2002.

[2]   U. K. Mishra, L. Shen, T. E. Kazior, and Y. F. Wu, "GaN-Based RF Power Devices and Amplifiers," *Proceedings of the IEEE,* vol. 96, pp. 287-305, 2008.

[3]   R. S. Pengelly, S. M. Wood, J. W. Milligan, S. T. Sheppard, and W. L. Pribble, "A Review of GaN on SiC High Electron-Mobility Power Transistors and MMICs," *IEEE Transactions on Microwave Theory and Techniques,* vol. 60, pp. 1764-1783, 2012.

[4]   M. J. Rosker, "Technologies for Next Generation T/R Modules," in *2007 IEEE Radar Conference*, 2007, pp. 944-947.

[5]   R. T. Kemerley, H. B. Wallace, and M. N. Yoder, "Impact of wide bandgap microwave devices on DoD systems," *Proceedings of the IEEE,* vol. 90, pp. 1059-1064, 2002.

[6]   D. N. McQuiddy, J. W. Wassel, J. B. LaGrange, and W. R. Wisseman, "Monolithic Microwave Integrated Circuits: An Historical Perspective," *IEEE Transactions on Microwave Theory and Techniques,* vol. 32, pp. 997-1008, 1984.

[7]   D. N. McQuiddy, "High volume applications for GaAs microwave and millimeter-wave ICs in military systems," in *Gallium Arsenide Integrated Circuit (GaAs IC) Symposium, 1989. Technical Digest 1989., 11th Annual*, 1989, pp. 3-6.

[8]   D. N. McQuiddy, R. L. Gassner, P. Hull, J. S. Mason, and J. M. Bedinger, "Transmit/receive module technology for X-band active array radar," *Proceedings of the IEEE,* vol. 79, pp. 308-341, 1991.

[9]   G. E. Brehm, "Multifunction MMIC history from a process technology perspective," *IEEE Transactions on Microwave Theory and Techniques,* vol. 38, pp. 1164-1170, 1990.

[10]   E. D. Cohen, "The MIMIC Program; A Retrospective," *IEEE Microwave Magazine,* vol. 13, pp. 77-88, 2012.

[11]   M. R. Lorenz, J. F. Woods, and R. J. Gambino, "Some electrical properties of the semiconductor β☐Ga2O3," *Journal of Physics and Chemistry of Solids,* vol. 28, pp. 403-404, 1967/03/01 1967.

[12]   T. Matsumoto, M. Aoki, A. Kinoshita, and T. Aono, "Absorption and Reflection of Vapor Grown Single Crystal Platelets of β-Ga 2 O 3," *Japanese Journal of Applied Physics,* vol. 13, p. 1578, 1974.

[13]   N. Ueda, H. Hosono, R. Waseda, and H. Kawazoe, "Anisotropy of electrical and optical properties in beta-Ga2O3 single crystals," *Applied Physics Letters,* vol. 71, pp. 933-935, Aug 18 1997.

[14]   N. Ueda, H. Hosono, R. Waseda, and H. Kawazoe, "Synthesis and control of conductivity of ultraviolet transmitting beta-Ga2O3 single crystals," *Applied Physics Letters,* vol. 70, pp. 3561-3563, Jun 30 1997.

[15]   J. Zhang, B. Li, C. Xia, G. Pei, Q. Deng, Z. Yang*, et al.*, "Growth and spectral characterization of β-Ga2O3 single crystals," *Journal of Physics and Chemistry of Solids,* vol. 67, pp. 2448-2451, 12// 2006.

[16]   J. Zhang, C. Xia, Q. Deng, W. Xu, H. Shi, F. Wu*, et al.*, "Growth and characterization of new transparent conductive oxides single crystals β-Ga2O3: Sn," *Journal of Physics and Chemistry of Solids,* vol. 67, pp. 1656-1659, 8// 2006.

[17]   M. Higashiwaki, K. Sasaki, M. H. Wong, T. Kamimura, K. Goto, K. Nomura*, et al.*, "Current Status of Gallium Oxide-Based Power Device Technology," in *2015 IEEE Compound Semiconductor Integrated Circuit Symposium (CSICS)*, 2015, pp. 1-4.

[18]   M. Higashiwaki, S. Kohei, M. Hisashi, K. Yoshinao, K. Akinori, K. Akito*, et al.*, "Recent progress in Ga 2 O 3 power devices," *Semiconductor Science and Technology,* vol. 31, p. 034001, 2016.

[19]   H. H. Tippins, "Optical Absorption and Photoconductivity in the Band Edge of beta-Ga2O3," *Physical Review,* vol. 140, pp. A316-A319, 10/04/ 1965.

[20]   M. Orita, H. Ohta, M. Hirano, and H. Hosono, "Deep-ultraviolet transparent conductive beta-Ga2O3 thin films," *Applied Physics Letters,* vol. 77, pp. 4166-4168, Dec 18 2000.

[21]   T. Onuma, S. Fujioka, T. Yamaguchi, M. Higashiwaki, K. Sasaki, T. Masui*, et al.*, "Correlation between blue luminescence intensity and resistivity in beta-Ga2O3 single crystals," *Applied Physics Letters,* vol. 103, Jul 22 2013.

[22]   M. Passlack, E. F. Schubert, W. S. Hobson, M. Hong, N. Moriya, S. N. G. Chu*, et al.*, "GA2O3 FILMS FOR ELECTRONIC AND OPTOELECTRONIC APPLICATIONS," *Journal of Applied Physics,* vol. 77, pp. 686-693, Jan 15 1995.

[23]   E. G. Víllora, K. Shimamura, K. Kitamura, and K. Aoki, "Rf-plasma-assisted molecular-beam epitaxy of β-Ga2O3," *Applied Physics Letters,* vol. 88, p. 031105, 2006.

[24]   T. Oshima, O. Takeya, and F. Shizuo, "Ga 2 O 3 Thin Film Growth on c -Plane Sapphire Substrates by Molecular Beam Epitaxy for Deep-Ultraviolet Photodetectors," *Japanese Journal of Applied Physics,* vol. 46, p. 7217, 2007.

[25]   T. P. Chow and R. Tyagi, "Wide bandgap compound semiconductors for superior high-voltage unipolar power devices," *IEEE Transactions on Electron Devices,* vol. 41, pp. 1481-1483, 1994.

[26]   P. B. Perry and R. F. Rutz, "The optical absorption edge of single-crystal AlN prepared by a close-spaced vapor process," *Applied Physics Letters,* vol. 33, pp. 319-321, 1978.

[27]   Qixin Guo and Akira Yoshida, "Temperature Dependence of Band Gap Change in InN and AlN," *Japanese Journal of Applied Physics,* vol. 33, p. 2453, 1994.

[28]   H. Yamashita, K. Fukui, S. Misawa, and S. Yoshida, "Optical properties of AlN epitaxial thin films in the vacuum ultraviolet region," *Journal of Applied Physics,* vol. 50, pp. 896-898, 1979.

[29]   W. M. Yim, E. J. Stofko, P. J. Zanzucchi, J. I. Pankove, M. Ettenberg, and S. L. Gilbert, "Epitaxially grown AlN and its optical band gap," *Journal of Applied Physics,* vol. 44, pp. 292-296, 1973.

[30]   J. Bauer, L. Biste, and D. Bolze, "Optical properties of aluminium nitride prepared by chemical and plasmachemical vapour deposition," *physica status solidi (a),* vol. 39, pp. 173-181, 1977.

[31]   J. Pastrňák and L. Roskovcová, "Optical Absorption Edge of AlN Single Crystals," *physica status solidi (b),* vol. 26, pp. 591-597, 1968.

[32]   A. Aleksov, M. Kubovic, N. Kaeb, U. Spitzberg, A. Bergmaier, G. Dollinger*, et al.*, "Diamond field effect transistors—concepts and challenges," *Diamond and Related Materials,* vol. 12, pp. 391-398, 3// 2003.

[33]   A. Aleksov, M. Kubovic, M. Kasu, P. Schmid, D. Grobe, S. Ertl*, et al.*, "Diamond-based electronics for RF applications," *Diamond and Related Materials,* vol. 13, pp. 233-240, 2// 2004.

[34]   A. Denisenko and E. Kohn, "Diamond power devices. Concepts and limits," *Diamond and Related Materials,* vol. 14, pp. 491-498, 3// 2005.

[35]   E. Kohn and A. Denisenko, "Concepts for diamond electronics," *Thin Solid Films,* vol. 515, pp. 4333-4339, 3/26/ 2007.

[36]   R. Roy, V. G. Hill, and E. F. Osborn, "Polymorphism of Ga2O3 and the System Ga2O3—H2O," *Journal of the American Chemical Society,* vol. 74, pp. 719-722, 1952/02/01 1952.

[37]   X. Du, W. Mi, C. Luan, Z. Li, C. Xia, and J. Ma, "Characterization of homoepitaxial β-Ga2O3 films prepared by metal–organic chemical vapor deposition," *Journal of Crystal Growth,* vol. 404, pp. 75-79, 10/15/ 2014.

[38]   D. E. Aspnes, G. P. Schwartz, G. J. Gualtieri, A. A. Studna, and B. Schwartz, "Optical Properties of GaAs and Its Electrochemically Grown Anodic Oxide from 1.5 to 6.0 eV," *Journal of The Electrochemical Society,* vol. 128, pp. 590-597, March 1, 1981 1981.

[39]   B. Bayraktaroglu and H. L. Hartnagel, "Invited paper. Anodic oxides on GaAs. I. Anodic native oxides on GaAs," *International Journal of Electronics,* vol. 45, pp. 337-352, 1978/10/01 1978.

[40]   H. Hasegawa and H. L. Hartnagel, "Anodic Oxidation of GaAs in Mixed Solutions of Glycol and Water," *Journal of The Electrochemical Society,* vol. 123, pp. 713-723, May 1, 1976 1976.

[41]   V. M. Kalygina, A. N. Zarubin, Y. P. Nayden, V. A. Novikov, Y. S. Petrova, O. P. Tolbanov*, et al.*, "Ga2O3 films formed by electrochemical oxidation," *Semiconductors,* vol. 45, pp. 1097-1102, 2011.

[42]   S. P. Murarka, "Thermal oxidation of GaAs," *Applied Physics Letters,* vol. 26, pp. 180-181, 1975.

[43]   G. P. Schwartz, G. J. Gualtieri, J. E. Griffiths, C. D. Thurmond, and B. Schwartz, "Oxide-Substrate and Oxide-Oxide Chemical Reactions in Thermally Annealed Anodic Films on GaSb , GaAs , and GaP," *Journal of The Electrochemical Society,* vol. 127, pp. 2488-2499, November 1, 1980 1980.

[44]   S. M. Spitzer, B. Schwartz, and G. D. Weigle, "Preparation and Stabilization of Anodic Oxides on GaAs," *Journal of The Electrochemical Society,* vol. 122, pp. 397-402, March 1, 1975 1975.

[45]   M. Passlack, M. Hong, J. P. Mannaerts, R. L. Opila, S. N. G. Chu, N. Moriya*, et al.*, "Low Dit, thermodynamically stable Ga2O3-GaAs interfaces: fabrication, characterization, and modeling," *IEEE Transactions on Electron Devices,* vol. 44, pp. 214-225, 1997.

[46]   S. P. Kowalczyk, J. R. Waldrop, and R. W. Grant, "INTERFACIAL CHEMICAL-REACTIVITY OF METAL CONTACTS WITH THIN NATIVE OXIDES OF GAAS," *Journal of Vacuum Science & Technology,* vol. 19, pp. 611-616, 1981 1981.

[47]   D. S. Ginley and C. Bright, "Transparent Conducting Oxides," *MRS Bulletin,* vol. 25, pp. 15-18, 2000.

[48]   R. G. Gordon, "Criteria for Choosing Transparent Conductors," *MRS Bulletin,* vol. 25, pp. 52-57, 2000.

[49]   B. G. Lewis and D. C. Paine, "Applications and Processing of Transparent Conducting Oxides," *MRS Bulletin,* vol. 25, pp. 22-27, 2000.

[50]   J. E. Medvedeva and C. L. Hettiarachchi, "Tuning the properties of complex transparent conducting oxides: Role of crystal symmetry, chemical composition, and carrier generation," *Physical Review B,* vol. 81, p. 125116, 03/17/ 2010.

[51]   M. Tadatsugu, "Transparent conducting oxide semiconductors for transparent electrodes," *Semiconductor Science and Technology,* vol. 20, p. S35, 2005.

[52]   C. Janowitz, V. Scherer, M. Mohamed, A. Krapf, H. Dwelk, R. Manzke*, et al.*, "Experimental electronic structure of In2O3 and Ga2O3," *New Journal of Physics,* vol. 13, Aug 16 2011.

[53]   S. M. Sze and G. Gibbons, "AVALANCHE BREAKDOWN VOLTAGES OF ABRUPT AND LINEARLY GRADED P-N JUNCTIONS IN GE SI GAAS AND GAP - (DOPANT EFFECTS IMPURITY EFFECTS T)," *Applied Physics Letters,* vol. 8, pp. 111-&, 1966 1966.

[54]   B. J. Baliga, "Power Semiconductor-Device Figure of Merit For High-Frequency Applications," *IEEE Electron Device Letters,* vol. 10, pp. 455-457, Oct 1989.

[55]   B. J. Baliga, "Semiconductors for High-Voltage, Vertical Channel Field-Eeffect Transistors," *Journal of Applied Physics,* vol. 53, pp. 1759-1764, Sep 1982.

[56]   J. L. Hudgins, G. S. Simin, E. Santi, and M. A. Khan, "An assessment of wide bandgap semiconductors for power devices," *IEEE Transactions on Power Electronics,* vol. 18, pp. 907-914, 2003.

[57]   R. Suzuki, S. Nakagomi, and Y. Kokubun, "Solar-blind photodiodes composed of a Au Schottky contact and a beta-Ga2O3 single crystal with a high resistivity cap layer," *Applied Physics Letters,* vol. 98, Mar 28 2011.

[58]   J. A. Rosero, J. A. Ortega, E. Aldabas, and L. Romeral, "Moving towards a more electric aircraft," *IEEE Aerospace and Electronic Systems Magazine,* vol. 22, pp. 3-9, 2007.

[59]   C. R. Avery, S. G. Burrow, and P. H. Mellor, "Electrical generation and distribution for the more electric aircraft," in *Universities Power Engineering Conference, 2007. UPEC 2007. 42nd International*, 2007, pp. 1007-1012.

[60]   R. T. Naayagi, "A review of more electric aircraft technology," in *Energy Efficient Technologies for Sustainability (ICEETS), 2013 International Conference on*, 2013, pp. 750-753.

[61]   K. C. Reinhardt and M. A. Marciniak, "Wide-bandgap power electronics for the More Electric Aircraft," in *Energy Conversion Engineering Conference, 1996. IECEC 96., Proceedings of the 31st Intersociety*, 1996, pp. 127-132 vol.1.

[62]   R. Szweda, "HEMT materials and devices," *III-Vs Review,* vol. 16, pp. 36-39, 2003/04/01 2003.

[63]   A. K. Geim and K. S. Novoselov, "The rise of graphene," *Nat Mater,* vol. 6, pp. 183-191, 03//print 2007.

[64]   Y. Tomm, P. Reiche, D. Klimm, and T. Fukuda, "Czochralski grown Ga2O3 crystals," *Journal of Crystal Growth,* vol. 220, pp. 510-514, 12// 2000.

[65]   Z. Galazka, K. Irmscher, R. Uecker, R. Bertram, M. Pietsch, A. Kwasniewski*, et al.*, "On the bulk β-Ga2O3 single crystals grown by the Czochralski method," *Journal of Crystal Growth,* vol. 404, pp. 184-191, 10/15/ 2014.

[66]   E. G. Villora, K. Shimamura, Y. Yoshikawa, K. Aoki, and N. Ichinose, "Large-size beta-Ga2O3 single crystals and wafers," *Journal of Crystal Growth,* vol. 270, pp. 420-426, Oct 1 2004.

[67]   S. Ohira, N. Suzuki, N. Arai, M. Tanaka, T. Sugawara, K. Nakajima*, et al.*, "Characterization of transparent and conducting Sn-doped β-Ga2O3 single crystal after annealing," *Thin Solid Films,* vol. 516, pp. 5763-5767, 7/1/ 2008.

[68]   H. Aida, K. Nishiguchi, H. Takeda, N. Aota, K. Sunakawa, and Y. Yaguchi, "Growth of beta-Ga2O3 Single Crystals by the Edge-Defined, Film Fed Growth Method," *Japanese Journal of Applied Physics,* vol. 47, pp. 8506-8509, Nov 2008.

[69]   K. Ghosh and U. Singisetti, "Calculation of electron impact ionization co-efficient in beta-Ga2O3," in *72nd Device Research Conference*, 2014, pp. 71-72.

[70]   M. Higashiwaki, K. Sasaki, A. Kuramata, T. Masui, and S. Yamakoshi, "Gallium oxide (Ga2O3) metal-semiconductor field-effect transistors on single-crystal beta-Ga2O3 (010) substrates," *Applied Physics Letters,* vol. 100, pp. 1-2, Jan 2 2012.

[71]   A. J. Green, K. D. Chabak, E. R. Heller, R. C. Fitch, M. Baldini, A. Fiedler*, et al.*, "3.8-MV/cm Breakdown Strength of MOVPE-Grown Sn-Doped beta-Ga2O3 MOSFETs," *IEEE Electron Device Letters,* vol. 37, pp. 902-905, 2016.

[72]   Z. Guo, A. Verma, X. Wu, F. Sun, A. Hickman, T. Masui*, et al.*, "Anisotropic thermal conductivity in single crystal β-gallium oxide," *Applied Physics Letters,* vol. 106, p. 111909, 2015.

[73]   C. J. Szwejkowski, N. C. Creange, K. Sun, A. Giri, B. F. Donovan, C. Constantin*, et al.*, "Size effects in the thermal conductivity of gallium oxide (β-Ga2O3) films grown via open-atmosphere annealing of gallium nitride," *Journal of Applied Physics,* vol. 117, p. 084308, 2015.

[74]   D. Shinohara and S. Fujita, "Heteroepitaxy of Corundum-Structured α-Ga 2 O 3 Thin Films on α-Al 2 O 3 Substrates by Ultrasonic Mist Chemical Vapor Deposition," *Japanese Journal of Applied Physics,* vol. 47, p. 7311, 2008.

[75]   T. Oshima, T. Nakazono, A. Mukai, and A. Ohtomo, "Epitaxial growth of γ-Ga2O3 films by mist chemical vapor deposition," *Journal of Crystal Growth,* vol. 359, pp. 60-63, 11/15/ 2012.

[76]   J. Kolodzey, E. A. Chowdhury, T. N. Adam, Q. Guohua, I. Rau, J. O. Olowolafe*, et al.*, "Electrical conduction and dielectric breakdown in aluminum oxide insulators on silicon," *IEEE Transactions on Electron Devices,* vol. 47, pp. 121-128, 2000.

[77]   J. W. McPherson, K. Jinyoung, A. Shanware, H. Mogul, and J. Rodriguez, "Trends in the ultimate breakdown strength of high dielectric-constant materials," *IEEE Transactions on Electron Devices,* vol. 50, pp. 1771-1778, 2003.

[78]   C. M. Osburn and E. J. Weitzman, "Electrical Conduction and Dielectric Breakdown in Silicon Dioxide Films on Silicon," *Journal of The Electrochemical Society,* vol. 119, pp. 603-609, May 1, 1972 1972.

[79]   E. Johnson, "Physical limitations on frequency and power parameters of transistors," *RCA review,* vol. 26, pp. 163-177, 1965.

[80]   R. W. Keyes, "Figure of merit for semiconductors for high-speed switches," *Proceedings of the IEEE,* vol. 60, pp. 225-225, 1972.

[81]   K. Il-Jung, S. Matsumoto, T. Sakai, and T. Yachi, "New power device figure of merit for high-frequency applications," in *Power Semiconductor Devices and ICs, 1995. ISPSD '95., Proceedings of the 7th International Symposium on*, 1995, pp. 309-314.

[82]   K. Shenai, R. S. Scott, and B. J. Baliga, "Optimum semiconductors for high-power electronics," *IEEE Transactions on Electron Devices,* vol. 36, pp. 1811-1823, 1989.

[83]   A. Q. Huang, "New unipolar switching power device figures of merit," *IEEE Electron Device Letters,* vol. 25, pp. 298-301, 2004.

[84]   H. Wang, F. Wang, and J. Zhang, "Power semiconductor device figure of merit for high-power-density converter design applications," *IEEE transactions on electron devices,* vol. 55, pp. 466-470, 2008.

[85]   M. Higashiwaki, K. Sasaki, A. Kuramata, T. Masui, and S. Yamakoshi, "Gallium oxide (Ga2O3) metal-semiconductor field-effect transistors on single-crystal β-Ga2O3 (010) substrates," *Applied Physics Letters,* vol. 100, p. 013504, 2012.

[86]   K. Sasaki, M. Higashiwaki, A. Kuramata, T. Masui, and S. Yamakoshi, "MBE grown Ga2O3 and its power device applications," *Journal of Crystal Growth,* vol. 378, pp. 591-595, 9/1/ 2013.

[87]   J. Isberg, J. Hammersberg, E. Johansson, T. Wikström, D. J. Twitchen, A. J. Whitehead*, et al.*, "High Carrier Mobility in Single-Crystal Plasma-Deposited Diamond," *Science,* vol. 297, pp. 1670-1672, 2002.

[88]   B. E. Foutz, S. K. O'Leary, M. S. Shur, and L. F. Eastman, "Transient electron transport in wurtzite GaN, InN, and AlN," *Journal of Applied Physics,* vol. 85, pp. 7727-7734, 1999.

[89]   K. Nomura, H. Ohta, K. Ueda, T. Kamiya, M. Hirano, and H. Hosono, "Thin-Film Transistor Fabricated in Single-Crystalline Transparent Oxide Semiconductor," *Science,* vol. 300, pp. 1269-1272, 2003.

[90]   H. Hosono, H. Ohta, M. Orita, K. Ueda, and M. Hirano, "Frontier of transparent conductive oxide thin films," *Vacuum,* vol. 66, pp. 419-425, 8/19/ 2002.

[91]   K. Nomura, H. Ohta, A. Takagi, T. Kamiya, M. Hirano, and H. Hosono, "Room-temperature fabrication of transparent flexible thin-film transistors using amorphous oxide semiconductors," *Nature,* vol. 432, pp. 488-492, 11/25/print 2004.

[92]   H. Kumomi, K. Nomura, T. Kamiya, and H. Hosono, "Amorphous oxide channel TFTs," *Thin Solid Films,* vol. 516, pp. 1516-1522, 2/15/ 2008.

[93]   E. Fortunato, H. Hosono, C. Granqvist, and J. Wager, "Advances in transparent electronics: From materials to devices I," *Thin Solid Films,* vol. 516, p. 1313, 2/15/ 2008.

[94]   H. Hosono, "Ionic amorphous oxide semiconductors: Material design, carrier transport, and device application," *Journal of Non-Crystalline Solids,* vol. 352, pp. 851-858, 6/15/ 2006.

[95]   S. Yoshioka, H. Hayashi, A. Kuwabara, F. Oba, K. Matsunaga, and I. Tanaka, "Structures and energetics of Ga 2 O 3 polymorphs," *Journal of Physics: Condensed Matter,* vol. 19, p. 346211, 2007.

[96]   I. Levin and D. Brandon, "Metastable Alumina Polymorphs: Crystal Structures and Transition Sequences," *Journal of the American Ceramic Society,* vol. 81, pp. 1995-2012, 1998.

[97]   R. Roy, V. G. Hill, and E. F. Osborn, "Polymorphs of Alumina and Gallia," *Industrial & Engineering Chemistry,* vol. 45, pp. 819-820, 1953/04/01 1953.

[98]   E. Chikoidze, H. J. von Bardeleben, K. Akaiwa, E. Shigematsu, K. Kaneko, S. Fujita*, et al.*, "Electrical, optical, and magnetic properties of Sn doped α-Ga2O3 thin films," *Journal of Applied Physics,* vol. 120, p. 025109, 2016.

[99]   M.-G. Ju, X. Wang, W. Liang, Y. Zhao, and C. Li, "Tuning the energy band-gap of crystalline gallium oxide to enhance photocatalytic water splitting: mixed-phase junctions," *Journal of Materials Chemistry A,* vol. 2, pp. 17005-17014, 2014.

[100]   H. He, R. Orlando, M. A. Blanco, R. Pandey, E. Amzallag, I. Baraille*, et al.*, "First-principles study of the structural, electronic, and optical properties of Ga2O3 in its monoclinic and hexagonal phases," *Physical Review B,* vol. 74, Nov 2006.

[101]   M. Marezio and J. P. Remeika, "Bond Lengths in the α-Ga2O3 Structure and the High-Pressure Phase of Ga2–xFexO3," *The Journal of Chemical Physics,* vol. 46, pp. 1862-1865, 1967.

[102]   G. Sinha, K. Adhikary, and S. Chaudhuri, "Sol–gel derived phase pure α-Ga2O3 nanocrystalline thin film and its optical properties," *Journal of Crystal Growth,* vol. 276, pp. 204-207, 3/15/ 2005.

[103]   G. T. Dang, T. Kawaharamura, M. Furuta, and M. W. Allen, "Mist-CVD Grown Sn-Doped alpha-Ga2O3 MESFETs," *Ieee Transactions on Electron Devices,* vol. 62, pp. 3640-3644, Nov 2015.

[104]   Y. Oshima, E. Víllora, and K. Shimamura, "Halide vapor phase epitaxy of twin-free α-Ga 2 O 3 on sapphire (0001) substrates," *Applied Physics Express,* vol. 8, p. 055501, 2015.

[105]   M. Oda, T. Rie, K. Hitoshi, T. Tomochika, S. Takahiro, and H. Toshimi, "Schottky barrier diodes of corundum-structured gallium oxide showing on-resistance of 0.1 mΩ·cm 2 grown by MIST EPITAXY ®," *Applied Physics Express,* vol. 9, p. 021101, 2016.

[106]   J. Ahman, G. Svensson, and J. Albertsson, "A Reinvestigation of [beta]-Gallium Oxide," *Acta Crystallographica Section C,* vol. 52, pp. 1336-1338, 1996.

[107]   S. Geller, "THE CRYSTAL STRUCTURE OF BETA-GA2O3," *Acta Crystallographica,* vol. 13, pp. 1023-1024, 1960 1960.

[108]   M. Zinkevich, F. M. Morales, H. Nitsche, M. Ahrens, M. Rühle, and F. Aldinger, "Microstructural and thermodynamic study of γ-Ga2O3," *Zeitschrift für Metallkunde,* vol. 95, pp. 756-762, 2004/09/01 2004.

[109]   M. Zinkevich and F. Aldinger, "Thermodynamic Assessment of the Gallium-Oxygen System," *Journal of the American Ceramic Society,* vol. 87, pp. 683-691, 2004.

[110]   R. Huang, H. Hayashi, F. Oba, and I. Tanaka, "Microstructure of Mn-doped γ-Ga2O3 epitaxial film on sapphire (0001) with room temperature ferromagnetism," *Journal of Applied Physics,* vol. 101, p. 063526, 2007.

[111]   H. Hayashi, R. Huang, H. Ikeno, F. Oba, S. Yoshioka, I. Tanaka*, et al.*, "Room temperature ferromagnetism in Mn-doped γ-Ga2O3 with spinel structure," *Applied Physics Letters,* vol. 89, p. 181903, 2006.

[112]   H. Hayashi, R. Huang, F. Oba, T. Hirayama, and I. Tanaka, "Epitaxial growth of Mn-doped γ-Ga2O3 on spinel substrate," *Journal of Materials Research,* vol. 26, pp. 578-583, 2011.

[113]   M. Orita, H. Hiramatsu, H. Ohta, M. Hirano, and H. Hosono, "Preparation of highly conductive, deep ultraviolet transparent β-Ga2O3 thin film at low deposition temperatures," *Thin Solid Films,* vol. 411, pp. 134-139, 5/22/ 2002.

[114]   K. Matsuzaki, H. Hiramatsu, K. Nomura, H. Yanagi, T. Kamiya, M. Hirano*, et al.*, "Growth, structure and carrier transport properties of Ga2O3 epitaxial film examined for transparent field-effect transistor," *Thin Solid Films,* vol. 496, pp. 37-41, Feb 1 2006.

[115]   B. Ollivier, R. Retoux, P. Lacorre, D. Massiot, and G. Ferey, "Crystal structure of [small kappa]-alumina: an X-ray powder diffraction, TEM and NMR study," *Journal of Materials Chemistry,* vol. 7, pp. 1049-1056, 1997.

[116]   K. Matsuzaki, H. Yanagi, T. Kamiya, H. Hiramatsu, K. Nomura, M. Hirano*, et al.*, "Field-induced current modulation in epitaxial film of deep-ultraviolet transparent oxide semiconductor Ga2O3," *Applied Physics Letters,* vol. 88, Feb 27 2006.

[117]   H. Hiramatsu, H. Ohta, W.-S. Seo, and K. Koumoto, "Thermoelectric Properties of (ZnO)$_5$In$_2$O$_3$Thin Films Prepared by r.f. Sputtering

Method," *Journal of the Japan Society of Powder and Powder Metallurgy,* vol. 44, pp. 44-49, 1997.

[118]   K. Hisashi, A. Ryoji, and T. Toshihiko, "Thermoelectric Properties of Highly Textured Ca-Doped (ZnO) m In 2 O 3 Ceramics," *Japanese Journal of Applied Physics,* vol. 43, p. 7133, 2004.

[119]   A. J. Freeman, K. R. Poeppelmeier, T. O. Mason, R. P. H. Chang, and T. J. Marks, "Chemical and Thin-Film Strategies for New Transparent Conducting Oxides," *MRS Bulletin,* vol. 25, pp. 45-51, 2000.

[120]   B. J. Ingram, G. B. Gonzalez, D. R. Kammler, M. I. Bertoni, and T. O. Mason, "Chemical and Structural Factors Governing Transparent Conductivity in Oxides," *Journal of Electroceramics,* vol. 13, pp. 167-175, 2004// 2004.

[121]   H. Kawazoe, N. Ueda, H. Un'no, T. Omata, H. Hosono, and H. Tanoue, "Generation of electron carriers in insulating thin film of MgIn2O4 spinel by Li+ implantation," *Journal of Applied Physics,* vol. 76, pp. 7935-7941, 1994.

[122]   H. Mizoguchi and P. M. Woodward, "Electronic Structure Studies of Main Group Oxides Possessing Edge-Sharing Octahedra: Implications for the Design of Transparent Conducting Oxides," *Chemistry of Materials,* vol. 16, pp. 5233-5248, 2004/12/01 2004.

[123]   R. D. Shannon, J. L. Gillson, and R. J. Bouchard, "Single crystal synthesis and electrical properties of CdSnO3, Cd2SnO4, In2TeO6 and CdIn2O4," *Journal of Physics and Chemistry of Solids,* vol. 38, pp. 877-881, 1977/01/01 1977.

[124]   M. Orita, M. Takeuchi, H. Sakai, and H. Tanji, "New Transparent Conductive Oxides with Y b F e 2 O 4 Structure," *Japanese Journal of Applied Physics,* vol. 34, p. L1550, 1995.

[125]   M. Orita, H. Tanji, M. Mizuno, H. Adachi, and I. Tanaka, "Mechanism of electrical conductivity of transparent InGaZnO4," *Physical Review B,* vol. 61, pp. 1811-1816, 01/15/ 2000.

[126]   J. E. Medvedeva, "Averaging of the electron effective mass in multicomponent transparent conducting oxides," *EPL (Europhysics Letters),* vol. 78, p. 57004, 2007.

[127]   J. B. Varley, J. R. Weber, A. Janotti, and C. G. Van de Walle, "Oxygen vacancies and donor impurities in beta-Ga2O3," *Applied Physics Letters,* vol. 97, Oct 4 2010.

[128]   P.-C. Chang, Z. Fan, W.-Y. Tseng, A. Rajagopal, and J. G. Lu, "β-Ga2O3 nanowires: Synthesis, characterization, and p-channel field-effect transistor," *Applied Physics Letters,* vol. 87, p. 222102, 2005.

[129]   J. B. Varley, A. Janotti, C. Franchini, and C. G. Van de Walle, "Role of self-trapping in luminescence and p-type conductivity of wide-band-gap oxides," *Physical Review B,* vol. 85, p. 081109, 02/27/ 2012.

[130]   C. Li, J.-L. Yan, L.-Y. Zhang, and G. Zhao, "Electronic structures and optical properties of Zn-doped β-Ga 2 O 3 with different doping sites," *Chinese Physics B,* vol. 21, p. 127104, 2012.

[131]   L.-Y. Zhang, J.-L. Yan, Y.-J. Zhang, and T. Li, "Effects of N-doping concentration on the electronic structure and optical properties of N-doped β-Ga 2 O 3," *Chinese Physics B,* vol. 21, p. 067102, 2012.

[132]   L. Zhang, J. Yan, Y. Zhang, T. Li, and X. Ding, "A comparison of electronic structure and optical properties between N-doped β-Ga2O3 and N–Zn co-doped β-Ga2O3," *Physica B: Condensed Matter,* vol. 407, pp. 1227-1231, 4/15/ 2012.

[133]   L. L. Liu, M. K. Li, D. Q. Yu, J. Zhang, H. Zhang, C. Qian*, et al.*, "Fabrication and characteristics of N-doped β-Ga2O3 nanowires," *Applied Physics A,* vol. 98, pp. 831-835, 2010.

[134]   K. Yamaguchi, "First principles study on electronic structure of β-Ga2O3," *Solid State Communications,* vol. 131, pp. 739-744, 9// 2004.

[135]   M. D. Santia, N. Tandon, and J. D. Albrecht, "Lattice thermal conductivity in beta-Ga2O3 from first principles," *Applied Physics Letters,* vol. 107, p. 4, Jul 2015.

[136] M. Handwerg, R. Mitdank, Z. Galazka, and S. F. Fischer, "Temperature-dependent thermal conductivity in Mg-doped and undoped β -Ga 2 O 3 bulk-crystals," *Semiconductor Science and Technology,* vol. 30, p. 024006, 2015.

[137] K. Shimamura, E. G. Víllora, T. Ujiie, and K. Aoki, "Excitation and photoluminescence of pure and Si-doped β-Ga2O3 single crystals," *Applied Physics Letters,* vol. 92, p. 201914, 2008.

[138] R. A. Laudise, J. B. Mullin, B. Mutaftschiev, and K. Nassau, "Dr. A. V. L. Verneuil: The man and the method," *Journal of Crystal Growth,* vol. 13, pp. 12-18, 1972/05/01 1972.

[139] M. Ueltzen, "The Verneuil flame fusion process: substances," *Journal of Crystal Growth,* vol. 132, pp. 315-328, 1993/09/01 1993.

[140] K. Nassau, ""Reconstructed" or "Geneva" ruby," *Journal of Crystal Growth,* vol. 5, pp. 338-344, 1969/10/01 1969.

[141] A. O. Chase, "Growth of β-Ga2, O3 by the Verneuil Technique," *Journal of the American Ceramic Society,* vol. 47, pp. 470-470, 1964.

[142] T. Harwig and J. Schoonman, "Electrical properties of β-Ga2O3 single crystals. II," *Journal of Solid State Chemistry,* vol. 23, pp. 205-211, 1978/01/15 1978.

[143] T. Harwig, G. J. Wubs, and G. J. Dirksen, "Electrical properties of β-Ga2O3 single crystals," *Solid State Communications,* vol. 18, pp. 1223-1225, 1976/01/01 1976.

[144] L. Binet and D. Gourier, "Origin of the blue luminescence of β-Ga2O3," *Journal of Physics and Chemistry of Solids,* vol. 59, pp. 1241-1249, 8// 1998.

[145] W. Zulehner, "Historical overview of silicon crystal pulling development," *Materials Science and Engineering: B,* vol. 73, pp. 7-15, 4/3/ 2000.

[146] P. H. Keck and M. J. E. Golay, "Crystallization of Silicon from a Floating Liquid Zone," *Physical Review,* vol. 89, pp. 1297-1297, 03/15/ 1953.

[147] N. Suzuki, S. Ohira, M. Tanaka, T. Sugawara, K. Nakajima, and T. Shishido, "Fabrication and characterization of transparent conductive Sn-doped β-Ga2O3 single crystal," *physica status solidi (c),* vol. 4, pp. 2310-2313, 2007.

[148] E. G. Víllora, K. Shimamura, Y. Yoshikawa, K. Aoki, and N. Ichinose, "Large-size β-Ga2O3 single crystals and wafers," *Journal of Crystal Growth,* vol. 270, pp. 420-426, 10/1/ 2004.

[149] Y. Tomm, J. M. Ko, A. Yoshikawa, and T. Fukuda, "Floating zone growth of β-Ga2O3: a new window material for optoelectronic device applications," *Solar Energy Materials and Solar Cells,* vol. 66, pp. 369-374, 2// 2001.

[150] G. Teal and E. Buehler, "Single-crystal germanium," *Proceedings of the IRE,* vol. 40, pp. 906-909, 1952.

[151] H. J. Scheel, "Historical aspects of crystal growth technology," *Journal of Crystal Growth,* vol. 211, pp. 1-12, 4/1/ 2000.

[152] P. W. Bridgman, "Certain Physical Properties of Single Crystals of Tungsten, Antimony, Bismuth, Tellurium, Cadmium, Zinc, and Tin," *Proceedings of the American Academy of Arts and Sciences,* vol. 60, pp. 305-383, 1925.

[153] J. Czochralski, "Ein neues Verfahren zur Messung der Kristallisations geschwindigkeit der Metalle," *Z. Physikal. Chemie,* vol. 92, p. 219, 1918.

[154] G. K. Teal and J. Little, "Growth of germanium single crystals," in *Physical review*, 1950, pp. 647-647.

[155] B. Ernest and G. K. Teal, "Process for producing semiconductive crystals of uniform resistivity," ed: Google Patents, 1956.

[156] D. Gernez, "Measurements of growlh rates," *Comptes Rendus (Paris)* vol. 95, p. 1278, 1882.

[157] G. Tammann, "Uber die Abhiingigkeit der Zahl der Kerne, welche sich in verschiedenen unterkhulten Flussigkeiten bilden, von der Temperatur," *Z. phys. Chem. (Leipzig),* vol. 25, pp. 441-479, 1898.

[158]   R. Uecker, "The historical development of the Czochralski method," *Journal of Crystal Growth,* vol. 401, pp. 7-24, 2014.

[159]   J. Czochralski, "Process of improving alloys and metals," ed: Google Patents, 1925.

[160]   P. E. Tomaszewski, "Jan Czochralski—father of the Czochralski method," *Journal of crystal growth,* vol. 236, pp. 1-4, 2002.

[161]   E. Talik, "Ninetieth anniversary of Czochralski method," *Journal of alloys and compounds,* vol. 442, pp. 70-73, 2007.

[162]   Z. Galazka, R. Uecker, K. Irmscher, M. Albrecht, D. Klimm, M. Pietsch*, et al.*, "Czochralski growth and characterization of β-Ga2O3 single crystals," *Crystal Research and Technology,* vol. 45, pp. 1229-1236, 2010.

[163]   Z. Galazka, R. Uecker, D. Klimm, K. Irmscher, M. Naumann, M. Pietsch*, et al.*, "Scaling-Up of Bulk β-Ga2O3 Single Crystals by the Czochralski Method," *ECS Journal of Solid State Science and Technology,* vol. 6, pp. Q3007-Q3011, 2017.

[164]   B. Chalmers, H. E. LaBelle, and A. I. Mlavsky, "Growth of controlled profile crystals from the melt: Part III — Theory," *Materials Research Bulletin,* vol. 6, pp. 681-690, 1971/08/01 1971.

[165]   H. LaBelle and A. Mlavsky, "Growth of controlled profile crystals from the melt: Part I-Sapphire filaments," *Materials Research Bulletin,* vol. 6, pp. 571-579, 1971.

[166]   H.-E. LaBelle, "Growth of controlled profile crystals from the melt: Part II-Edge-defined, film-fed growth (EFG)," *Materials Research Bulletin,* vol. 6, pp. 581-589, 1971.

[167]   H. LaBelle, "EFG, the invention and application to sapphire growth," *Journal of Crystal Growth,* vol. 50, pp. 8-17, 1980.

[168]   B. Chalmers, H. LaBelle, and A. Mlavsky, "Edge-defined, film-fed crystal growth," *Journal of Crystal Growth,* vol. 13, pp. 84-87, 1972.

[169]   T. Masui, K. Koshi, K. DOIOKA, and Y. Yamaoka, "Ga2O3-BASED SINGLE CRYSTAL SUBSTRATE," ed: Google Patents, 2015.

[170]   S. Watanabe, K. IIzuka, K. DOIOKA, H. Matsubara, and T. Masui, "Method for growing beta-ga2o3-based single crystal," ed: Google Patents, 2016.

[171]   S. Watanabe, D. Wakimoto, K. IIzuka, K. Koshi, and T. Masui, "METHOD FOR GROWING B-Ga2O3 SINGLE CRYSTAL," ed: Google Patents, 2015.

[172]   K. Koshi, T. Masui, and M. Takizawa, "METHOD FOR CULTIVATING BETA-Ga2O3 SINGLE CRYSTAL, AND BETA-Ga2O3-SINGLE-CRYSTAL SUBSTRATE AND METHOD FOR PRODUCING SAME," ed: Google Patents, 2016.

[173]   K. Koshi, H. Matsubara, and S. Watanabe, "METHOD FOR GROWING ß-Ga2O3 SINGLE CRYSTAL," ed: Google Patents, 2014.

[174]   K. Koshi, S. Watanabe, M. Takizawa, Y. Yamaoka, D. Wakimoto, and M. Watanabe, "Beta-Ga2O3-Based Single Crystal Substrate," ed: Google Patents, 2015.

[175]   K. Koshi, S. Watanabe, M. Takizawa, Y. Yamaoka, D. Wakimoto, and M. Watanabe, "β-Ga 2 O 3-based single crystal substrate," ed: US Patent 9,349,915, 2016.

[176]   T. Oishi, Y. Koga, K. Harada, and M. Kasu, "High-mobility beta-Ga2O3 (201) single crystals grown by edge-defined film-fed growth method and their Schottky barrier diodes with Ni contact," *Applied Physics Express,* vol. 8, pp. 1-3, Mar 2015.

[177]   Z. Galazka, D. Klimm, K. Irmscher, R. Uecker, M. Pietsch, R. Bertram*, et al.*, "MgGa2O4 as a new wide bandgap transparent semiconducting oxide: Growth and properties of bulk single crystals," *Physica Status Solidi a-Applications and Materials Science,* vol. 212, pp. 1455-1460, Jul 2015.

[178]   R. A. Laudise, J. B. Mullin, B. Mutaftschiev, G. Garton, S. H. Smith, and B. M. Wanklyn, "Crystal growth from the flux systems PbO☐V2O5 and Bi2O3☐V2O5," *Journal of Crystal Growth,* vol. 13, pp. 588-592, 1972/05/01 1972.

[179]   V. I. Chani, K. Inoue, K. Shimamura, K. Sugiyama, and T. Fukuda, "Segregation coefficients in β-Ga2O2: Cr crystals grown from a B2O3 based flux," *Journal of Crystal Growth,* vol. 132, pp. 335-336, 1993/09/01 1993.

[180]   A. B. Chase and J. A. Osmer, "Localized Cooling in Flux Crystal Growth," *Journal of the American Ceramic Society,* vol. 50, pp. 325-328, 1967.

[181]   M. Takashi, A. Masaharu, K. Akira, and A. Tomoyoshi, "Absorption and Reflection of Vapor Grown Single Crystal Platelets of β-Ga 2 O 3," *Japanese Journal of Applied Physics,* vol. 13, p. 1578, 1974.

[182]   K. Hoshikawa, E. Ohba, T. Kobayashi, J. Yanagisawa, C. Miyagawa, and Y. Nakamura, "Growth of β-Ga2O3 single crystals using vertical Bridgman method in ambient air," *Journal of Crystal Growth,* vol. 447, pp. 36-41, 8/1/ 2016.

[183]   V. Maslov, V. Krymov, M. Blashenkov, A. Golovatenko, and V. Nikolaev, "β-Ga2O3 crystal growing from its own melt," *Technical Physics Letters,* vol. 40, pp. 303-305, 2014.

[184]   S. Uda, H. Inaba, J. Harada, and K. Hoshikawa, "Growth of langasite via Bridgman technique along [], [] and [] for piezoelectric applications," *Journal of Crystal Growth,* vol. 271, pp. 229-237, 10/15/ 2004.

[185]   S. Uda, S.-Q. Wang, N. Konishi, H. Inaba, and J. Harada, "Growth technology of piezoelectric langasite single crystal," *Journal of Crystal Growth,* vol. 275, pp. 251-258, 2/15/ 2005.

[186]   K. Hoshikawa, J. Osada, Y. Saitou, E. Ohba, C. Miyagawa, T. Kobayashi*, et al.*, "Vertical Bridgman growth of sapphire—Seed crystal shapes and seeding characteristics," *Journal of Crystal Growth,* vol. 395, pp. 80-89, 6/1/ 2014.

[187]   K. Sasaki, A. Kuramata, T. Masui, E. G. Villora, K. Shimamura, and S. Yamakoshi, "Device-Quality beta-Ga2O3 Epitaxial Films Fabricated by Ozone Molecular Beam Epitaxy," *Applied Physics Express,* vol. 5, pp. 1-3, Mar 2012.

[188]   O. Takayoshi, O. Takeya, and F. Shizuo, "Ga 2 O 3 Thin Film Growth on c -Plane Sapphire Substrates by Molecular Beam Epitaxy for Deep-Ultraviolet Photodetectors," *Japanese Journal of Applied Physics,* vol. 46, p. 7217, 2007.

[189]   O. Hironori, K. Masao, S. Kohei, K. Akito, H. Masataka, and S. S. James, "Systematic investigation of the growth rate of β-Ga 2 O 3 (010) by plasma-assisted molecular beam epitaxy," *Applied Physics Express,* vol. 7, p. 095501, 2014.

[190]   P. Vogt and O. Bierwagen, "The competing oxide and sub-oxide formation in metal-oxide molecular beam epitaxy," *Applied Physics Letters,* vol. 106, p. 081910, 2015.

[191]   K. Sasaki, M. Higashiwaki, A. Kuramata, T. Masui, and S. Yamakoshi, "Growth temperature dependences of structural and electrical properties of Ga2O3 epitaxial films grown on β-Ga2O3 (010) substrates by molecular beam epitaxy," *Journal of Crystal Growth,* vol. 392, pp. 30-33, 4/15/ 2014.

[192]   H. Okumura, K. Masao, S. Kohei, K. Akito, H. Masataka, and S. S. James, "Systematic investigation of the growth rate of β-Ga 2 O 3 (010) by plasma-assisted molecular beam epitaxy," *Applied Physics Express,* vol. 7, p. 095501, 2014.

[193]   R. Kumaran, T. Tiedje, S. E. Webster, S. Penson, and W. Li, "Epitaxial Nd-doped α-(Al1−xGax)2O3 films on sapphire for solid-state waveguide lasers," *Optics Letters,* vol. 35, pp. 3793-3795, 2010/11/15 2010.

[194]   J. J. Tietjen and J. A. Amick, "The preparation and properties of vapor-deposited epitaxial GaAs1− x P x using arsine and phosphine," *Journal of the Electrochemical Society,* vol. 113, pp. 724-728, 1966.

[195]   J. K. Abrokwah, T. N. Peck, R. A. Walterson, G. E. Stillman, T. S. Low, and B. Skromme, "High purity GaAs grown by the hydride vpe process," *Journal of Electronic Materials,* vol. 12, pp. 681-699, 1983.

[196]   A. Usui, S. Haruo, S. Akira, and A. A. Yamaguchi, "Thick GaN Epitaxial Growth with Low Dislocation Density by Hydride Vapor Phase Epitaxy," *Japanese Journal of Applied Physics,* vol. 36, p. L899, 1997.

[197]   K. Nomura, K. Goto, R. Togashi, H. Murakami, Y. Kumagai, A. Kuramata*, et al.*, "Thermodynamic study of β-Ga2O3 growth by halide vapor phase epitaxy," *Journal of Crystal Growth,* vol. 405, pp. 19-22, 11/1/ 2014.

[198]   H. Murakami, N. Kazushiro, G. Ken, S. Kohei, K. Katsuaki, T. Quang Tu*, et al.*, "Homoepitaxial growth of β-Ga 2 O 3 layers by halide vapor phase epitaxy," *Applied Physics Express,* vol. 8, p. 015503, 2015.

[199]   Y. Oshima, E. G. Víllora, and K. Shimamura, "Quasi-heteroepitaxial growth of β-Ga2O3 on off-angled sapphire (0 0 0 1) substrates by halide vapor phase epitaxy," *Journal of Crystal Growth,* vol. 410, pp. 53-58, 1/15/ 2015.

[200]   H. W. Kim and N. H. Kim, "Synthesis of βGa2O3 nanowires by an MOCVD approach," *Applied Physics A,* vol. 81, pp. 763-765, 2005.

[201]   D. J. Comstock and J. W. Elam, "Atomic Layer Deposition of Ga2O3 Films Using Trimethylgallium and Ozone," *Chemistry of Materials,* vol. 24, pp. 4011-4018, Nov 13 2012.

[202]   G. A. Battiston, R. Gerbasi, M. Porchia, R. Bertoncello, and F. Caccavale, "Chemical vapour deposition and characterization of gallium oxide thin films," *Thin Solid Films,* vol. 279, pp. 115-118, 1996/06/01 1996.

[203]   L. Miinea, S. Suh, S. G. Bott, J.-R. Liu, W.-K. Chu, and D. M. Hoffman, "Synthesis of aluminium and gallium fluoroalkoxide compounds and the low pressure metal-organic chemical vapor deposition of gallium oxide films," *Journal of Materials Chemistry,* vol. 9, pp. 929-935, 1999.

[204]   M. Valet and D. M. Hoffman, "Synthesis of Homoleptic Gallium Alkoxide Complexes and the Chemical Vapor Deposition of Gallium Oxide Films," *Chemistry of Materials,* vol. 13, pp. 2135-2143, 2001/06/01 2001.

[205]   H. W. Kim and N. H. Kim, "Growth of gallium oxide thin films on silicon by the metal organic chemical vapor deposition method," *Materials Science and Engineering: B,* vol. 110, pp. 34-37, 6/25/ 2004.

[206]   X. J. Du, Z. Li, C. N. Luan, W. G. Wang, M. X. Wang, X. J. Feng*, et al.*, "Preparation and characterization of Sn-doped beta-Ga2O3 homoepitaxial films by MOCVD," *Journal of Materials Science,* vol. 50, pp. 3252-3257, Apr 2015.

[207]   C.-Y. Huang, R.-H. Horng, D.-S. Wuu, L.-W. Tu, and H.-S. Kao, "Thermal annealing effect on material characterizations of β-Ga2O3 epilayer grown by metal organic chemical vapor deposition," *Applied Physics Letters,* vol. 102, p. 011119, 2013.

[208]   W. Mi, J. Ma, Z. Zhu, C. Luan, Y. Lv, and H. Xiao, "Epitaxial growth of Ga2O3 thin films on MgO (110) substrate by metal–organic chemical vapor deposition," *Journal of Crystal Growth,* vol. 354, pp. 93-97, 9/1/ 2012.

[209]   L. Kong, J. Ma, C. Luan, W. Mi, and Y. Lv, "Structural and optical properties of heteroepitaxial beta Ga2O3 films grown on MgO (100) substrates," *Thin Solid Films,* vol. 520, pp. 4270-4274, 4/30/ 2012.

[210]   D. Gogova, G. Wagner, M. Baldini, M. Schmidbauer, K. Irmscher, R. Schewski*, et al.*, "Structural properties of Si-doped β-Ga2O3 layers grown by MOVPE," *Journal of Crystal Growth,* vol. 401, pp. 665-669, 9/1/ 2014.

[211]   G. Wagner, M. Baldini, D. Gogova, M. Schmidbauer, R. Schewski, M. Albrecht*, et al.*, "Homoepitaxial growth of β-Ga2O3 layers by metal-organic vapor phase epitaxy," *physica status solidi (a),* vol. 211, pp. 27-33, 2014.

[212] M. Baldini, M. Albrecht, A. Fiedler, K. Irmscher, D. Klimm, R. Schewski, *et al.*, "Semiconducting Sn-doped beta-Ga2O3 homoepitaxial layers grown by metal organic vapour-phase epitaxy," *Journal of Materials Science,* vol. 51, pp. 3650-3656, Apr 2016.

[213] G. Wagner, M. Baldini, D. Gogova, M. Schmidbauer, R. Schewski, M. Albrecht, *et al.*, "Homoepitaxial growth of β-Ga2O3 layers by metal-organic vapor phase epitaxy," *physica status solidi (a),* vol. 211, pp. 27-33, 2014.

[214] A. Smith and R. Rodriguez-Clemente, "Morphological differences in ZnO films deposited by the pyrosol technique: effect of HCl," *Thin Solid Films,* vol. 345, pp. 192-196, 5/21/ 1999.

[215] J. G. Lu, T. Kawaharamura, H. Nishinaka, Y. Kamada, T. Ohshima, and S. Fujita, "Zno-based thin films synthesized by atmospheric pressure mist chemical vapor deposition," *Journal of Crystal Growth,* vol. 299, pp. 1-10, 2/1/ 2007.

[216] H. Nishinaka, K. Toshiyuki, and F. Shizuo, "Low-Temperature Growth of ZnO Thin Films by Linear Source Ultrasonic Spray Chemical Vapor Deposition," *Japanese Journal of Applied Physics,* vol. 46, p. 6811, 2007.

[217] T. Kawaharamura, N. Hiroyuki, and F. Shizuo, "Growth of Crystalline Zinc Oxide Thin Films by Fine-Channel-Mist Chemical Vapor Deposition," *Japanese Journal of Applied Physics,* vol. 47, p. 4669, 2008.

[218] B. Gottlieb, R. Koropecki, R. Arce, R. Crisalle, and J. Ferron, "Characterization of fluorine-doped tin oxide produced by the pyrosol method," *Thin Solid Films,* vol. 199, pp. 13-21, 1991/04/01 1991.

[219] J.-M. Laurent, A. Smith, D. S. Smith, J.-P. Bonnet, and R. R. Clemente, "Morphology and physical properties of SnO2-based thin films deposited by the pyrosol process from dibutyltindiacetate," *Thin Solid Films,* vol. 292, pp. 145-149, 1997/01/05 1997.

[220] K. H. Yoon and J. S. Song, "Effects of solvents and carrier gases on the electrical and optical properties of pyrosol-deposited SnO2-based films," *Thin Solid Films,* vol. 224, pp. 203-208, 1993/03/15 1993.

[221] G. Gordillo, L. C. Moreno, W. de la Cruz, and P. Teheran, "Preparation and characterization of SnO2 thin films deposited by spray pyrolysis from SnCl2 and SnCl4 precursors," *Thin Solid Films,* vol. 252, pp. 61-66, 1994/11/15 1994.

[222] Y. Kamada, K. Toshiyuki, N. Hiroyuki, and F. Shizuo, "Linear-Source Ultrasonic Spray Chemical Vapor Deposition Method for Fabrication of ZnMgO Films and Ultraviolet Photodetectors," *Japanese Journal of Applied Physics,* vol. 45, p. L857, 2006.

[223] M. Oda, J. Kikawa, A. Takatsuka, R. Tokuda, T. Sasaki, K. Kaneko, *et al.*, "Vertical Schottky barrier diodes of B-Ga2O3 fabricated by mist epitaxy," in *2015 73rd Annual Device Research Conference (DRC)*, 2015, pp. 137-138.

[224] A. Smith, "Pyrosol deposition of ZnO and SnO2 based thin films: the interplay between solution chemistry, growth rate and film morphology," *Thin Solid Films,* vol. 376, pp. 47-55, 11/1/ 2000.

[225] K. Kaneko, N. Taichi, K. Itsuhiro, and F. Shizuo, "Fabrication of Highly Crystalline Corundum-Structured α-(Ga 1- x Fe x) 2 O 3 Alloy Thin Films on Sapphire Substrates," *Applied Physics Express,* vol. 2, p. 075501, 2009.

[226] H. Ito, K. Kentaro, and F. Shizuo, "Growth and Band Gap Control of Corundum-Structured α-(AlGa) 2 O 3 Thin Films on Sapphire by Spray-Assisted Mist Chemical Vapor Deposition," *Japanese Journal of Applied Physics,* vol. 51, p. 100207, 2012.

[227] K. Kaneko, K. Hitoshi, I. Hiroshi, and F. Shizuo, "Evaluation of Misfit Relaxation in α-Ga 2 O 3 Epitaxial Growth on α-Al 2 O 3 Substrate," *Japanese Journal of Applied Physics,* vol. 51, p. 020201, 2012.

[228] K. Akaiwa and F. Shizuo, "Electrical Conductive Corundum-Structured α-Ga 2 O 3 Thin Films on Sapphire with Tin-Doping Grown by Spray-Assisted Mist Chemical Vapor Deposition," *Japanese Journal of Applied Physics,* vol. 51, p. 070203, 2012.

[229] T. Kawaharamura, T. D. Giang, and F. Mamoru, "Successful Growth of Conductive Highly Crystalline Sn-Doped α-Ga 2 O 3 Thin Films by Fine-Channel Mist Chemical Vapor Deposition," *Japanese Journal of Applied Physics,* vol. 51, p. 040207, 2012.

[230] S. J. Pearton, "Ion implantation doping and isolation of III–V semiconductors," *Nuclear Instruments and Methods in Physics Research Section B: Beam Interactions with Materials and Atoms,* vol. 59, pp. 970-977, 1991/07/01 1991.

[231] S. J. Pearton, "Ion implantation for isolation of III-V semiconductors," *Materials Science Reports,* vol. 4, pp. 313-363, 1990/01/01 1990.

[232] S. J. Pearton, J. M. Poate, F. Sette, J. M. Gibson, D. C. Jacobson, and J. S. Williams, "Ion implantation in GaAs," *Nuclear Instruments and Methods in Physics Research Section B: Beam Interactions with Materials and Atoms,* vol. 19, pp. 369-380, 1987/01/01 1987.

[233] K. Sasaki, M. Higashiwaki, A. Kuramata, T. Masui, and S. Yamakoshi, "Si-Ion Implantation Doping in beta-Ga2O3 and Its Application to Fabrication of Low-Resistance Ohmic Contacts," *Applied Physics Express,* vol. 6, Aug 2013.

[234] M. Razeghi, "Short-wavelength solar-blind detectors-status, prospects, and markets," *Proceedings of the IEEE,* vol. 90, pp. 1006-1014, 2002.

[235] L. Li, E. Auer, M. Liao, X. Fang, T. Zhai, U. K. Gautam*, et al.*, "Deep-ultraviolet solar-blind photoconductivity of individual gallium oxide nanobelts," *Nanoscale,* vol. 3, pp. 1120-1126, 2011.

[236] Y. Li, T. Tokizono, M. Liao, M. Zhong, Y. Koide, I. Yamada*, et al.*, "Efficient Assembly of Bridged β-Ga2O3 Nanowires for Solar-Blind Photodetection," *Advanced Functional Materials,* vol. 20, pp. 3972-3978, 2010.

[237] P. Feng, J. Y. Zhang, Q. H. Li, and T. H. Wang, "Individual β-Ga2O3 nanowires as solar-blind photodetectors," *Applied Physics Letters,* vol. 88, p. 153107, 2006.

[238] D. Guo, Z. Wu, P. Li, Y. An, H. Liu, X. Guo*, et al.*, "Fabrication of β-Ga2O3 thin films and solar-blind photodetectors by laser MBE technology," *Optical Materials Express,* vol. 4, pp. 1067-1076, 2014/05/01 2014.

[239] D. Y. Guo, Z. P. Wu, Y. H. An, X. C. Guo, X. L. Chu, C. L. Sun*, et al.*, "Oxygen vacancy tuned Ohmic-Schottky conversion for enhanced performance in beta-Ga2O3 solar-blind ultraviolet photodetectors," *Applied Physics Letters,* vol. 105, Jul 14 2014.

[240] S. Nakagomi, T. Momo, S. Takahashi, and Y. Kokubun, "Deep ultraviolet photodiodes based on β-Ga2O3/SiC heterojunction," *Applied Physics Letters,* vol. 103, p. 072105, 2013.

[241] R. Suzuki, S. Nakagomi, Y. Kokubun, N. Arai, and S. Ohira, "Enhancement of responsivity in solar-blind β-Ga2O3 photodiodes with a Au Schottky contact fabricated on single crystal substrates by annealing," *Applied Physics Letters,* vol. 94, p. 222102, 2009.

[242] M. Mohamed, K. Irmscher, C. Janowitz, Z. Galazka, R. Manzke, and R. Fornari, "Schottky barrier height of Au on the transparent semiconducting oxide beta-Ga2O3," *Applied Physics Letters,* vol. 101, Sep 24 2012.

[243] K. Sasaki, M. Higashiwaki, A. Kuramata, T. Masui, and S. Yamakoshi, "Ga2O3 Schottky Barrier Diodes Fabricated by Using Single-Crystal β–Ga2O3 (010) Substrates," *IEEE Electron Device Letters,* vol. 34, pp. 493-495, 2013.

[244] M. Higashiwaki, K. Sasaki, T. Kamimura, M. H. Wong, D. Krishnamurthy, A. Kuramata*, et al.*, "Depletion-mode Ga2O3 metal-oxide-semiconductor field-effect transistors on beta-Ga2O3 (010) substrates and temperature dependence of their device characteristics," *Applied Physics Letters,* vol. 103, pp. 1-4, Sep 16 2013.

[245]   M. H. Wong, K. Sasaki, A. Kuramata, S. Tamakoshi, and M. Higashiwaki, "Field-Plated Ga2O3 MOSFETs with a Breakdown Voltage of Over 750 V," *IEEE Electron Device Letters,* vol. 37, pp. 212 - 215, 2016.

[246]   W. S. Hwang, A. Verma, H. Peelaers, V. Protasenko, S. Rouvimov, H. Xing*, et al.*, "High-voltage field effect transistors with wide-bandgap β-Ga2O3 nanomembranes," *Applied Physics Letters,* vol. 104, p. 203111, 2014.

[247]   S. R. Thomas, G. Adamopoulos, Y.-H. Lin, H. Faber, L. Sygellou, E. Stratakis*, et al.*, "High electron mobility thin-film transistors based on Ga2O3 grown by atmospheric ultrasonic spray pyrolysis at low temperatures," *Applied Physics Letters,* vol. 105, Sep 1 2014.

[248]   M. J. Tadjer, N. A. Mahadik, V. D. Wheeler, E. R. Glaser, L. Ruppalt, A. D. Koehler*, et al.*, "Editors' Choice Communication—A (001) β-Ga2O3 MOSFET with +2.9 V Threshold Voltage and HfO2 Gate Dielectric," *ECS Journal of Solid State Science and Technology,* vol. 5, pp. P468-P470, January 1, 2016 2016.

[249]   M. H. Wong, K. Sasaki, A. Kuramata, S. Yamakoshi, and M. Higashiwaki, "Anomalous Fe diffusion in Si-ion-implanted beta-Ga2O3 and its suppression in Ga2O3 transistor structures through highly resistive buffer layers," *Applied Physics Letters,* vol. 106, Jan 19 2015.

[250]   M. W. Allen, S. M. Durbin, and J. B. Metson, "Silver oxide Schottky contacts on n-type ZnO," *Applied Physics Letters,* vol. 91, p. 053512, 2007.

[251]   G. T. Dang, T. Kawaharamura, M. Furuta, and M. W. Allen, "Metal-Semiconductor Field-Effect Transistors With InGaZnO Channel Grown by Nonvacuum-Processed Mist Chemical Vapor Deposition," *IEEE Electron Device Letters,* vol. 36, pp. 463-465, 2015.

[252]   J. A. Cooper and A. Agarwal, "SiC power-switching devices - The second electronics revolution?," *Proceedings of the Ieee,* vol. 90, pp. 956-968, Jun 2002.

[253]   J. Spitz, M. R. Melloch, J. A. Cooper, and M. A. Capano, "2.6 kV 4H-SiC lateral DMOSFET's," *Ieee Electron Device Letters,* vol. 19, pp. 100-102, Apr 1998.

[254]   A. Elasser and T. P. Chow, "Silicon carbide benefits and advantages for power electronics circuits and systems," *Proceedings of the Ieee,* vol. 90, pp. 969-986, Jun 2002.